



LUND UNIVERSITY

Combustion Engine Models for Hybrid Vehicle System Development

Strandh, Petter

2002

[Link to publication](#)

Citation for published version (APA):

Strandh, P. (2002). *Combustion Engine Models for Hybrid Vehicle System Development*. [Licentiate Thesis, Combustion Engines]. Division of Combustion Engines, Lund Institute of Technology.

Total number of authors:

1

General rights

Unless other specific re-use rights are stated the following general rights apply:

Copyright and moral rights for the publications made accessible in the public portal are retained by the authors and/or other copyright owners and it is a condition of accessing publications that users recognise and abide by the legal requirements associated with these rights.

- Users may download and print one copy of any publication from the public portal for the purpose of private study or research.
- You may not further distribute the material or use it for any profit-making activity or commercial gain
- You may freely distribute the URL identifying the publication in the public portal

Read more about Creative commons licenses: <https://creativecommons.org/licenses/>

Take down policy

If you believe that this document breaches copyright please contact us providing details, and we will remove access to the work immediately and investigate your claim.

LUND UNIVERSITY

PO Box 117
221 00 Lund
+46 46-222 00 00

Combustion Engine Models for Hybrid Vehicle System Development

Petter Strandh

Division of Combustion Engines
Department of Heat and Power Engineering
Lund Institute of Technology
Lund 2002

Till Desirée och Emma.

Department of Heat and Power Engineering
Lund Institute of Technology
Box 118
SE-221 00 LUND
Sweden

E-mail: petter.strandh@vok.lth.se
WWW: <http://www.vok.lth.se/>

ISSN 0282–1990
ISRN LUTMDN / TMHP -- 02 / 7003 -- SE

©2002 by Petter Strandh. All rights reserved.
Printed in Sweden by Media-Tryck,
Lund University, Lund 2002

Abstract

This report is part of a project that is called *Generic hybrid systems*. Its objective is to simulate and investigate electric hybrid drive trains.

The goal of this work has been to develop combustion engine models that are computer efficient, but still has the potential of giving both qualitative and quantitative results. For instance, if the model is run in a less ideal manner the model will show an increase in both fuel consumption and exhaust emissions.

Both a spark ignition (SI or Otto) engine as well as a compression ignition (CI or Diesel) engine model have been developed.

The SI-engine model has been partially validated through the use of transient testing.

The thesis also contains a proof of concept study that is called TES - *Transient Emission Sampling*, which is a method for measuring exhaust emissions during transients.

Acknowledgments

I have many people to thank for their involvement in this thesis. First at hand is my main supervisor Rolf Egnell. It is mainly his ideas that I have expanded in this work. Also big thanks goes to Prof Gunnar Lundholm for accepting me as a PhD student and taking care of the practicalities.

I also thank Bengt Johansson whose great knowledge about combustion engines have helped from time to time.

Other people at the department are my room mates, Magnus Christensen, Olof Erlandsson and Ola Stenlåås. Our discussion about everything from work to life has been very giving and fruitful.

Also the rest of the guys at the department deserves big thanks for the extremely nice camaraderie I have seen over the past years.

For my colleagues at the Department of Industrial Electrical Engineering and Automation: First we have my partner in this project, Karin Jonasson, whose work on the hybrid vehicle made it possible for me to test my models on a entirely new level. This work would not have been done at all without the help of Professor Mats Alaküla. Christian Andersson has also been of great value to the project.

For all the practical work that has been done I have mainly Jan-Erik Nilsson to thank for getting the lab engine work properly. For the TES project Bengt Simonsson was of invaluable help.

For help with computers I have to thank Krister Olsson and Olof Strömstedt.

Finally I thank my wife Desirée and my little daughter Emma, for being there for me.

Contents

1. Introduction	1
1.1 Background	1
1.2 Previous work by the author	2
1.3 Method and objective	2
1.4 Outline of the thesis	3
1.5 List of publications	3
2. Vehicle Modeling Theory	4
2.1 Why simulate?	4
2.2 Previous projects	5
2.3 Modeling combustion engines	6
3. Hybrid Vehicle Modelling	8
3.1 Different hybrid topologies	11
4. Modeling Diesel Engines for Hybrid Vehicles	14
4.1 Modeling Diesel specific components	14
4.2 EGR	21
4.3 Diesel engine implementation in Simulink	25
4.4 Diesel exhaust emission transient correction	28
4.5 Simulation results	33
5. Modeling SI-Engines for Hybrid Vehicles	39
5.1 The air flow model	39
5.2 The fuel supply	45
5.3 Implementation of the λ time delays	47
5.4 Model implementation in Simulink	48
5.5 Simulation time scale	49
5.6 Simulation results	50

6. Validation with TES	54
6.1 TES - How does it work?	55
6.2 The setup	55
6.3 Equipment used	55
6.4 Data acquisition setup	56
6.5 Measurements	56
6.6 Results	58
7. Summary and Conclusions	61
7.1 Summary	61
7.2 Engine sources	61
7.3 Future work	62
8. Bibliography	63
A. Dictionary	65
B. A small Simulink tutorial	66
B.1 How it all comes together	66
B.2 A small example - the low pass filter	67
B.3 A simple naturally aspirated SI engine	67
C. Simulink graphs	69
C.1 The CI engine	69
C.2 The SI engine	74
D. Discussion about the thesis	78
E. Modeling SI Engines for Hybrid Vehicles	80
F. Comparative Study of Generic Hybrid Topologies	90
G. Norpie - paper	103

1

Introduction

1.1 Background

The background to this project is that there has been several efforts in enhancing hybrid electric vehicle technology. The objective is to, from a bird's-eye view, solve the complex puzzle of hybrid vehicles.

The main problems are:

- What topology should the hybrid use?
- Which prime mover is best suited?
- What is the optimum power flow through a hybrid vehicle?

Previous hybrid related activities at LTH

The hybrid activities at LTH started in 1992 when a master' thesis was carried out on the subject of optimizing the running strategy of a series city bus hybrid that was being developed by SL (The Stockholms municipal bus company). See Reference [1].

This effort was then followed by a deeper analysis by Morten Hemmingsson in his licentiate thesis, Reference [2]. This was an optimization study of the entire drive train of a hybrid bus. It was complemented with practical studies with a real combustion engine in the laboratory.

Another parallel activity at LTH was carried out by Christian Andersson with his licentiate thesis, see Reference [3], where he simulated and validated a series hybrid electric city bus that was fueled with natural gas.

1.2 Previous work by the author

Below follows a short review of what brought me to the subject of this thesis:

Ion current measurements

Part of my first work at the department was to carry out ion current measurements on a turbocharged SAAB 2.3 liter engine. In ion current measurements the spark plus is used as a sensor for detecting engine knock and misfire. Ion current measurements have also the potential of predicting the air fuel ratio. Some work was also done on an atmospheric burner to complement the engine measurements. These efforts resulted in an SAE paper, Reference [4], which I presented at the SAE Congress in Detroit 1998.

Conversion of a hybrid electric bus to run on ethanol

When the ion current project was concluded, my following project was to convert the fuel system on a hybrid electric bus from gasoline to an ethanol based fuel, called E85 (which is basically 85% ethanol and 15% gasoline). There was also an effort in reducing the exhaust emissions from the vehicle. The project report can be found in Reference [5].

1.3 Method and objective

The goal of the present work is to contribute to the development of hybrid vehicles, and to increase the knowledge of how to simulate combustion engines in a easy and computer efficient manner.

Simple models

It had been the desire of the author to make simple models. This will have a twofold impact on its end use. Simple models are of course easier to understand than complex ones. But also, which is more important, a simple model that is understood will have a greater potential of actually being used.

1.4 Outline of the thesis

First, there is a chapter which deals with vehicle modeling theory. This is a summary of different approaches for simulating vehicles. The next chapter deals with the specifics of hybrid vehicle components and how they are approached. The two subsequent chapters deal with the specifics of Diesel engine and spark ignition engine modelling. Next chapter describes a method to measure transient emissions.

1.5 List of publications

- *Simulation and verification of a hybrid bus*, was written by Christian Andersson, Karin Jonasson, myself and Mats Alaküla. My contribution to this paper was to help collect the data for the combustion engine model, and advice on how to utilize the engine to minimize emissions. The paper was presented by Christian Andersson at the NORPIE conference in Ålborg, Denmark, 2000.
- *Modeling SI-engines for Hybrid Vehicles*, written by myself and Rolf Egnell. The paper is based on my SI-engine model which is presented here in Chapter 5. The paper was presented by me at the SAE Congress in Detroit, USA, 2001.
- *Comparative Study of Generic Hybrid Topologies*, was written by Karin Jonasson, myself and Mats Alaküla. My contribution was the SI-engine model which is a part of the hybrid vehicle model. The paper was presented by Karin, at the EVS¹, Berlin, Germany, 2001.

¹Electric Vehicle Symposium

2

Vehicle Modeling Theory

In this chapter, different ways of simulating vehicles on the road are discussed.

2.1 Why simulate?

Why simulate, is the question one should ask oneself before starting. Answer: To get a better understanding of how things work and, when dealing with large complex machines, it is the only possibility for understanding how their components interact. How to foresee how a machine is going to react when being run in a new way, can preferably be obtained with the use of simulation.

When a model describes reality in a correct manner it is possible to determine how a machine is going to operate in different configurations. It can be used for optimization of the machine, where trying all the possible configurations in practice is too expensive and time consuming. Simulation models can also be used for training purposes, so that mistakes can be made without damage to hardware.

Vehicle simulations

Vehicle simulations are for example used to determine the performance and fuel consumption of new vehicles. Other applications are for planning the structure of the road network, where different layouts are compared to determine which concept is the safest, and which has the least impact on the environment.

There are also applications that are used for determining the total amount of exhaust emission for a region or for an entire country.

2.2 Previous projects

VehProp was a Swedish vehicle modeling project that was run in the mid nineties, see Reference [6]. Its goal was to produce a large modular library to aid in the analysis and development of new vehicles by simulating the vehicle drive train with regard to stability, performance, energy use and exhaust emissions.

In the early stages of the project the simulating tool was Simulink. However, it was found to be too slow when dealing with the large structures that make up an entire vehicle.

The next choice was Dymola which is a more refined modelling language. In Dymola solving a problem is done in two stages. First the problem is described in an object oriented manner where all components are connected together. Every component is described with its governing equation. Secondly, the entire model is translated into one program that describes the entire system. During the translation of the system, every equation is simplified and put into a system matrix. The matrix system is described as a DAE (Differential Algebraic Equations). See Reference [7].

These steps made the simulation go very fast. But still, when one wants to simulate the entire vehicle, with everything included such as driver, drive train, combustion engine and catalyst, the simulation is too slow, which causes the time between iterations to become too long to be a useful tool.

2.3 Modeling combustion engines

Simulation of combustion engines can be done in different time scales. There are several different methods for everything from micro time scale models used for calculating individual species in the cylinder to mean value models. In the following section the most commonly used methods are described, as is their respective usability.

Quasi stationary modeling¹

When is a model considered to be quasi stationary? The actual value, for example a specific exhaust emission of interest, is taken from a table, using the current engine speed and load. This method does not take any consideration to whether the engine is stationary or if it is just passing by in a fast transient where the actual operation point happens to be the mean value.

One reason is that engine data are measured at constant conditions, it is easy just interpolating the desired values from a table. For stationary engines this might be a nice approach but not for vehicles that nearly never operate stationary.

Statistical models

There are some literature examples that use statistical models that has been fitted from a large volume of data, thereby constructing a composite car, see Reference [8]. These models are then used to determine the performance and characteristics of a fleet of vehicles. The problem with these kinds of models is that the composite car will not represent any car, and the characteristics of one model will influence the engine fleet in a biased way.

In the Reference [8], conclusions were drawn on how the air fuel ratio impacts emissions, based on these statistical models. However, these relations can be obtained from combustion engine literature.

Cycle resolved modeling

Cycle resolved models are based on cycle by cycle calculations. Every part of the cycle is considered from gas exchange to combustion. The cycle resolved approach is usually used to study the formation of emissions and other phenomena such as engine knock.

The method has different degrees of complexity.

¹When parameters do not change during the time window.

- Zero dimensional,
which is when the cylinder composition is regarded as mean values. In some cases, the cylinder is divided into several zones, but these zones doesn't have any spatial resolution.
- Quasi dimensional,
basically the same as zero dimensional, but the main gas is divided into small packets representing different properties of the gas bulk.
- Multi-dimensional model,
this model has a spatial resolution, taking into account mass transfer between different zones.

Cycle resolved modeling is not the best way to approach vehicle simulation as the simulation time is long, setup time is also long and the quality of the information is better than what is required for vehicle simulations.

QSTC - Quasi stationary transient compensated models

The models presented in this thesis are basically quasi stationary models, where components that are affected by transients are modeled more thoroughly.

The Diesel engine model For Diesel engines whose main governing load component is the turbocharger, it is important to take this component into consideration. When a Diesel engine is forced to increase its torque faster then the turbocharger can respond, the result will be large amounts of soot emissions. This is explained in more detail in Chapter 4.

The SI engine model In a SI-engine the main crucial factor for emission control is how well λ is controlled. This is affected by such factors as the engine control unit response, and wall-wetting. The SI engine is explained in more detail in Chapter 5.

3

Hybrid Vehicle Modelling

A hybrid vehicle means that the vehicle is powered by two sources. These two sources are usually a battery powered electric motor and some sort of fuel powered prime mover. The prime mover is usually in the shape of a combustion engine.

The aim is to model a drive cycle with correct transient responsiveness. The simulation model is run from the driver's point of view. The driver is implemented as a PID-controller which controls the amount of power that is applied on the wheels. By changing the control parameters for the driver, three different driver signatures were developed, presented as slow, normal and fast.

The main problem with the SI engine is its poor part load efficiency. Figure 3.1 shows the efficiency of a SI engine. As can be seen, the efficiency is maximal close to full torque and at moderate speeds; this is true for naturally aspirated engines. For turbocharged engines the maximum efficiency is at lower torque. During normal driving, the engine is seldom operating in this area.

The efficiency characteristic of the Diesel engine is similar to that of the SI engine. However the efficiency is generally higher and especially at lower torque the efficiency is much higher. But in order to achieve maximal efficiency it is important to run the engine at high load and moderate engine speed, see Figure 3.2.

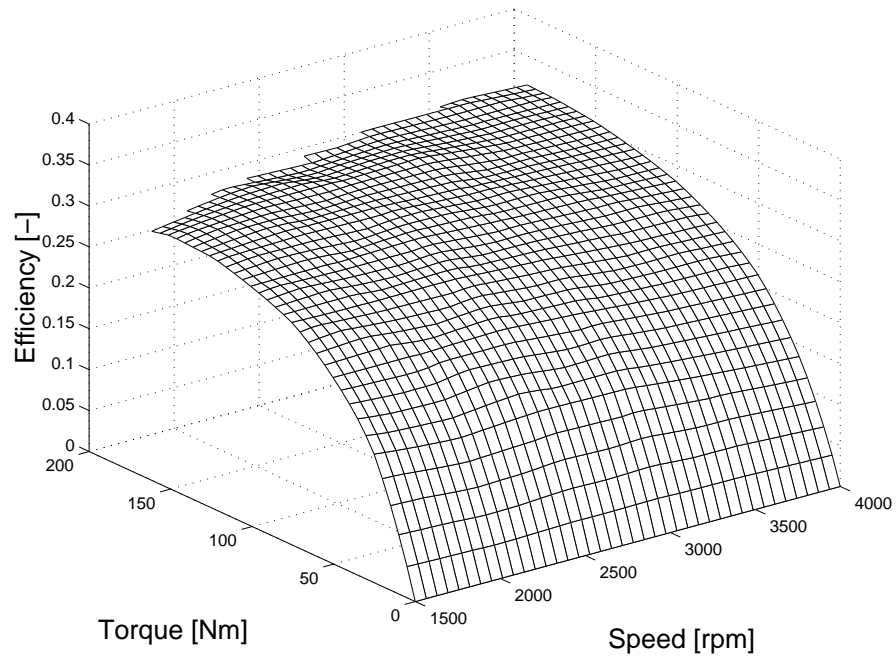


Figure 3.1 The efficiency of an automotive SI engine.

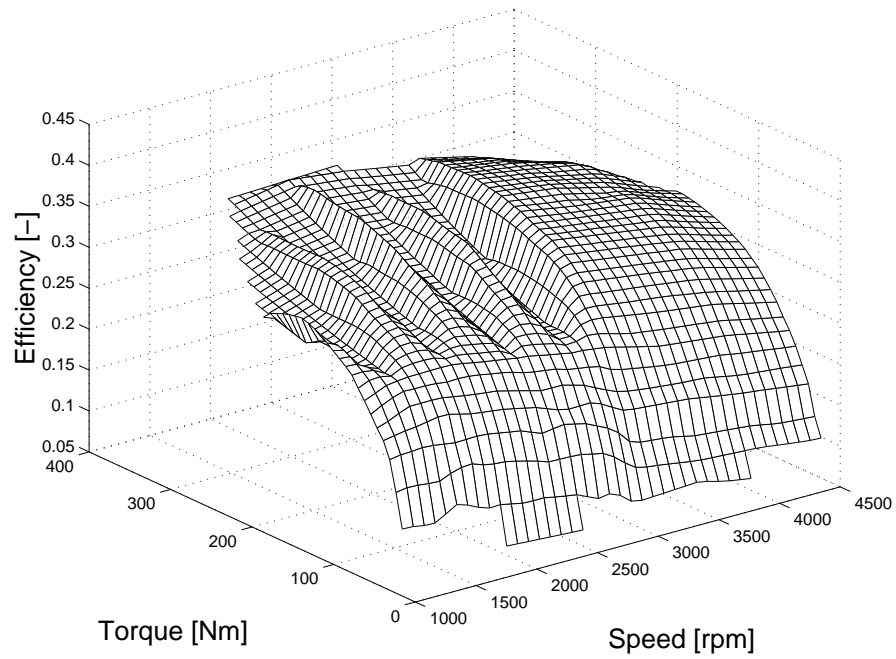


Figure 3.2 The efficiency of an automotive Diesel engine.

The strengths and weaknesses

The hybrid vehicle strength lies in its ability to:

- Utilize the optimal load points of the combustion engine.
- Regenerative Braking
In a standard vehicle, all brake energy is dissipated into heat in the brakes. If the brake energy could be recycled, a reduction in fuel consumption of up to 30% is attainable.
- Prime mover sizing
During strong accelerations it is possible to use the electrical motor together with the battery in parallel with the IC-engine to augment the acceleration, whereby a smaller IC and for the application smaller engine can be used.
- Idle shut off
In a conventional vehicle the engine is run at idle when it is standing in a queue or at traffic lights. In a hybrid it is possible have engine shutdown and start the engine with an ISG¹.
- Performance and drivability
Since a hybrid drive line has more degrees of freedom than a conventional direct drive, it is possible to increase drivability.

The hybrid vehicle weakness is the:

- Vehicle complexity
In order to accommodate all technology, the degree of complexity of the vehicle is increased, which causes an increase in cost and maintenance. More machinery and battery cause the weight to increase as well.

¹Integrated Starter-Generator

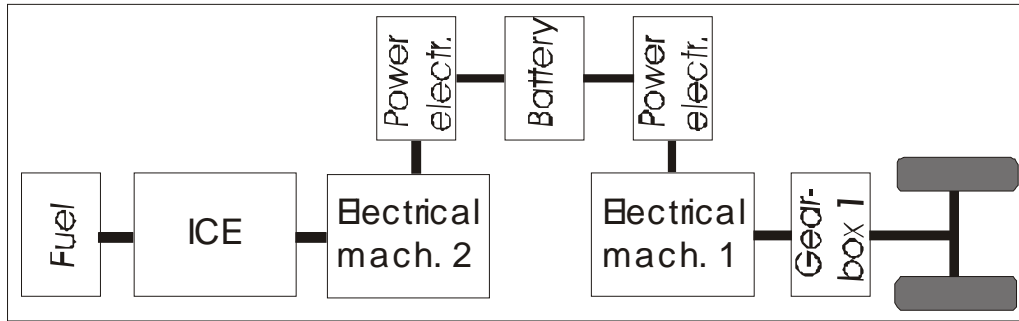
3.1 Different hybrid topologies

Below the different hybrid topologies are described. Figure 3.3 shows the principal layouts.

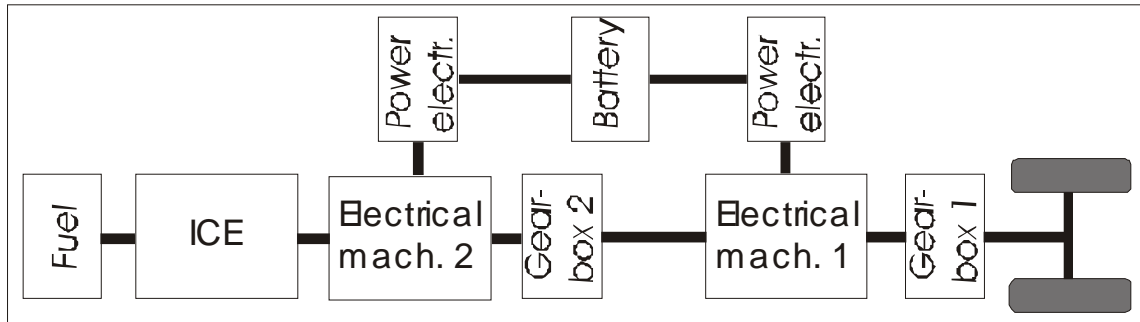
- *The parallel hybrid.* The parallel hybrid vehicle has a combination of drive systems where each driving shaft is connected to an energy source. There is a direct mechanical connection between the ICE and the wheels, which reduces the drive losses from the prime mover to the wheels, hence the overall efficiency increases.
- *The series hybrid.* Series hybrid vehicles have a combination of energy sources. There is no mechanical connection between the prime mover and the wheels. Therefore all energy from the prime mover to the wheels has to be converted into electrical energy after it can be brought to electrical motors of the wheels. This facilitates the ICE to be turned off in sensitive areas, zero emission zones. The main drawback is that the electrical drives and motor have to be able to take care of large amounts of power, which makes them expensive. The main advantage is that the combustion engine can be run in an optimal manner.
- *The Strigear hybrid.* The Strigear hybrid is actually a combination of a parallel and a series hybrid vehicle. By replacing the single electrical machine in a parallel hybrid with two, with a clutch between them, it is possible to switch between the two modes. The on-board computers are given the task to compare the predicted overall losses from the two hybrid concepts. The best solution is chosen, i.e. the clutch is engaged or disengaged. The name Strigear is a short form of sequentially run, triple gearbox connected engine/motor hybrid.
- *The complex hybrid.* The Power Split Hybrid (PSH), also called complex, combined or dual hybrid vehicle, has a blurred transformation between the series and parallel hybrid state. A planetary gearbox is used with two electrical machines (one on the ring wheel, one on the solar wheel and the ICE connected to the planet carrier). At most operating points some of the prime energy flows from the ICE directly to the wheels as in a parallel hybrid, and some flows via the electrical machines as in a series hybrid. The proportion between these two energy flows is speed dependent and at a certain speed it works as a pure parallel hybrid. In most other operating points it is partially

a series hybrid, which means several conversions of the energy that flows the series way from the prime energy source to the wheels.

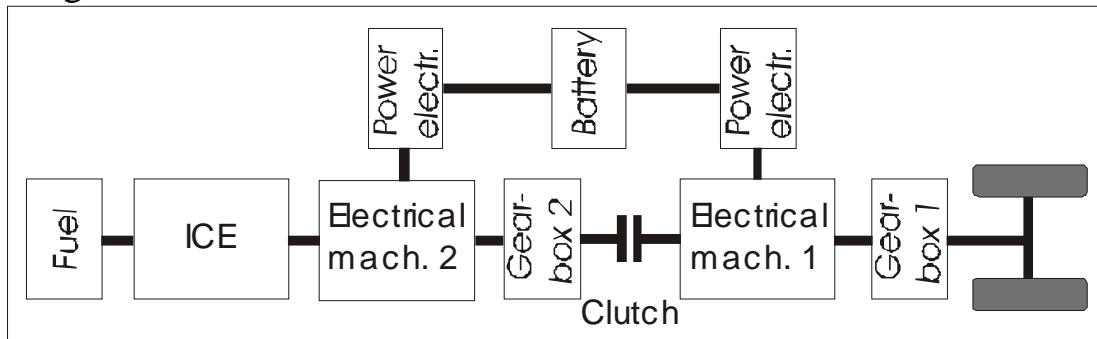
Series



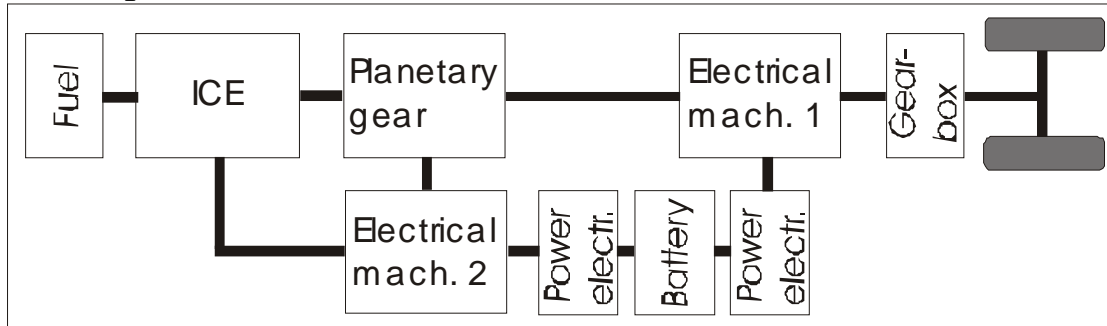
Parallel



Strigear



Powersplit

**Figure 3.3** Layout of different hybrid topologies.

4

Modeling Diesel Engines for Hybrid Vehicles

The Diesel engine is, thanks to its high efficiency and high durability, an attractive power source for most vehicle applications. With the forthcoming use of SCR¹, NOx storage technology and efficient particulate traps the Diesel engine has the potential to compete emissionwise with the Otto engine. Utilizing a hybrid drive train together with a Diesel engine has the potential of achieving a very high overall efficiency.

The main problem with the present-day Diesel engine is that, at part load or at near idle operation, the specific NOx emissions are high.

However, with state of the art catalysts, there is the possibility of reducing NOx at lower exhaust temperatures. Drawbacks are cost and complexity of exhaust after-treatment systems.

A simulation model concept is here presented where stationary engine data are used for transient simulations. In order to have correct behavior, the model is corrected for the effects of turbocharging (turbo lag). This is done in order to take transient effects into consideration.

4.1 Modeling Diesel specific components

The following section contains a presentation of the major components that make up the Diesel engine model.

The parts discussed here are the inlet and exhaust manifolds, the pumping action of the engine, the turbocharger as well as the intercooler and the EGR circuit.

¹Selective Catalytic Reduction of NOx

The mass balance of the inlet manifold

The inlet manifold is the heart of the basic emptying-and-filling model. The manifold is filled with air from the intercooler. The gas flow out of the manifold is dependent on the pumping action of the engine which in turn is affected by the volumetric efficiency.

The mass balance of the inlet manifold is described by Equation 4.1, $\dot{m}_{manifold}$ is the net flow of air into the manifold, $\dot{m}_{throttle}$ is the mass flow entering the manifold through the throttle and \dot{m}_{engine} is the mass flow exiting the manifold, thus entering the engine body.

$$\dot{m}_{manifold} = \dot{m}_{throttle} - \dot{m}_{engine} \quad (4.1)$$

The pressure in the manifold $P_{manifold}$ is calculated from the equation of state, where R is the gas constant and $T_{manifold}$ the gas temperature. See Equation 4.2

$$P_{manifold} = \frac{\dot{m}_{manifold} R T_{manifold}}{V_{manifold}} \quad (4.2)$$

The exhaust manifold gas mass and the intercooler gas mass are calculated in the same way as the inlet manifold by using a mass balance.

Exhaust manifold

The incoming exhaust mass flow comes from the engine cylinders. The outgoing mass flow rate is coupled to the action of the exhaust turbine.

The mass of gas in the exhaust manifold gives the manifold gas pressure which then acts on the turbine. Pressure and mass flow gives the operating point of the turbine.

In Reference [9] it is stated that there is no need for an exhaust manifold since its time constant is so small that neglecting it does not affect the accuracy of the simulation. This is so because of the high exhaust temperature which causes the volume flow to be high. An exhaust manifold is still used in this model to improve turbine model stability.

The intercooler

The purpose of the intercooler is to cool the compressed hot gas from the compressor. The lower the inlet temperature of the air entering the engine, the higher the density, which means more air mass into the engine. It also means lower NOx emissions because of the lower temperature.

In the model the intercooler has been implemented as an extra volume between the compressor and the inlet manifold. The intercooler is assumed

to lower the temperature to a constant level. No heat transfer calculations were made.

Engine gas exchange

On the output side of the emptying and filling inlet manifold model there is the engine body with the pumping action of the pistons. The volume flow into the engine is based on volumetric efficiency, engine displacement and engine speed, see Equation 4.3, where ω is the engine speed, η_v is the volumetric efficiency which comes from measured data, and V_{engine} the engine displacement.

$$\dot{V}(\omega, \eta_v) = \eta_v \frac{V_{engine} * \omega}{4\pi} \quad (4.3)$$

The density is determined with Equation 4.4, where the integrated mass of air in the manifold, $m_{manifold}$ from Equation 4.1 is used. $V_{manifold}$ is the volume of the inlet manifold.

$$\rho = \frac{m_{manifold}}{V_{manifold}} \quad (4.4)$$

When the density is known the volume flow can be re-calculated into mass flow, see Equation 4.5.

$$\dot{m}_{engine} = \rho \dot{V}(\omega, \eta_v) \quad (4.5)$$

The volumetric efficiency is not 100%. It varies with load and engine speed. The main reasons are:

- The pressure ratio over the engine, inlet manifold pressure to exhaust manifold pressure
- Residual gases
- Tuning phenomena

In Figure 4.1, the volumetric efficiency can be seen as function of engine load, BMEP, and speed.

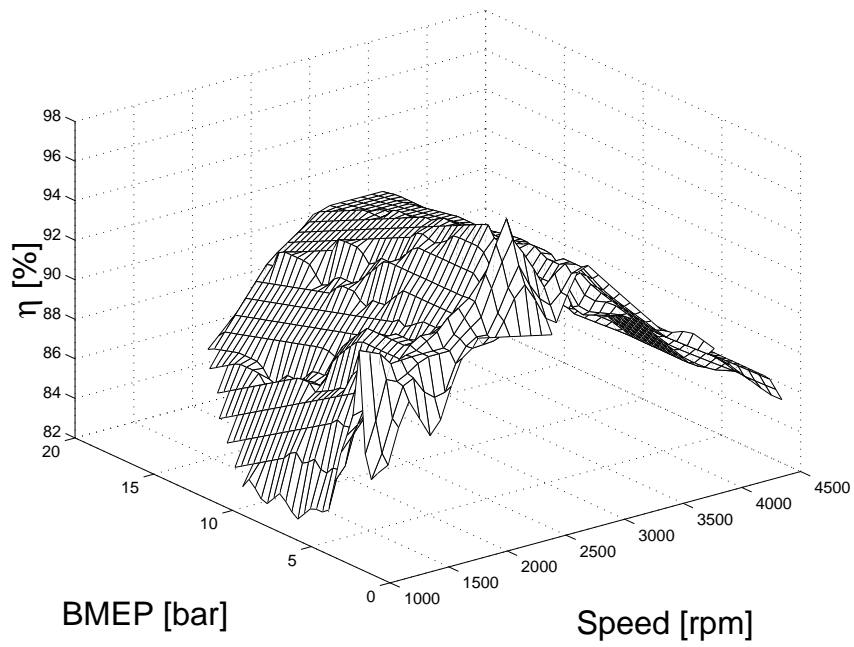


Figure 4.1 Volumetric efficiency vs Speed and BMEP. Data from a 2.5 liter passenger car Diesel engine.

The turbocharger

One of the most influential components of the Diesel engine is the turbocharger. It uses exhaust energy to supercharge the engine. This increases the output power by allowing more fuel to be injected.

The transient responsiveness of the Diesel engine is to a great extent given by the ability of the turbocharger to deliver sufficient air so that the λ isn't too low. If the λ is too low, large amount of soot will be formed. When doing a fast transient, the maximum load change is dependent on how fast the turbocharger is able to change its rotational speed.

The turbocharger performance in the model is given as tabled data. Here it has been chosen to use tables to describe the turbocharger, as opposed to using a mathematical model.

The following look-up tables are used:

- CF = Compressor Flow (corrected speed, corrected mass flow)
- CE = Compressor Efficiency (pressure ratio, corrected mass flow)
- TF = Turbine Flow (pressure ratio)
- TE = Turbine Efficiency (pressure ratio)

The compressor

The characteristics of a turbo-compressor can be seen in Figure 4.2. This figure shows the influence of the mass flow on pressure ratio and efficiency.

The compressor speed is normalized according to Equation 4.6, where ω^* is the corrected speed in the figure and ω_{real} is the real speed. T_{norm} is the normalization temperature which is compared to T which is the actual gas temperature.

$$\omega^* = \frac{\omega_{real}}{\sqrt{\frac{T}{T_{norm}}}} \quad (4.6)$$

The mass flow is corrected according to Equation 4.7, where \dot{m}^* is the corrected mass flow as seen in the figure. \dot{m}_{real} is the actual mass flow. P_{1c} is the pressure before the compressor and P_{norm} is a normalization pressure from the original mapping of the compressor.

$$\dot{m}^* = \frac{\dot{m}_{real} P_{1c}}{P_{norm}} \sqrt{\frac{T}{T_{norm}}} \quad (4.7)$$

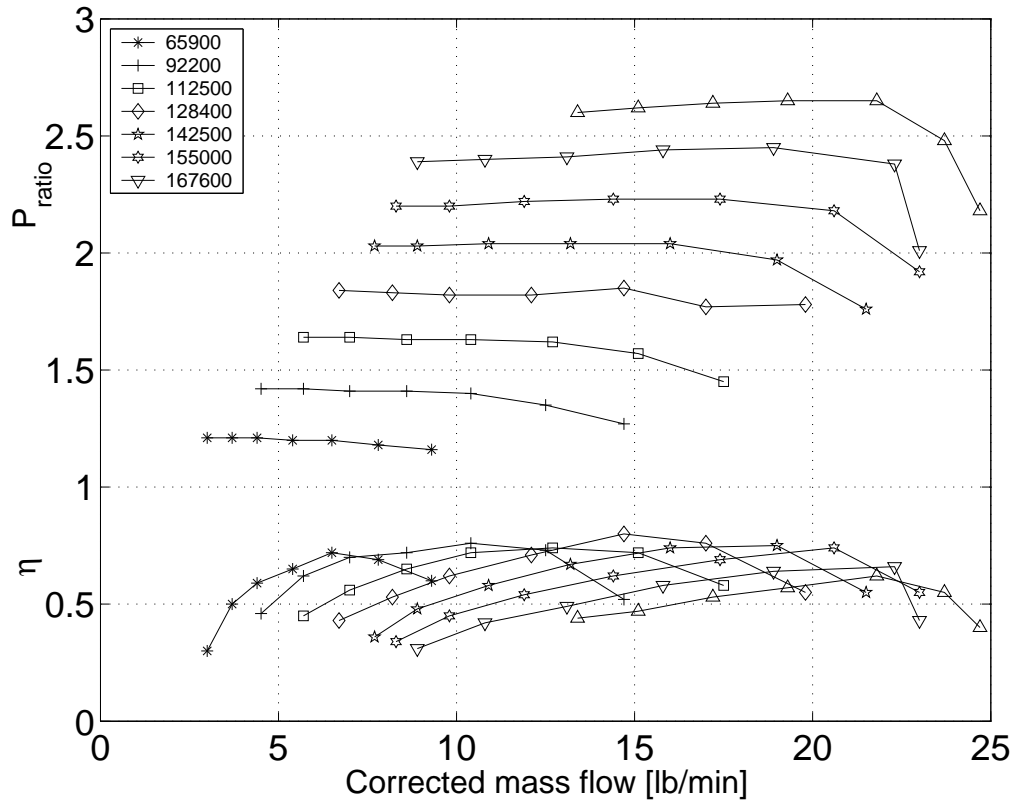


Figure 4.2 Diesel engine turbocharger compressor diagram.

When dealing with this kind of simulation it is best to get the mass flow from a given pressure ratio, since there will be a given pressure in the inlet manifold. But as can be seen in Figure 4.2, it is very difficult to do this, since a small deviation in pressure ratio results in a large deviation in mass flow.

A more stable solution is obtained if the mass flow rate is given and the pressure ratio is calculated. The mass flow is given by the use of a virtual area restriction that acts over the compressor. The main idea is an analogy of electric potential over a resistance.

The potential over a resistance of given by Equation 4.8, where U is the potential, R is the resistance and I is the current. The analogy is R to area restriction, I to mass flow and U to pressure.

$$U = (R I) \quad (4.8)$$

This analogy is used to get a more stable solution around the compressor. The original idea came from Reference [10], where an intercooler was used to tell the mass flow. In this model a virtual area restriction is used

after the compressor. The pressure ratio over this restriction gives the mass flow through the compressor.

Equation 4.9 is used for calculating the torque of the compressor, where M_{comp} is the compressor torque. \dot{m}_{comp} is the mass flow through the compressor. T_{bc} is the temperature before the turbine and c_p the constant pressure specific heat. P_{c1} is the pressure before and P_{c2} after the compressor. The pressure ratio is based on total pressures. κ is the ratio of specific heats. ω is the rotational speed and η_{comp} the compressor efficiency.

$$M_{comp} = \frac{\dot{m}_{comp} T_{bc} c_p \left(\frac{P_{c2}}{P_{c1}} \right)^{\left(\frac{\kappa-1}{\kappa} - 1 \right)}}{\omega \eta_{comp}} \quad (4.9)$$

The turbine

The influence of the turbine shaft speed on mass flow rate and pressure ratio is very low. Hence it is excluded from the calculation, where the only pressure ratio is used to give the mass flow and efficiency. Figure 4.3 shows the performance of a passenger car sized turbocharger turbine.

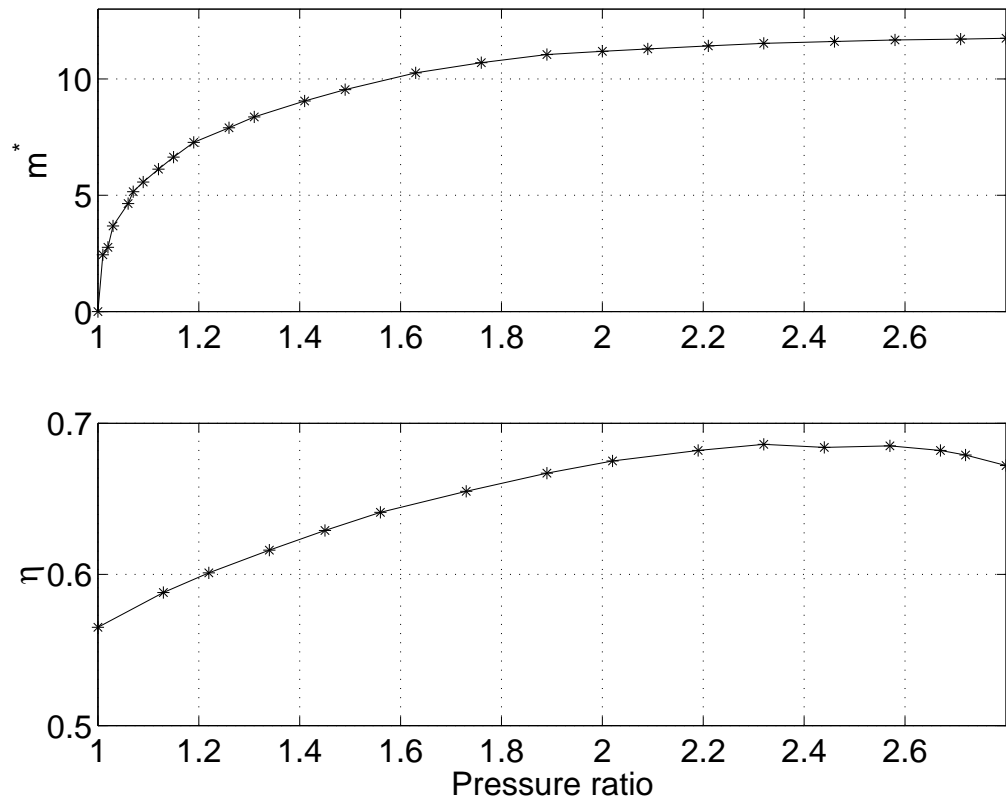


Figure 4.3 Diesel engine turbocharger turbine characteristics.

The upper graph shows mass flow as a function of pressure ratio. The mass flow rate in the figure is the mass flow parameter. This equation comes from the turbine manufacturer, see Equation 4.10, where \dot{m}^{**} is the mass flow parameter. \dot{m}_{turb} is the actual mass flow through the turbine. T_{exh} is the exhaust gas temperature and P_{exh} is the exhaust pressure.

The lower graph shows turbine efficiency as a function of pressure ratio.

$$\dot{m}^{**} = \dot{m}_{turb} \frac{\sqrt{T_{exh}}}{P_{exh}} \quad (4.10)$$

The produced torque by the turbine is calculated through Equation 4.11, where M_{turb} is the turbine torque, \dot{m}_{turb} mass flow through the turbine, T_{exh} exhaust temperature. c_p is the specific heat of the gas, P_{t1} is before and P_{t2} is after the turbine; κ is the ratio of specific heats and ω is the rotational speed of the turbine.

$$M_{turb} = \frac{\dot{m}_{turb} T_{exh} c_p (1 - (\frac{P_{t2}}{P_{t1}})^{\frac{\kappa-1}{\kappa}}) \eta_{turb}}{\omega} \quad (4.11)$$

Turbocharger speed

Equation 4.12 shows the dynamic equation used for the turbocharger, where J_{turbo} is the inertia, M_{turb} the turbine torque from Equation 4.11 and M_{comp} the compressor torque from Equation 4.9.

$$\frac{d\omega}{dt} = \left(\frac{M_{turb} - M_{comp}}{J_{turbo}} \right) \quad (4.12)$$

4.2 EGR

EGR is used to lower NOx emissions by diluting the inlet air with inert gas which lowers the combustion temperature.

In this model EGR is replacing part of the the air that goes into the cylinder.

The EGR flow is driven by the pressure difference between the inlet and exhaust manifolds. By putting a valve between those two manifolds it is possible to control the EGR rate.

As EGR will replace part of the air, the mixture will lower the maximum power of the engine. During transients the EGR flow is shut off to allow a faster response of the turbocharger, due to higher exhaust temperatures and increased mass flow.

There are two ways of defining the EGR rate, it can be based on the total mass, m_{total} , to the EGR mass, m_{EGR} , see Equation 4.13. But also on the total mass of air, m_{air} , to the mass of EGR, see Equation 4.14.

$$EGR_1 = \left(\frac{m_{EGR}}{m_{total}} \right) \quad (4.13)$$

$$EGR_2 = \left(\frac{m_{EGR}}{m_{air}} \right) \quad (4.14)$$

Figure 4.4 shows the EGR *landscape* of a passenger car Diesel engine. There are lots of EGR in the low speed and low load area, to keep the NOx emissions low, especially during drive cycle tests. In Figure 4.4, the definition of EGR is the one defined in Equation 4.13.

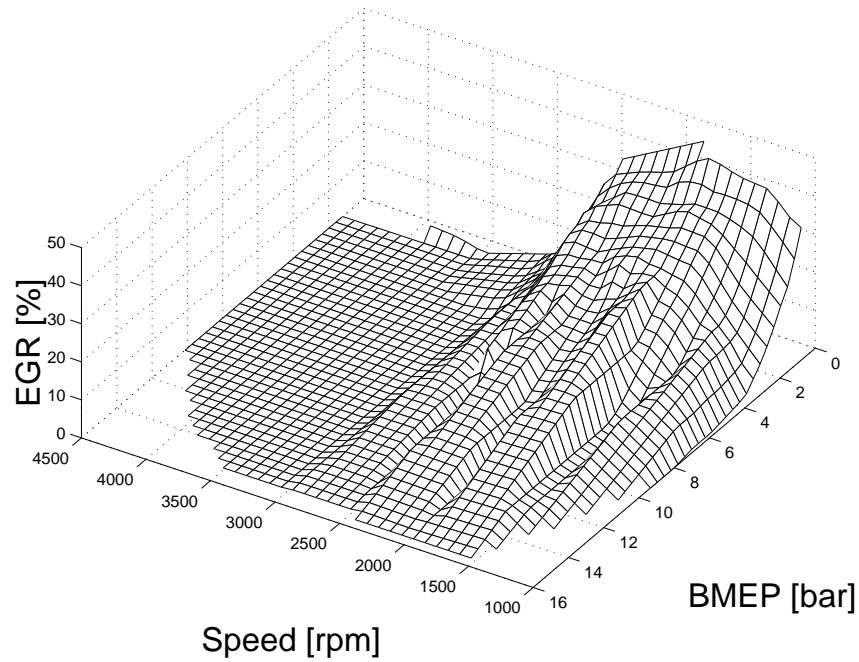


Figure 4.4 Diesel engine EGR rate at different loads.

Exhaust temperature characteristics

The exhaust gas temperature is the most important parameter for both catalyst performance and for the exhaust turbine. The main objective in the model has been to give the correct exhaust temperature for the turbocharger.

The exhaust temperature is determined by a simple empirical linear function based on λ . It is also dependent on engine speed, because of the lower per cycle total heat loss at high engine speeds.

$$T_{exhaust} = f(\lambda, \omega) \quad (4.15)$$

Torque build-up in Diesel engines

The torque build-up in a Diesel engine is more complex than that in a SI-engine. The torque is, as in the SI-engine, a function of engine speed, fuel flow and air flow. A SI-engine operates at stoichiometric conditions, but in the Diesel engine λ varies with load.

In a quasi-stationary simulation there is no additional torque build-up when running transient, because of the time it takes for the turbocharger to reach steady state. This is because there are no internal states to be changed.

When the engine changes its load point and the turbocharger is not at steady state, the engine will operate outside the defined space of stationary measurements. The question is then: How is the torque calculated when the engine isn't operating at steady state?

The proposed solution here is to base the torque on a numeric table that gives the engine torque at defined conditions, in this case where $\lambda = 1$. The engine torque at $\lambda = 1$ is divided by the actual λ value, see Equation 4.16, where \dot{m}_{air} is mass flow air and ω is the engine speed.

$$M_{engine\ CI} = \frac{M(\dot{m}_{air}, \omega)_{\lambda=1}}{\lambda} \quad (4.16)$$

A numerical table is made to correspond with the real engine. Figure 4.5 shows the λ landscape for a Diesel engine.

Figure 4.6 shows \dot{m}_{fuel} landscape for a passenger car Diesel engine.

The λ -value varies from 1.2 to 7. During transients it can vary even more.

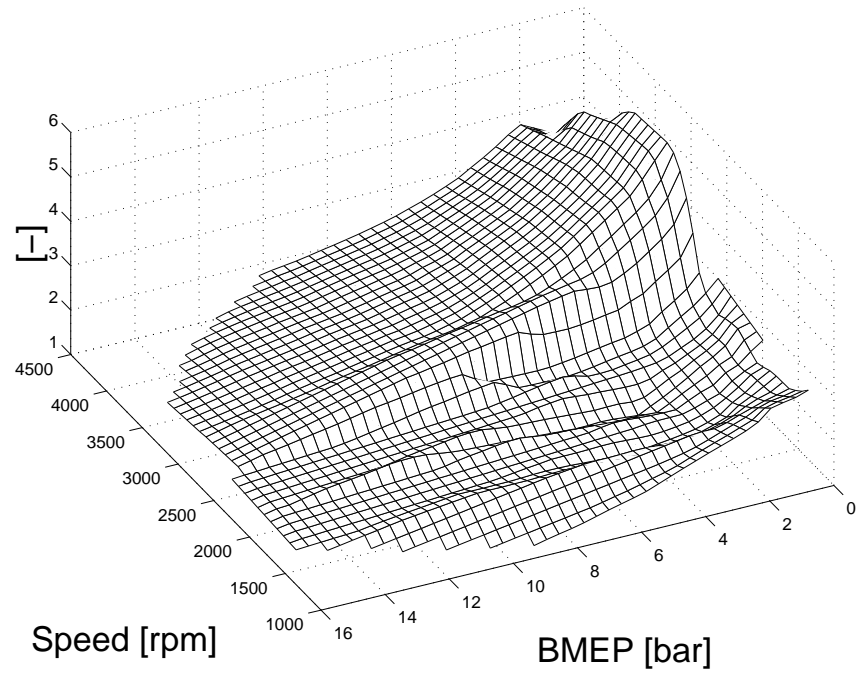


Figure 4.5 Diesel engine λ landscape.

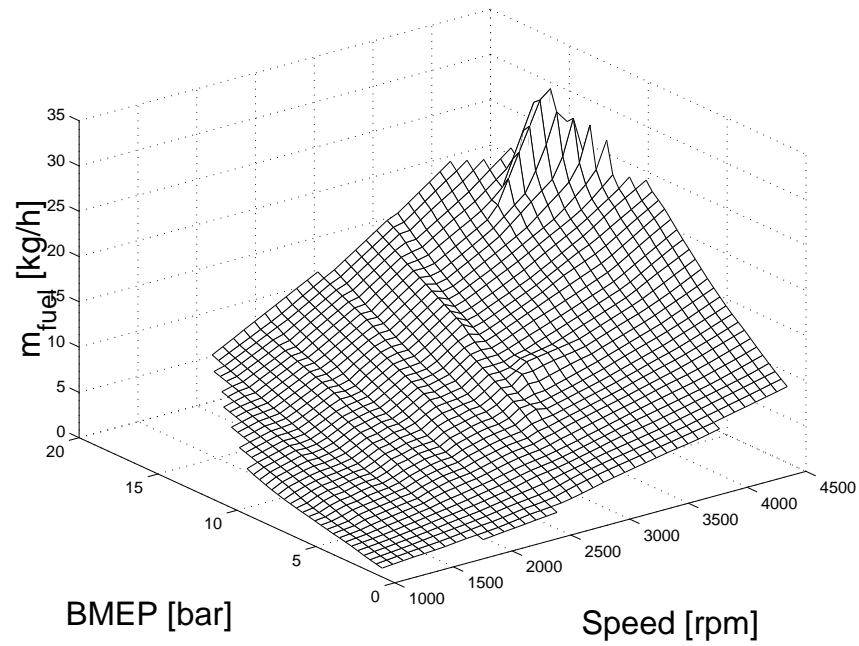


Figure 4.6 Diesel fuel flow landscape.

4.3 Diesel engine implementation in Simulink

The following section deals with how the implementation was done with regard to theory.

The following section is a tour of the main circuit of the Diesel engine model. The following table shows only the external information flow in the model, the inner workings can be found in Appendix C on page 69, where most Simulink boxes are presented. Appendix B has a small tutorial for those of you that does not have prior knowledge of Simulink.

1. The turbocharger. It is treated as in section 4.1 on page 18. Inputs to the module are:

- (a) P_{bt} , Pressure before the turbine
- (b) \dot{m}_{comp} , Mass air flow through the compressor
- (c) T_{bt} , Temperature before turbine
- (d) P_{at} , Pressure after the turbine
- (e) P_{bc} , Pressure before the compressor
- (f) T_{bc} , Temperature before the compressor

The output signals are:

- (a) $\dot{m}_{turbine}$, mass air flow through turbine
- (b) P_{ac} , Pressure after the compressor
- (c) ω_{turbo} , Turbo shaft speed

2. The intercooler. The purpose of this is to cool the hot inlet air from the compressor, thus increasing the density of the air. It serves as an extra manifold prior to the main inlet manifold. The intercooler in the model lowers the temperature to a constant level. Input is:

- (a) $\dot{m}_{ic\ in}$, Mass flow in to intercooler

Output is:

- (a) $\dot{m}_{ic\ out}$, $\dot{m}_{manifold}$, Mass flow out of intercooler

The mass flow going out of the intercooler is determined by variable area that is implemented as a throttle body, Section 5.1, on page 40.

3. The inlet manifold. Implemented as in Chapter 4.1 on page 15.

- (a) \dot{m}_{in} , Mass flow rate into the manifold
- (b) \dot{m}_{out} , Mass flow rate out of the manifold

The outputs are:

- (a) $\rho_{manifold}$, Density in the manifold
- (b) $P_{manifold}$, Pressure in the manifold

4. Pumping action of the pistons. Determines the amount of air going into the engine body. Here the engine is assumed to consume a particular amount of volume flow. This volume flow is also depending on volumetric efficiency. See also Chapter 4.1 on page 16.

- (a) $\rho_{manifold}$. Density in the manifold
- (b) ω_{engine} , Engine speed

The output is:

- (a) $\dot{m}_{out \text{ of manifold}}$ which is the same as \dot{m}_{engine}

5. Engine body cycle delay. This is the time where cycle gases are part of the working cycle. For example, if there is a sudden increase in air pressure it will take one engine cycle before it reaches the exhaust manifold and the turbine. It is implemented as a variable time delay.

- (a) \dot{m}_{engine}
- (b) ω_{engine} . Engine speed

The output is:

- (a) $\dot{m}_{exhaust}$.

6. The exhaust manifold. Inputs are:

- (a) $\dot{m}_{turbine}$, mass flow through the turbine
- (b) $\dot{m}_{exhaust}$, mass flow into the exhaust manifold
- (c) $T_{exhaust}$, exhaust temperature before the turbine

The output is:

- (a) $P_{exhaust \text{ manifold}}$

The EGR implementation

The EGR circuit consists of two modules, an EGR valve and an EGR controller. The EGR valve is simply a throttle valve which is the same as described in section 5.1, on page 40. The EGR drive force is the higher pressure in the exhaust manifold compared to that at the inlet.

The EGR controller is implemented as a PI-controller, where the set value from Figure 4.4 on page 22 is compared to the engine delivered EGR rate.

4.4 Diesel exhaust emission transient correction

This section has some discussions regarding how to compensate for the exhaust emissions when the engine doesn't run at steady state.

The emissions from the engine are obtained from measured data.

Now, what are the emission levels from an engine in a non-stationary operating point?

The approach is to take emission data from static engine measurements, together with the understanding of how engine characteristics affects the formation of emissions when the engine runs outside its steady state regime. This is done by trying to find easily identifiable trends when looking at steady state exhaust emissions.

By plotting the emissions as functions of λ and emission index $[g/kg]$, it is possible to identify how the exhaust emissions vary with different transients. The relationships are explained by logic reasoning. These are then implemented into mathematical expressions intended to be parts of the model.

EGR

Another important factor to take into consideration is the use of EGR, for example when the engine is subjected to a load change, where EGR flow can differ from the stationary case. In order to get the fastest acceleration on the turbocharger the EGR rate is decreased. When the engine runs at steady state operation and at low load, the engine has a large amount of EGR in order to keep NOx emissions low.

Effect on CO

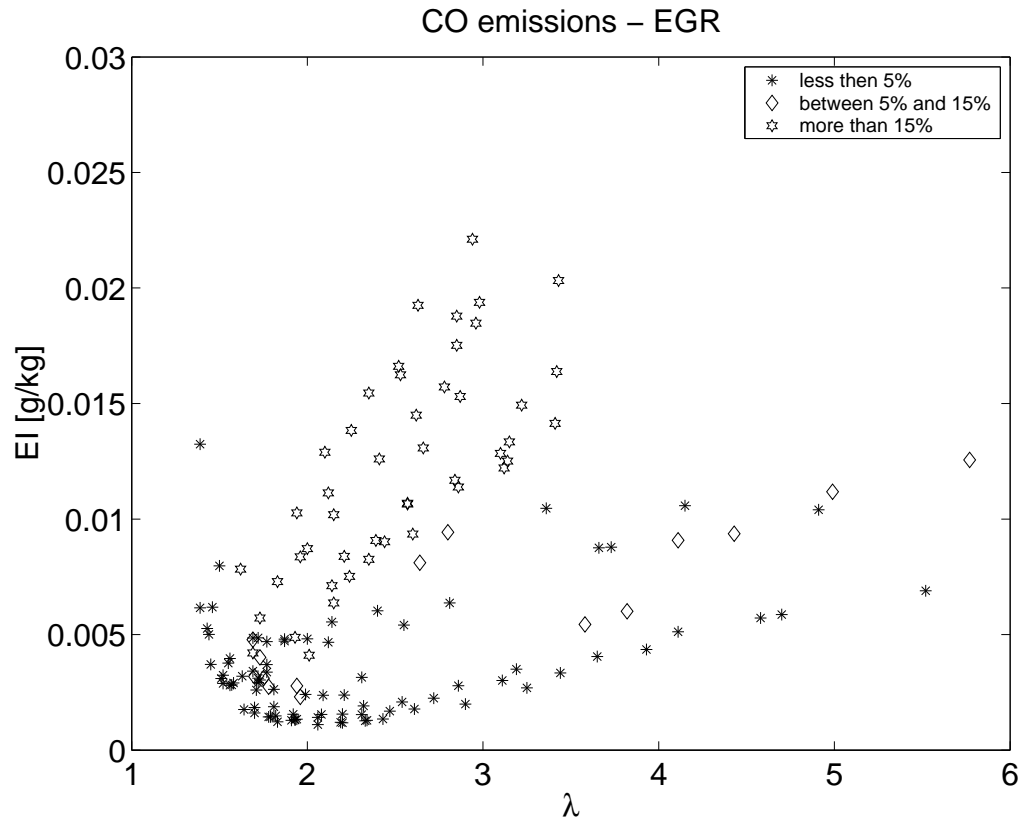


Figure 4.7 Steady state emission of CO versus λ at different EGR levels.

Figure 4.7 shows how carbon monoxide is correlated to λ . Carbon monoxide emissions tend to increase at higher λ . This is caused by lower temperature which results in poor oxidation.

The figure shows how emission index of CO goes up as λ is raised. It also shows how emission index increases as λ goes below 1.5. This says that a low λ -value will cause the CO to be high. As the EGR rate increases, higher λ will cause the EI to increase.

Effect on NOx

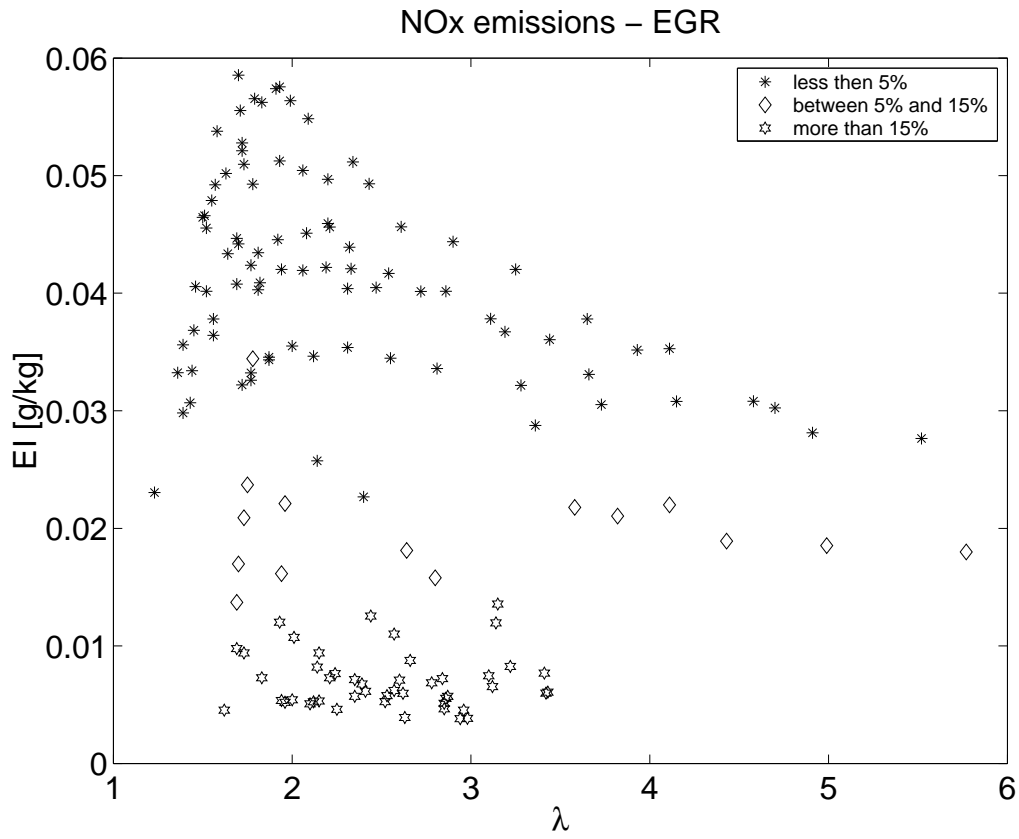


Figure 4.8 Correlation of NOx with EGR.

Figure 4.8 shows how nitrogen oxide is correlated to λ . The effect of EGR on NOx is that it will reduce the combustion temperature and hence reduce the NOx formation. Also an increase in EGR lowers the NOx formation due to lower oxygen concentration.

The figure shows that the higher rate of EGR lowers the NOx emission index.

Effect on HC

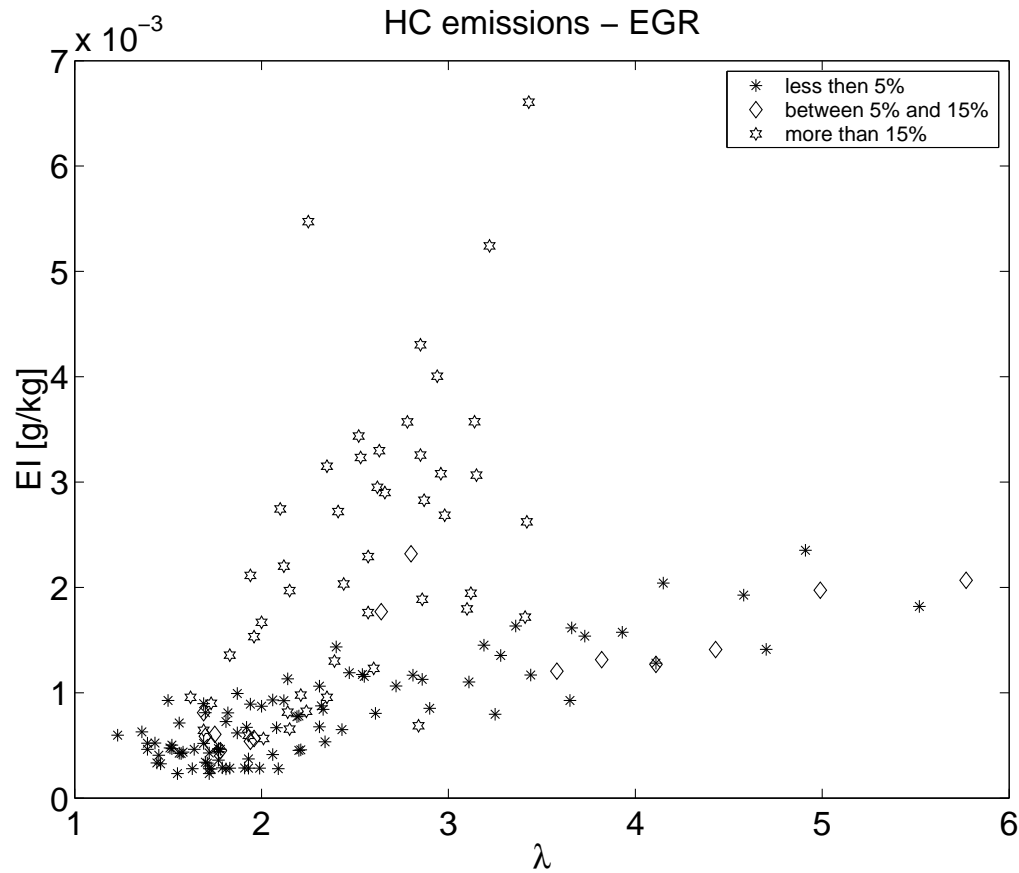


Figure 4.9 Correlation of HC with EGR.

Figure 4.9 shows hydrocarbon emission index correlated against λ . The basic causes of hydrocarbon emissions are over-leaning and fuel droplets from the sac of the injector. At idle the engine operates under very lean conditions. HC emissions are increased when running at high engine speeds when burn time is short, at high speeds and at low load there is a very lean mixture.

The figure shows that high λ and high EGR rates increases the HC emission index.

Effect on Particles

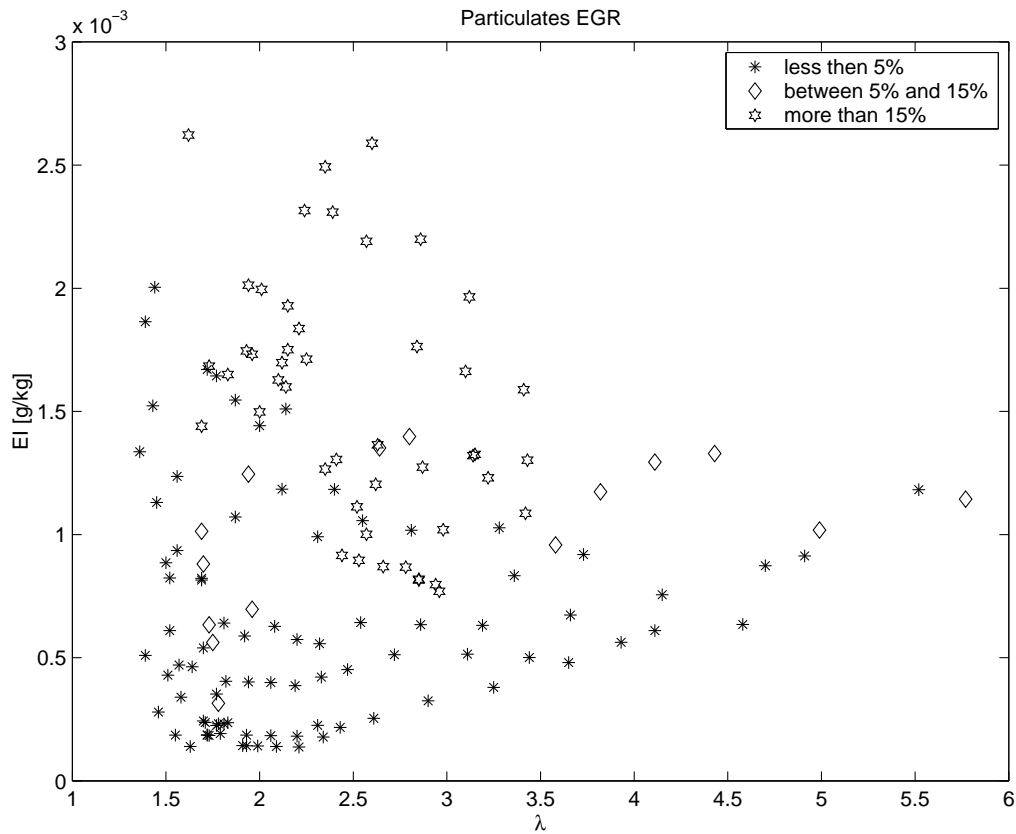


Figure 4.10 Correlation of particulates with EGR.

Particles are formed during the early diffusive combustion and oxidized during the latter part of the combustion phase, after the injection has ended.

As can be seen in Figure 4.10 the trend is that high EGR and low λ cause a high emission index of particulates. By looking at points with low amount of EGR, it is possible to see a trend similar to that of CO.

4.5 Simulation results

Here follows a demonstration series of the capabilities of the model.

Load step test

The first example to be presented is a load change at constant engine speed. See Figure 4.11.

According to number the plots contain the following.

1. M_{input} , The set engine torque
2. M_{engine} , The engine output torque
3. λ , air fuel eqv. ratio
4. $T_{exhaust}$, Engine Exhaust Temperature
5. $\omega_{turbine}$, Turbine speed [rad/s].

The requested load is added quite suddenly, and still the engine response is quite fast. Note how the exhaust temperature decreases as λ increases while the exhaust turbine picks up speed.

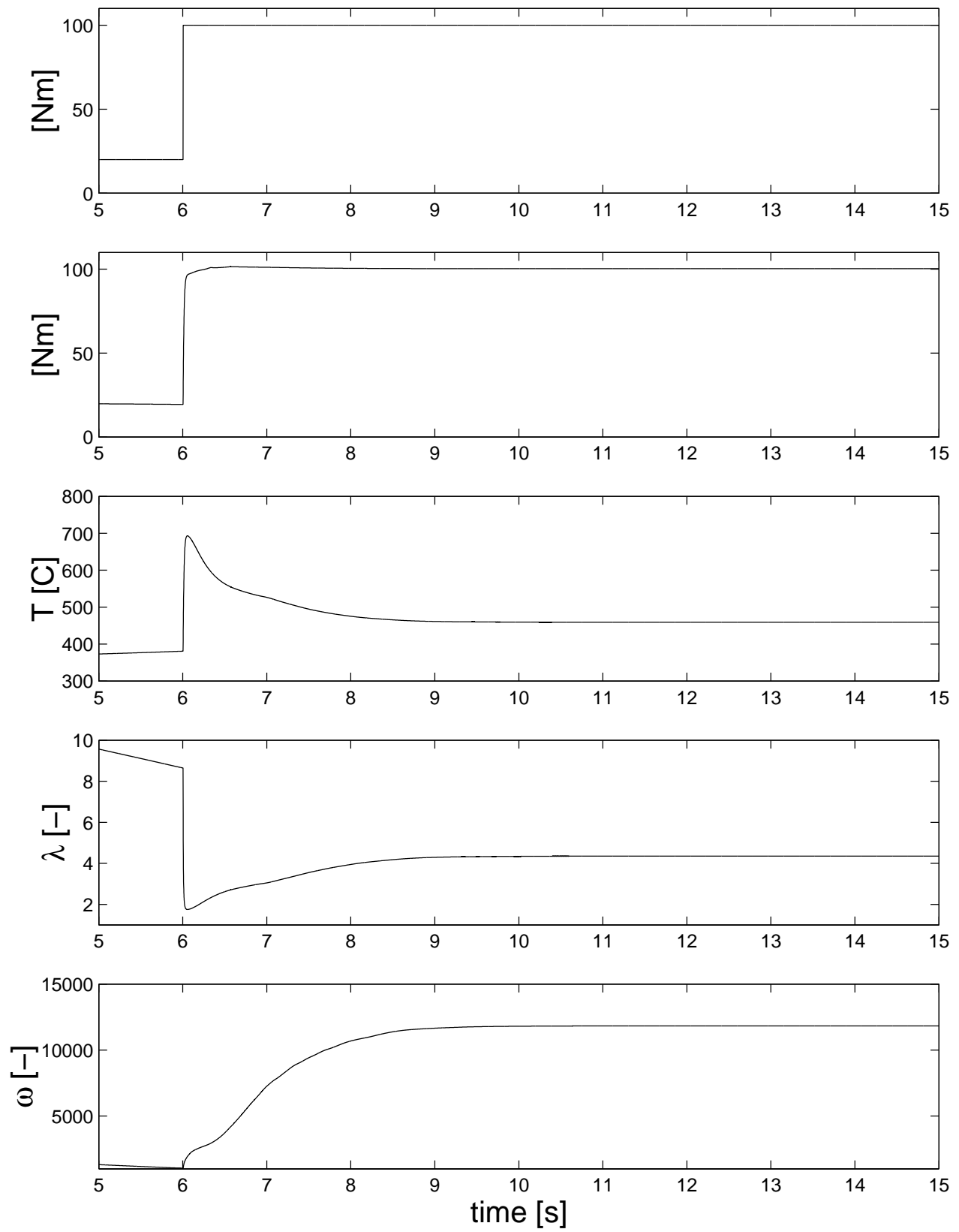


Figure 4.11 Diesel engine model with a step load change.

Heavy step load change

Figure 4.12 shows a heavy load change. To avoid excessive amounts of soot the model is equipped with a function to limit the injected fuel to avoid soot until the turbocharger is able to provide sufficient amount of air. This function limits the exhaust temperature as well as the λ -value.

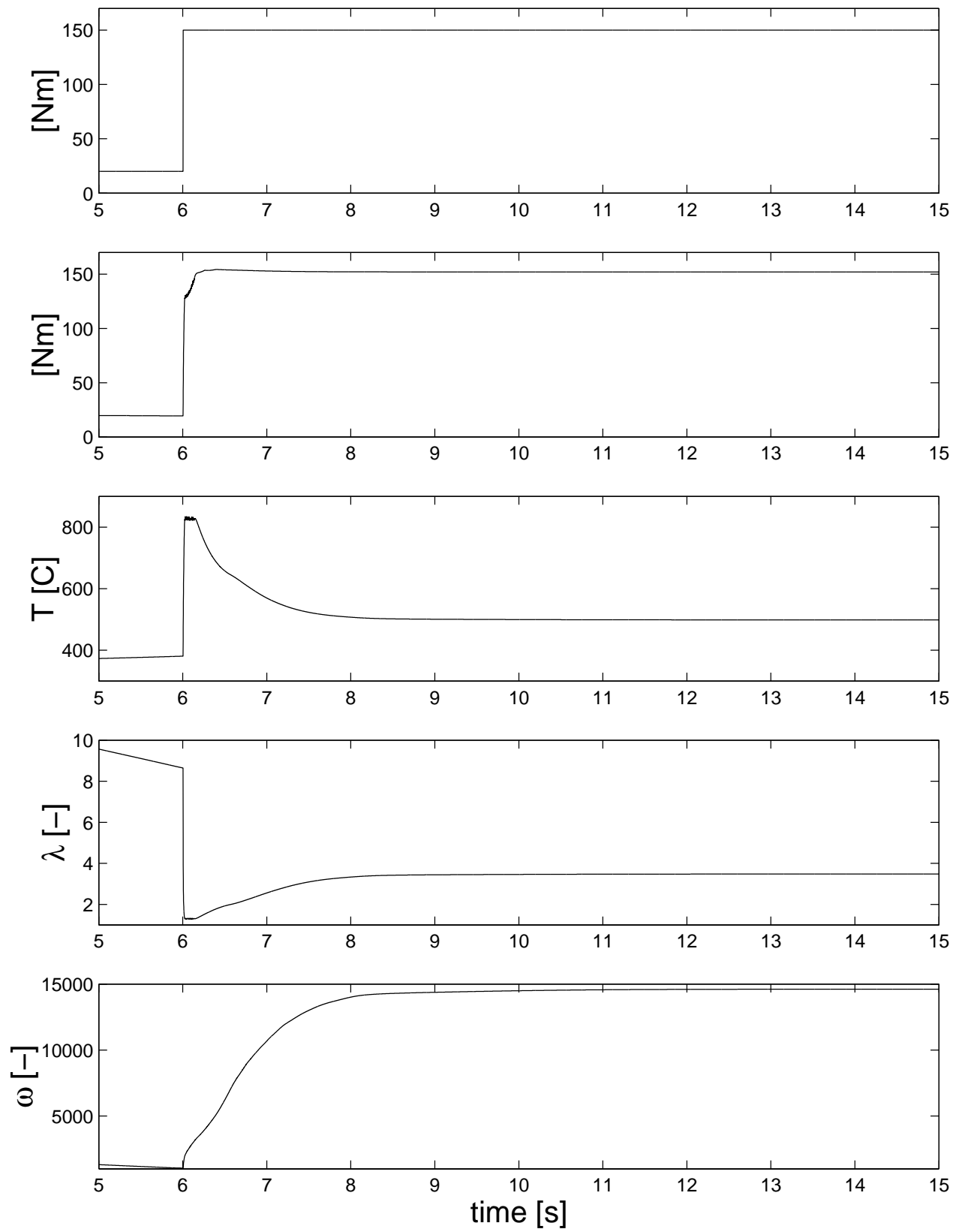


Figure 4.12 Diesel engine model with a heavy step load change.

Load ramp test

Figure 4.13 shows a ramp test. Here the turbocharger, with good margin, is able to provide sufficient amount of air without having the risk for soot formation.

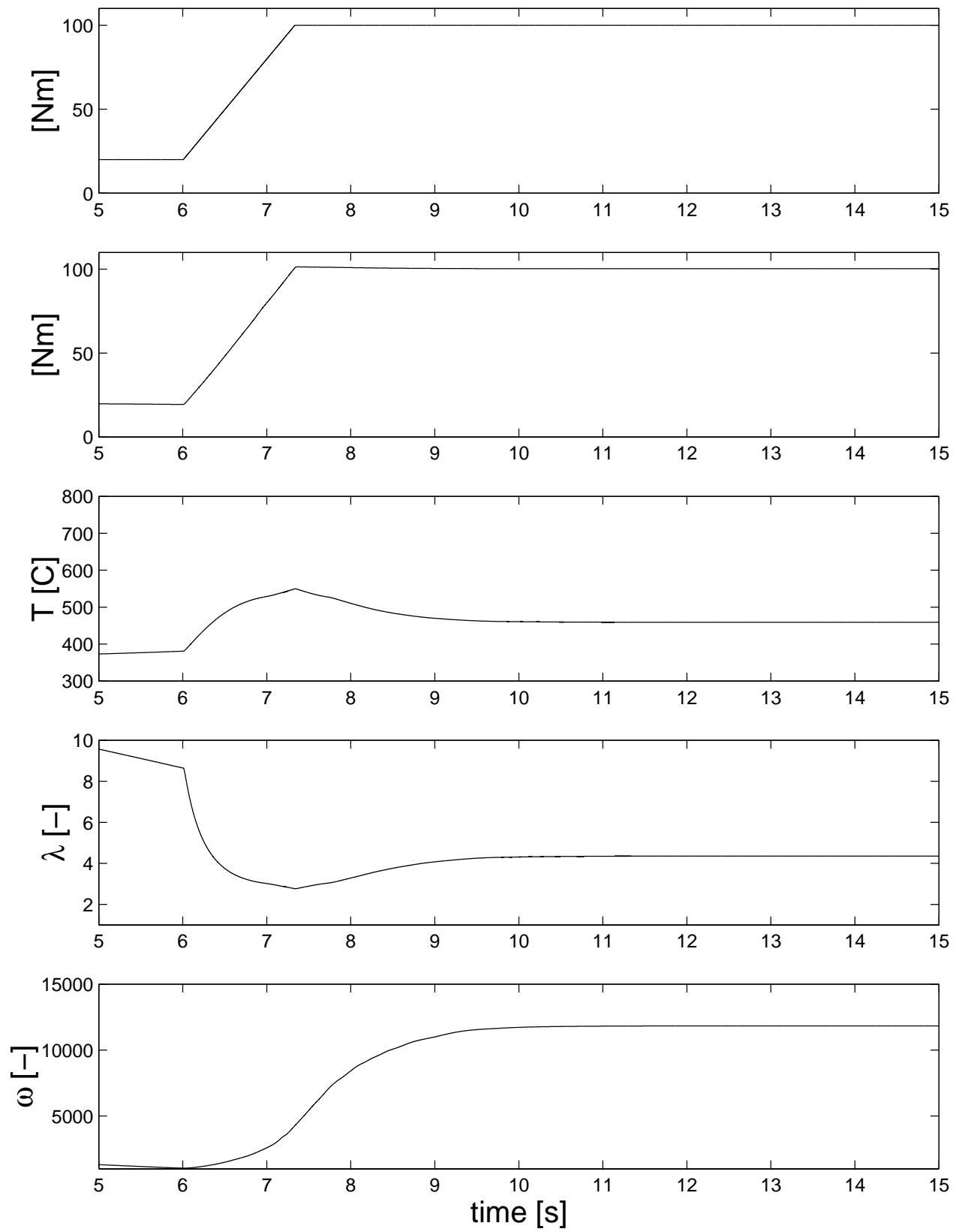


Figure 4.13 Diesel engine model ramp load change.

5

Modeling SI-Engines for Hybrid Vehicles

This chapter explains and discusses the model for an SI engine. The model is thought to be used in the study of vehicle propulsion, and was mainly developed for hybrid vehicle studies.

The model tries to fill the space between the simple quasi stationary model and the more complicated and time consuming cycle resolved model. The main goal was to develop a model that could give an answer to how transients affect emissions. A quasi stationary engine will not show any signs of being subjected to transients. A cycle resolved model would do this but at the cost of a more complex model and longer simulation times.

The basis for this model is data collected during stationary measurements. Required data are torque, air flow, fuel flow and emissions.

The simulation model can be categorized into three major parts:

- The air flow model. This part consists of the throttle, inlet manifold, engine body (pumping action of the pistons) and exhaust manifold.
- The fuel flow model. This part consists of fuel injection and a wall wetting model.
- The fuel control model (closed loop λ -control) where λ is detected with a λ -sensor that has a time constant.

5.1 The air flow model

The goal of this part of the model is to calculate the mass flows through the engine. This is the result of three parts:

- The throttle, which controls the amount of air that is let into the inlet manifold. Mass flow through the throttle is governed by the difference pressure and throttle area.
- The engine pumping action. To determine the mass flow into the cylinders, the density in the inlet manifold has to be known.
- The inlet manifold, which contains the main state, air mass in the manifold. When the air mass is known, both density and pressure difference for the throttle is known.

The throttle

The throttle controls the amount of air that is let into the inlet manifold. Equations that describe a compressible gas flows through an area restriction are used. Whenever there is a pressure difference, there will be a flow over the throttle governed by the property of the gas, the area restriction and pressure ratio, see Equation 5.3.

There are two equations describing the mass flow. One is used for critical pressure ratio, and the other is used for sub critical pressure ratio. A critical pressure ratio means that the velocity in the throttle is sonic.

With the ideal gas law, critical pressure ratio is given by Equation 5.1, where Π is the pressure ratio and κ is the ratio of specific heats.

$$\Pi = \left(\frac{2}{\kappa + 1} \right)^{\frac{\kappa}{\kappa - 1}} \quad (5.1)$$

The κ value for air is 1.4 and this gives a critical pressure ratio of 0.5283. When the pressure ratio is critical, Equation 5.2 is used, otherwise Equation 5.3.

$$\dot{m}_{th} = \frac{C_D A_{th} P_a}{\sqrt{RT}} \kappa^{1/2} \left(\frac{2}{\kappa + 1} \right)^{\frac{\kappa + 1}{2(\kappa - 1)}} \quad (5.2)$$

$$\dot{m}_{th} = \frac{C_D A_{th} P_a}{\sqrt{RT}} \left(\frac{P_m}{P_a} \right)^{\frac{1}{\kappa}} \sqrt{\frac{2\kappa}{\kappa - 1} \left[1 - \left(\frac{P_m}{P_a} \right)^{\frac{\kappa - 1}{\kappa}} \right]} \quad (5.3)$$

Where:

C_D	[-]	discharge coefficient
κ	[-]	ratio of specific heats
R	[kJ/(kg * K)]	gas constant
T	[K]	gas temperature
A_{th}	[m ²]	throttle area
Π	[-]	pressure ratio

Pumping action

The engine body is looked upon as a displacement pump with a volume flow as a function of engine speed(ω) and volumetric efficiency (η_v), see Equation 5.4. The air mass flow entering the engine body is determined by the density (ρ) in the inlet manifold, Equation 5.5.

$$\dot{V} = \eta_v \frac{V_{engine} * \omega}{4\pi} \quad (5.4)$$

$$\dot{m}_{engine} = \rho * \dot{V}(\omega) \quad (5.5)$$

Where:

V_{engine}	[m ³]	engine displacement
ω	[rad/s]	engine speed
η_v	[-]	volumetric efficiency
\dot{V}	[m ³ /s]	volume flow through the engine
ρ	[kg/m ³]	density
\dot{m}_{engine}	[kg/s]	mass flow through the engine

The inlet manifold

When air is drawn into the engine, Equation 5.5, a balance is formed by the air going into the engine and the air being sucked into the manifold via the throttle, Equation 5.6. This couples the air flow through the throttle to the pressure in the manifold, while density in the manifold determines how much air is drawn into the engine.

$$\dot{m}_{manifold} = \dot{m}_{throttle} - \dot{m}_{engine} \quad (5.6)$$

The equation of state yields Equation 5.7 and 5.8.

$$\rho = \frac{m_{inlet\ manifold}}{V_{manifold}} \quad (5.7)$$

$$P_{manifold} = \frac{m_{inlet\ manifold} R T}{V_{manifold}} \quad (5.8)$$

Where:

$\dot{m}_{manifold}$	$[kg/s]$	mass flow of air in the manifold
$\dot{m}_{throttle}$	$[kg/s]$	mass flow air to the manifold
\dot{m}_{engine}	$[kg/s]$	mass air flow to the engine
$m_{inlet\ manifold}$	$[kg]$	mass of air in the manifold
$V_{manifold}$	$[m^3]$	manifold volume
ρ	$[kg/m^3]$	density
$P_{manifold}$	$[Pa]$	pressure in manifold
R	$[kJ/(kg * K)]$	gas constant
T	$[K]$	temperature

Torque formation in SI engines

The air mass flow, \dot{m}_{engine} , from the inlet manifold combined with a stoichiometric air fuel ratio, will under stationary conditions give the output torque of the engine.

Figure 5.1 shows the connection between engine speed, torque and fuel flow.

If the table is turned over so that the parameters are engine speed and fuel flow which gives torque, then the torque formation from the air engine can be calculated.

Equation 5.9 gives the mass air flow m_{air} from the fuel flow \dot{m}_{fuel} and the stoichiometric relationship $(A/F)_s$.

$$\dot{m}_{air} = \dot{m}_{fuel} \cdot (A/F)_s \quad (5.9)$$

We now have an air flow table similar to Figure 5.1, but with air flow on the y-axis instead of on the z-axis, see Equation 5.10.

$$\dot{m}_{air} = f(M, \omega) \quad (5.10)$$

What is needed is a table where air mass flow (\dot{m}_{air} and engine speed ω give engine torque $M_{engine @(\lambda=1)}$ as in Equation 5.11.

$$M_{engine @(\lambda=1)} = f(\dot{m}_{air}, \omega) \quad (5.11)$$

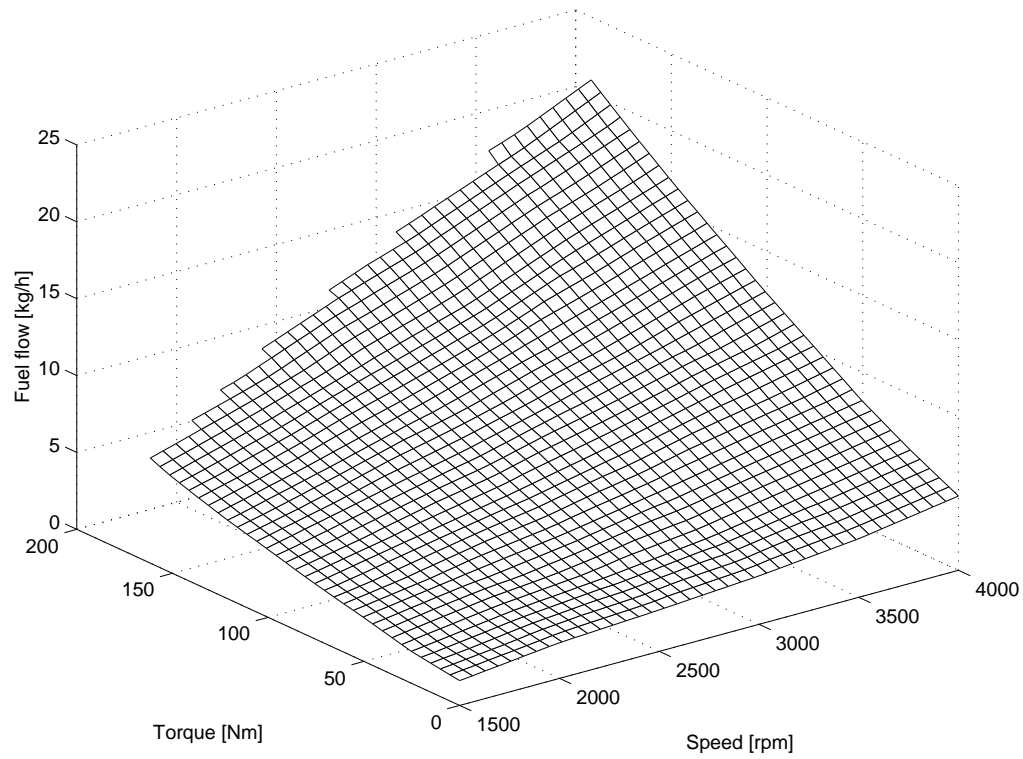


Figure 5.1 Fuel consumption.

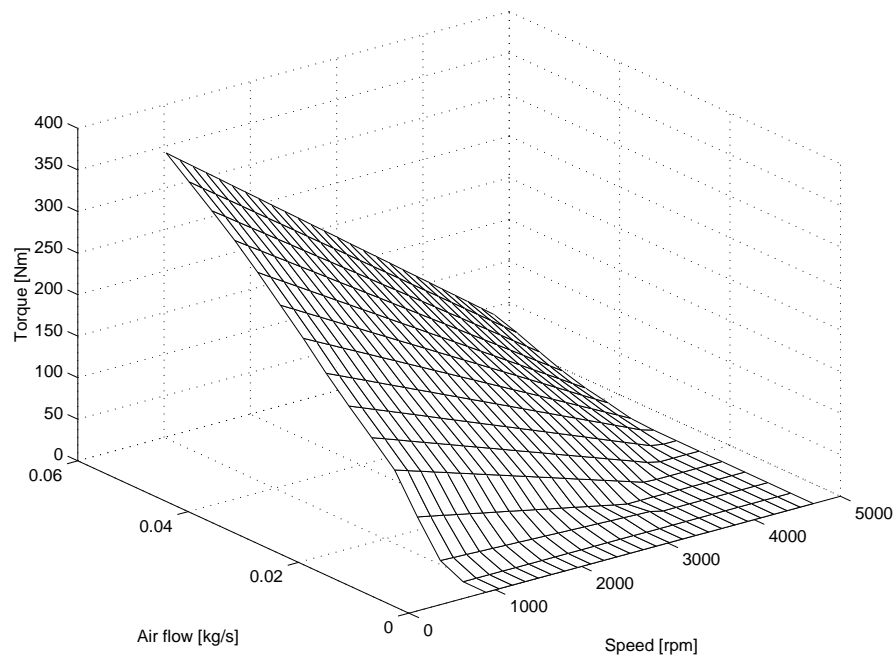


Figure 5.2 SI engine air map.

Figure 5.2 shows the resulting air map with the axis according to Equation 5.11.

Since the model calculates the λ in the engine, the torque from the air map is then corrected for this, see Figure 5.3. At λ -values just below 1 there is a small increase in the torque which is caused by better volumetric efficiency. As the λ -value is increased the torque is decreased because of reduced fuel flow: less fuel, less work. As λ approaches values near and above 1.5 a SI-engine usually begins to misfire. This explains the fast torque reduction as λ is increased.

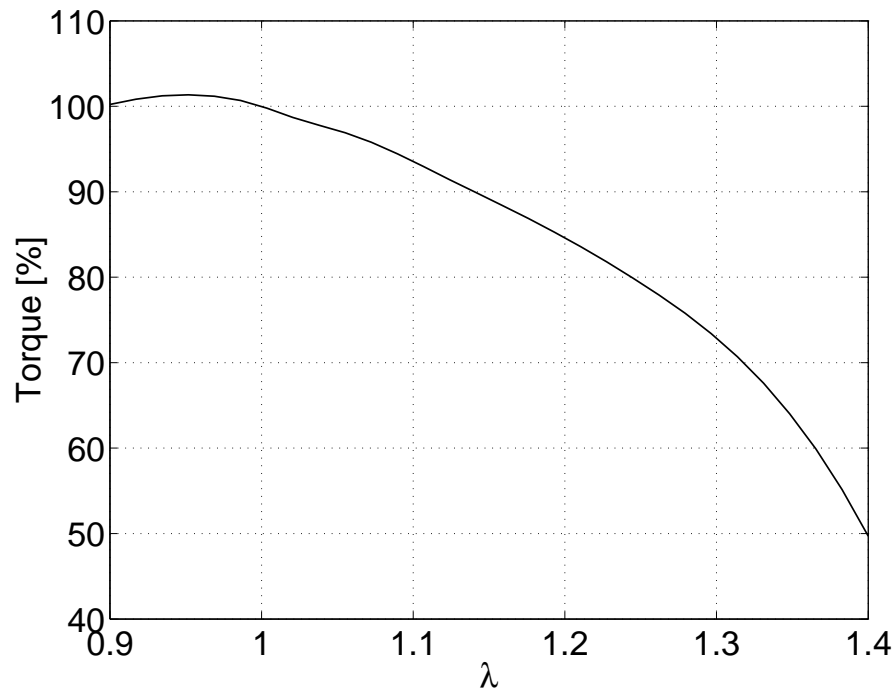


Figure 5.3 Torque compensation as function of λ .

5.2 The fuel supply

The instantaneous air flow at different operation points is calculated with the air model. In a real engine air flow information can be picked by a sensor before the throttle, or it can be calculated with the speed-density method. With this latter method the air flow is calculated from pressure and temperature in the manifold together with the knowledge of volumetric efficiency.

In the model, fuel flow is calculated from using air flow at two different points, either at the throttle for simulating a mass flow meter or at the inlet manifold outlet for simulating speed-density.

The closed loop λ control

In Equation 5.14, the term $f(\lambda_{meas})$ is the closed loop control of λ . It determines whether the λ_{meas} value is above or below 1. If the λ value is low it will ramp down the fuel flow until the value goes high, and vice versa. There is a limitation on the amplitude to prevent it from going too far.

Wall-wetting

In the ideal case fuel would go directly from the injector into the cylinder. However, part of the fuel that is injected into the port will stick to the walls. This is known as *wall wetting*. Wall wetting effects can also come from reverse flow which takes place during the early part of the intake stroke and during the valve overlap period. This causes the fuel that has been injected on the inlet valve to be thrown backwards into the manifold.

Wall wetting is influenced by several parameters.

- Geometrical: how much of the injected fuel that reaches its destination without being trapped on the inlet manifold wall.
- Inlet manifold surface, how well the fuel can be stored on the wall.
- Temperature at what rate the fuel is evaporated into the manifold bulk gas.
- Gas velocity in the inlet manifold. With higher engine speed the probability of fuel being drawn with the gas increases.

Tuning wall wetting factors

In the current model there are two factors that can be tuned in order to simulate reality.

The model used to describe the wall wetting originates from the PhD thesis, reference [11]. In that thesis, wall wetting effects are thoroughly investigated. Equation 5.12 describes how the fuel into the cylinder is a function of injected fuel $\dot{m}_{fuel\ injected}$, engine speed ω , inlet manifold pressure P_{inlet} , the wall wetting fuel mass m_{film} , and the time constant of the fuel film τ . The last term in the equation is a measure of fuel vaporization from the inlet manifold walls.

$$\dot{m}_{f\ engine} = f(\dot{m}_{fuel\ injected}, \omega, \dot{m}_{air}, P_{inlet}) + \frac{m_{film}}{\tau_{puddle}} \quad (5.12)$$

In paper [12], the use of different parameters for controlling wall wetting at different operating points is suggested. They use both least-square fittings and Kalman filtering methods. They had an extensive data base of transient tests run at different conditions.

Equation 5.13 shows the wall wetting fuel mass balance in the inlet manifold, where \dot{m}_{film} is the change in wall wetting fuel mass, $\dot{m}_{fuel\ injected}$ is the injected fuel and $\dot{m}_{fuel\ engine}$ is the fuel that ends up in the engine body.

$$\dot{m}_{film} = \dot{m}_{fuel\ injected} - \dot{m}_{fuel\ engine} \quad (5.13)$$

Fuel flow control

The principles and function of the computer-controlled fuel system in vehicles are complex, and their inner details are classified as *TOP SECRET* by the manufacturers. The behavior of the ECU changes throughout the production of the vehicle model, since the manufacturer keeps optimizing the design this makes it next to impossible to accurately model engine performance.

The current model receives its air flow information either from a simulated signal that comes from the throttle module, or one that comes from the inlet port using the speed-density method. This is easily changed by a simple rerouting in the Simulink model.

To determine the amount of fuel to be injected information regarding air flow, and in a closed loop system the real measured or calculated λ value, is required. In Equation 5.14 the L is the closed loop function described below. The Closed loop function L , means that the fuel flow is ramped rich and lean in the normal SI-engine fashion.

In Equation 5.15 λ_{meas} is a function of the time delay for the engine cycle, t_{engine} , the time delay from the plug flow in the exhaust manifold, $t_{exhaust}$, and finally from the characteristic time of the λ -sensor, τ_{sensor} .

$$\dot{m}_{fuel\ inj} = \dot{m}_{air} AFS + L(\lambda_{meas}) \quad (5.14)$$

$$\lambda_{meas} = f(\lambda_{real}, t_{engine}, t_{exhaust}, \tau_{sensor}) \quad (5.15)$$

Where:

$\dot{m}_{fuel\ inj}$	[kg/s]	fuel to be injected
\dot{m}_{air}	[kg/s]	air going into the engine
AFS	[—]	stoichiometric air fuel ratio
λ_{real}	[—]	real air fuel ratio in the engine
λ_{meas}	[—]	"measured" air fuel ratio
t_{engine}	[s]	time delay through the engine
$t_{exhaust}$	[s]	time delay through the manifold
τ_{sensor}	[s]	time constant of the λ -sensor

5.3 Implementation of the λ time delays

The global lambda in the engine comes from the ratio of air mass flow into the engine and mass flow of fuel that enters the engine. In order to implement closed loop λ control, the response of the λ -sensor has to be simulated. The following section describes how this is done.

Engine body delay

First, the charge of fuel and air resides inside the engine for the duration of an engine cycle (t_{engine}), which is a function of engine speed (ω). It is the time of one engine cycle (two revolutions) as shown in Equation 5.16.

$$t_{engine} = \frac{120}{\omega[rpm]} = \frac{4\pi}{\omega[rad/s]} \quad (5.16)$$

Exhaust manifold delay

Secondly comes the time that the exhaust gases resides in the exhaust manifold. Here the flow is regarded as a plug flow which means that there is no mixing along the flow direction. This serves as a transport delay for the exhaust gases to reach the λ -sensor. Plug flow is described with Equation 5.17, where t is time, s is distance and q is a volume segment.

$$V_{plugflow} = \int_{t-d(t)}^t q(s)ds \quad (5.17)$$

In Simulink the plug flow time delay is solved by using a variable time delay function, where the λ value is stored in a memory for the time it takes for the exhaust gases to go from the exhaust port to the λ -sensor. Equation 5.18 gives the time delay, where V_{exh} is the volume of the exhaust system from the exhaust port to the λ -sensor, ρ is the density in the inlet manifold and \dot{m}_{engine} is the mass flow of exhaust from the engine.

$$t_{plugflow} = \frac{V_{exh} \rho}{\dot{m}_{engine}} \quad (5.18)$$

λ -sensor delay Thirdly, the λ sensor characteristics are implemented as a low pass filter, Equation 5.19, where λ_{meas} is the signal from the λ -sensor, λ_{calc} is the calculated λ -value from the exhaust manifold and τ is the time constant of the sensor.

$$\lambda_{meas} = \frac{1}{\tau} \frac{d}{dt} (\lambda_{calc} - \lambda_{meas}) \quad (5.19)$$

The λ -sensor in a vehicle is binary and will only indicate the existence or lack of oxygen in the exhaust gases. When it is used to control the λ -value, it only indicates if λ is above or below 1; there is no interest in the amplitude of the signal. This would otherwise be a problem since the low pass filter would change the amplitude.

Emissions

The factors that influence the regulated emissions as function of λ are well known. The engine out emission level is adjusted with regard to the actual λ value.

These relations are well known and can be observed in [13].

5.4 Model implementation in Simulink

Figure 5.4 shows the implementation from section 5.1.

Appendix B contains a small tutorial to help understand how Simulink works. The arrows show in which way information flows in the model. As can be seen Simulink has a fixed causality. The box labeled Manifold contains Equation 5.6 which is integrated by Simulink to give the mass in the manifold. When the mass is known equations 5.7 and 5.8 yield density and inlet pressure.

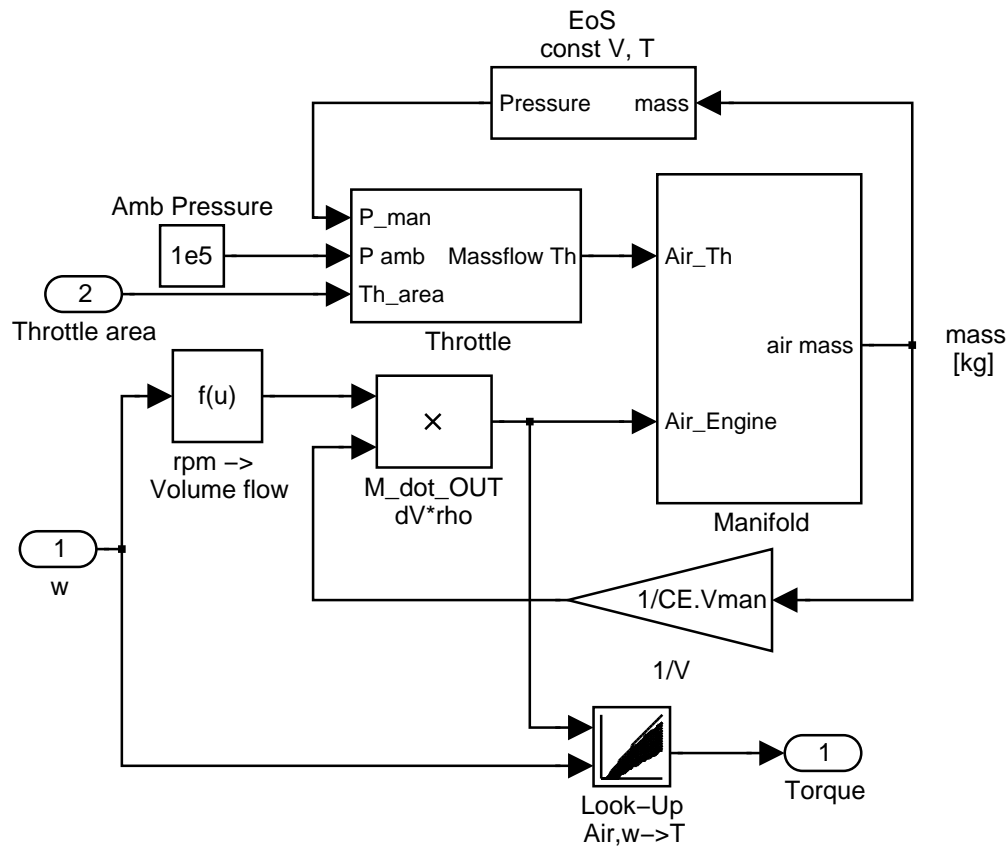


Figure 5.4 Simulink® program air model.

5.5 Simulation time scale

The time scale for the inlet manifold is about 0.1 s. A longer time step usually results in a faster simulation, but that is not always the case. The other reason for short time steps is the closed loop λ -control. In order to have a good resolution, a time step of 0.01 s was used. Using much longer times steps would affect the λ closed loop control. Smaller step size does not affect the solution.

5.6 Simulation results

In the simulations shown here the engine is subjected to a step shaped increase in torque. What is interesting to know is that λ goes lean because the air motion reacts faster than the fuel control. The simulations were run at an engine speed of 2000 rpm. The wall wetting parameters as well as λ integrating gains were adjusted to optimally correspond to the measurements done for TES project, for more details see Chapter 6.

Figure 5.5 shows the results from a simulation where the model is subjected to a step change in torque. The upper graph shows the requested torque, the middle shows the resulting torque and the lower graph shows λ . As anticipated the λ -value increases during the transient. This is a result of a delay in the fuel system, and wall wetting.

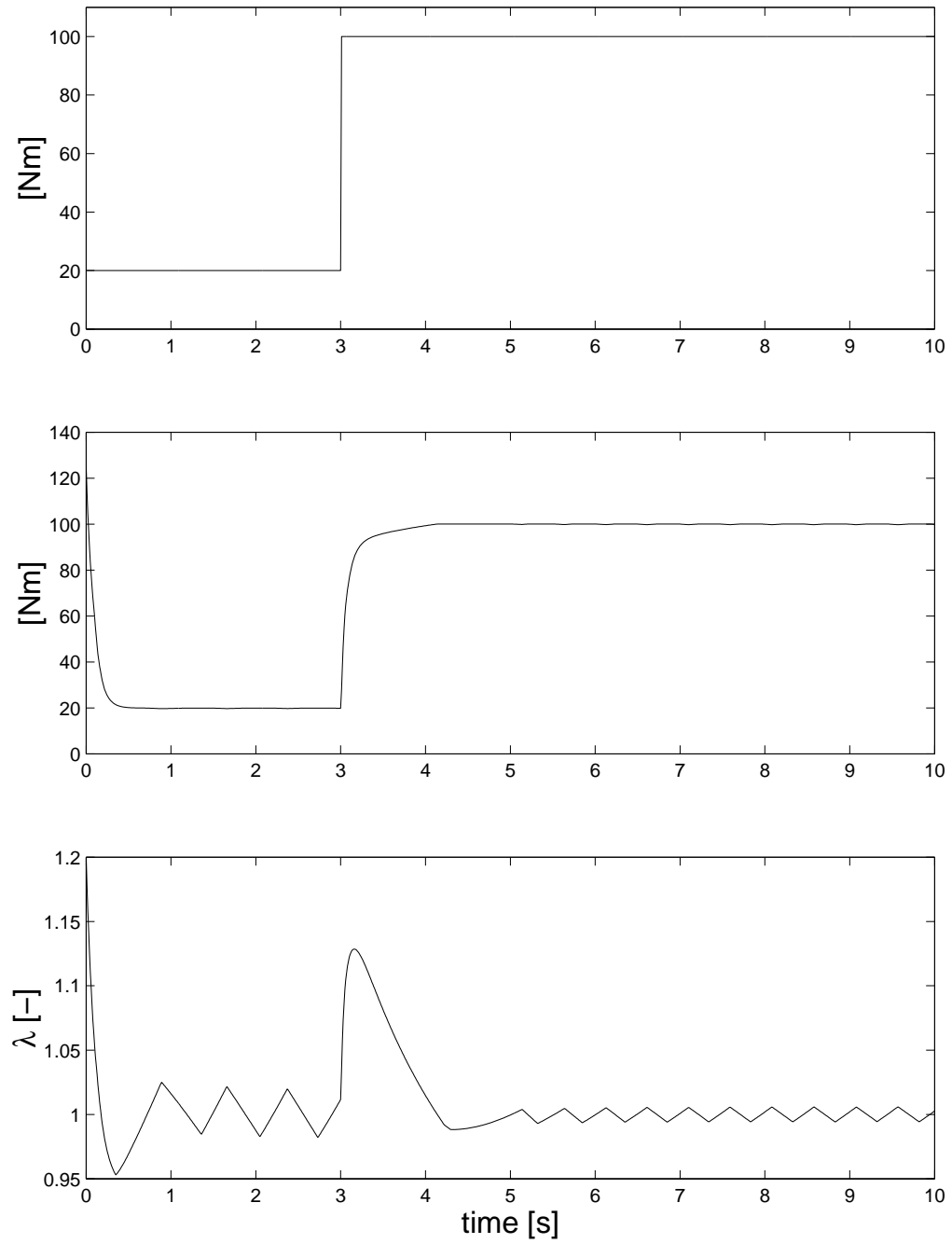


Figure 5.5 Simulation test of an increasing torque step change.

Figure 5.6 shows a negative torque step. The upper graph shows the requested torque, the middle shows the resulting torque and the lower graph shows λ . This simulation shows that the engine is running rich during the negative transient, which is caused by wall-wetting effects.

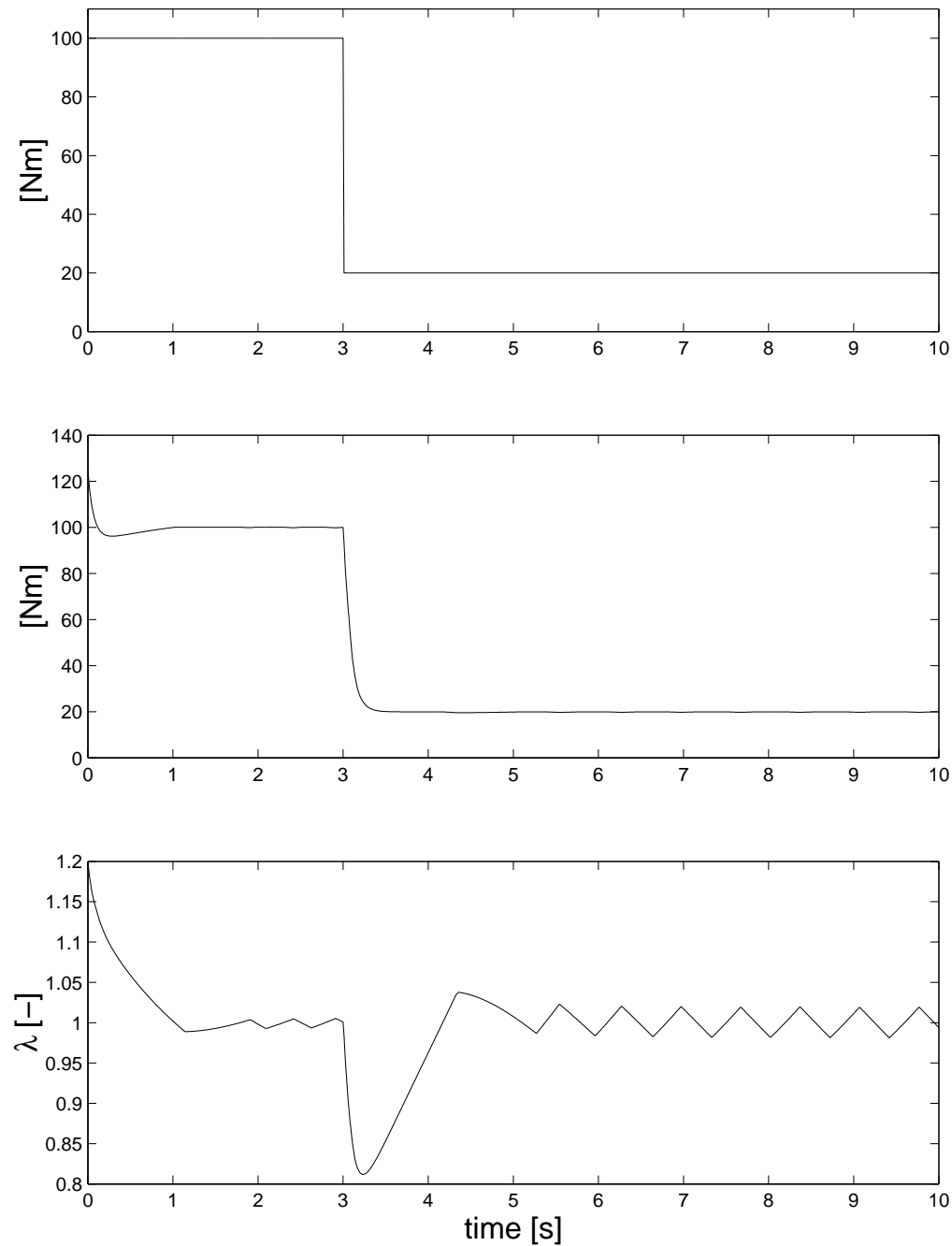


Figure 5.6 Simulation test of an decreasing torque step change.

Figure 5.7 show a torque ramp. The upper graph shows the requested torque, the middle shows the resulting torque and the lower graph shows λ . The slope of the torque curve is so slow that the λ control is able to keep up. There is only a slight rich spike.

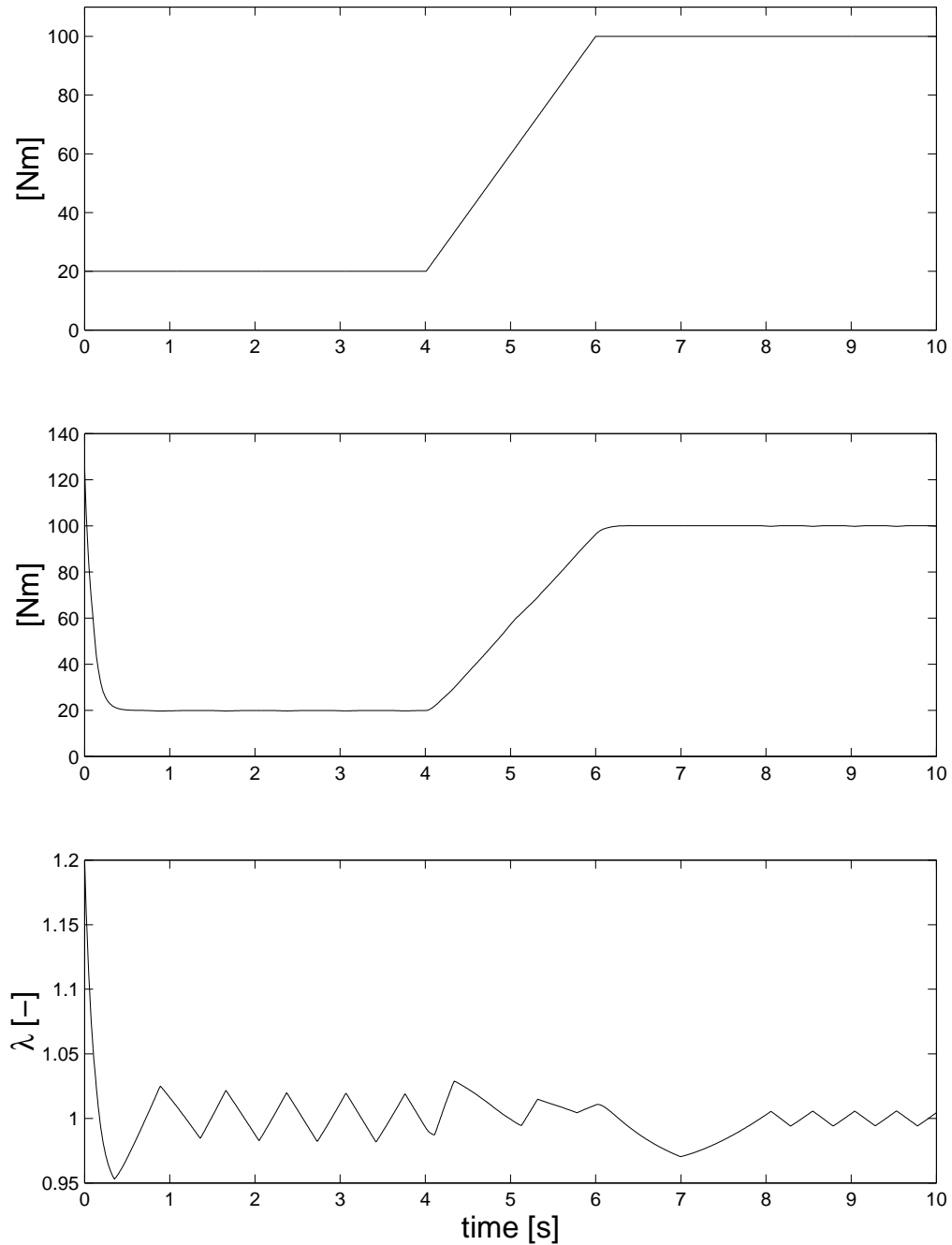


Figure 5.7 Simulation of an increasing ramp test.

6

Validation with TES

TES is short for *Transient Emission Sampling*. It is a method for measuring transient emissions. The project report can be found in Reference [14]. There are two ways of measuring emissions from combustion engines:

These are stationary measurements and drive cycle measurements.

- The stationary measurements are performed as the engine operates under stationary conditions. As standard emissions instruments have a time constant from 1 up to 30 seconds, the instruments have sufficient time to get a stable readings.
- Drive cycle measurements are usually performed on a vehicle on a dynamometer. Here the driver tries to follow the speed trace presented to him on a monitor. The emissions are collected in a bag to be analyzed afterwards.

None of these methods have the ability to measure transient emissions. The main reason for this is the time constant of the measuring device. The time frame for a transient emission *puff* is in the order of tenths of seconds. The time constant for a typical emission measuring systems is in the range of 1 to 30 seconds, see Reference [15].

There are devices for measuring HC and NO, on a cycle resolved timescale. But these devices were not an option because of budget restraints, so an alternative solution was sought instead.

The project was performed as a *proof of concept study*. It was done only to see whether or not it was possible to measure transient emissions with this method, but also to try to validate the models described earlier.

6.1 TES - How does it work?

The main idea is to let the engine and the brake be transient controlled by having the engine perform a loop in the speed and load domain. By doing this the engine will continuously be in a transient state. A valve is opened to redirect the emission flow during the interesting part of the loop into an temporary emission storage (a bag) for later analysis.

6.2 The setup

The test engine was a SAAB 2.3l 16 valve engine. It is a naturally aspirated engine with port injection. It was in production in 1994, powering the SAAB 9000 model.

The engine is mounted on a test bench connected to an eddy current brake. The eddy current brake can only brake, it cannot drive the engine. This makes it impossible to run tests where the engine is motored, like for example a motored braking.

After the exhaust manifold there is a Y - coupling. At one end the catalyst and the muffler is connected and at the other there is a sampling valve. The sampling valve is pneumatically/electrically controlled by a computer.

A personal computer was used as a logger, and was also used for controlling the sample valve operation. The sampling speed of the logger was 20 Hz. Sampling was performed by an AD card. However, the sample speed of the emission instrument was 1 Hz because of its slower response.

The valve was opened at a given engine torque. As it takes work to increase and decrease the engine speed caused by the inertia of the engine and brake, inlet manifold pressure was used to indicate the engine torque. The valve was then opened for given duration in time.

What are the problems with this method?

- Difficult to determine specific emissions due to problem with measuring the fuel consumption
- Because the emissions where not analyzed on line, how did they vary?
- From which part of the loop did the sampled emissions come from?

6.3 Equipment used

Below follows a summary of the equipment used in the experiments:

- Personal Computer, for logging data and emission information. The control program was written in C++. It was chosen for its flexibility and low overhead.
- Data acquisition card, a Microstar DAP 3000a, used for logging and controlling the valve.
- Pierburg emission measuring system. Its response time is too slow to directly resolve the transient. It has the capability to measure HC (hydrocarbons), NO_x (Nitrogen oxide), CO (Carbon monoxide), CO₂ (Carbon dioxide) and O₂ (Oxygen).
- ETAS Broad band lambda sensor.
- Heinzmann throttle servo. The Heinzmann speed controller is originally used for controlling the operation of combustion engine GenSets¹. The controller was found to be unsuitable for the kind of control that was needed in this project. So, an alternative controller for servo power was used. Only the Heinzmann servo and Heinzmann electronics for feedback control was used.

6.4 Data acquisition setup

The valve was controlled from the acquisition program that was running on the PC. So when the program decided to operate the valve a command was sent to the DAP card which then opened or closed the valve.

Exhaust emission data was collected with serial communication from the Pierburg emission sampler. Since everything was handled by the same program it was possible to have a time step on every sample, to help to recombine the two data streams, logging and emission.

6.5 Measurements

The measurements were performed with the engine brake set at a constant speed, and a throttle servo was used to control the torque.

The throttle servo was connected to a signal generator. By doing this it was possible to control the shape, frequency and amplitude of the throttle servo movement, in a repeatable fashion.

¹Generator connected to a Combustion engine used as a power supply

Figure 6.1 shows how torque and speed varies when running the setup. The load-speed change varies anticlockwise. The torque that is shown is the calculated engine torque, see Equation 6.1.

$$M_{ICE} = M_{Brake} + J \frac{d\omega}{dt} \quad (6.1)$$

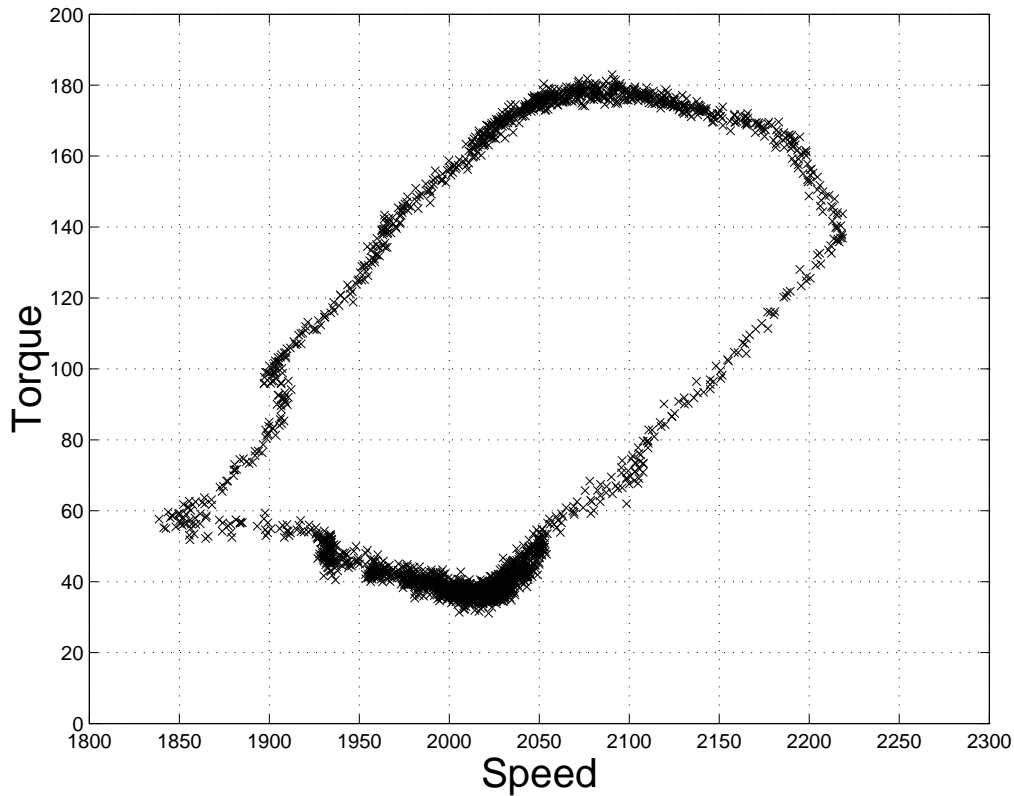


Figure 6.1 Speed and load change with the TES setup.

Figures 6.2 and 6.3 show how the valve was operated during measurements. Typically the valve was activated when passing the mean torque value, and it was active for a fixed time. In these figures the duration for the valve opening was set to 0.5 second.

Valve control

The valve was controlled by the logger program. Inlet pressure was used as indicator of engine torque, since the measured torque at the brake is affected by inertia. First the engine was started in its load cycle. Then the program detected the maximal and minimal value of the inlet pressure, as the mean value was used to trigger the valve. By using a series of logical

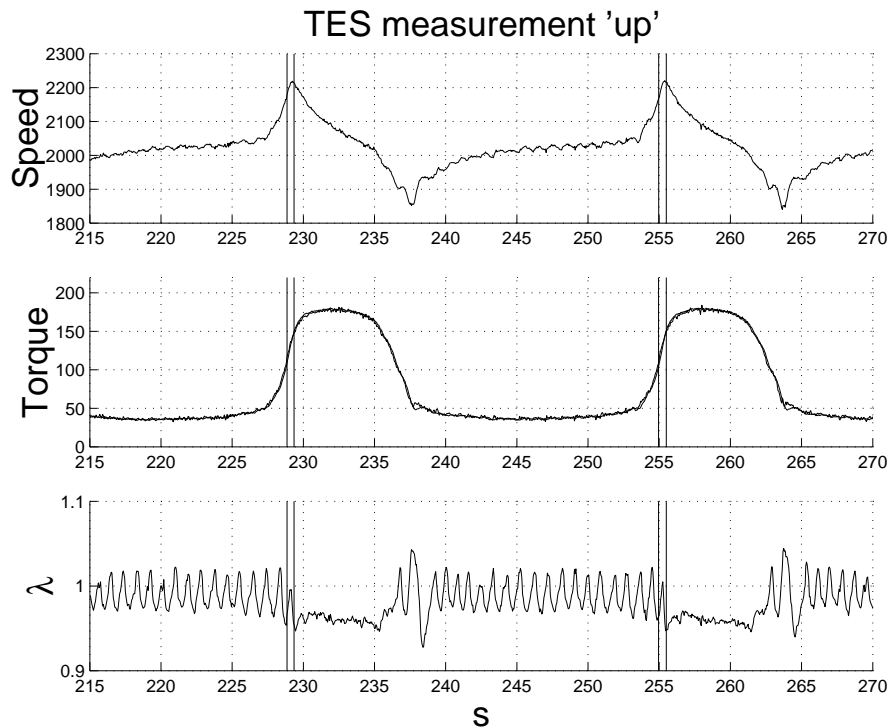


Figure 6.2 Valve opening at rising torque.

conditions it was possible to activate the valve on both rising and falling torque.

6.6 Results

The main effort in the project was a proof-of-concept study of TES, that is to see if it was a feasible method. A major part of the work was to make it function. There were lots of issues to be dealt with: What kind of valve should be used to divert the exhaust flow into the bag during sampling? What kind of dimensions should be chosen for the pipes? How to control the engine load change?

Table 6.1 shows the difference in emissions when comparing stationary measurements to exhaust gas measured during transient operation for increasing torque.

The exhaust compositions look a bit contradictory. For transient operation the higher concentration of CO, HC together with a lower concentration in NO_x, would clearly indicate that the engine ran fuel rich. But still there is plenty of oxygen present. This could be explained as either oxygen is

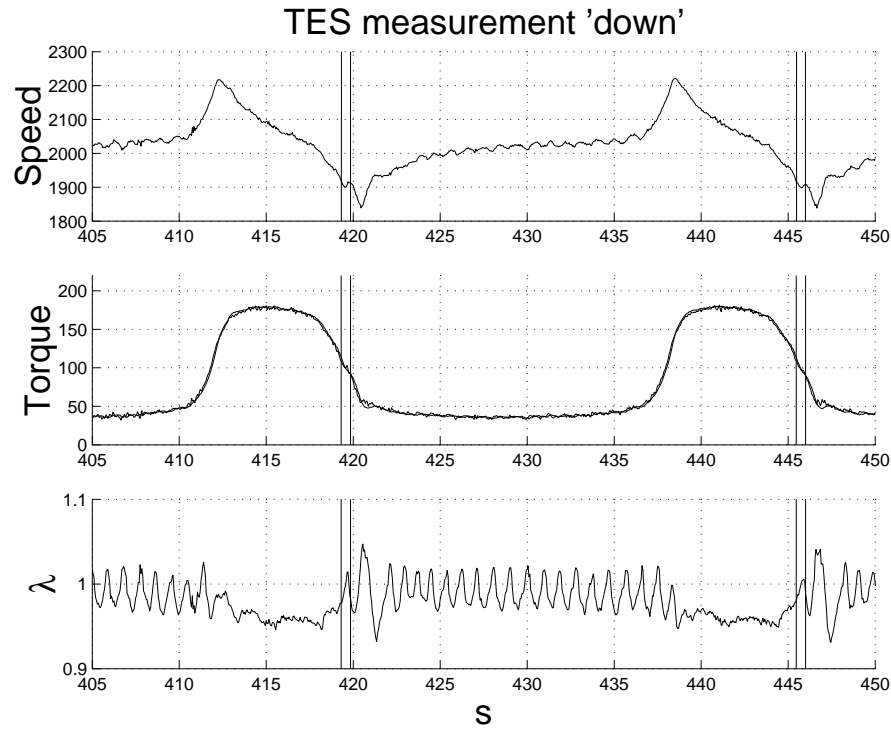


Figure 6.3 Valve opening at falling torque.

Emission		Transient operation	Stationary operation
CO	[%]	2.25	0.4
HC	[ppm]	1200	1880
NO _x	[ppm]	2200	3500
O ₂	[%]	2.0	0.88

Table 6.1 TES measurement: Before catalyst, increasing torque.

leaking into the system. Another explanation is that the engine could be misfiring during the transient.

Wall wetting would give a leaner mixture. But the engine ECU probably has acceleration enrichment which would explain the richer mixture.

Table 6.2 shows the difference in emissions when comparing stationary measurements to exhaust gas measured during transient operation for decreasing torque.

This exhaust composition is also a bit contradictory. The higher content of CO and HC with lower NO_x indicate a rich mixture.

Wall wetting would here account for the mixture being rich because

Emission	Transient operation	Stationary operation
CO [%]	3.3	0.8
HC [ppm]	1000	720
NO _x [ppm]	1400	2500
O ₂ [%]	1.0	0.72

Table 6.2 TES measurement: before the catalyst, decreasing load.

of the lower inlet pressure would increase the vaporization from the inlet manifold walls. But here the ECU could decide to shut off the fuel to because of anticipated use of motor braking.

7

Summary and Conclusions

7.1 Summary

In this project simulation models that has the capability of simulating different kinds of combustion engines have been developed.

It has been showed in this thesis that it is possible to create dynamic response engine models from using combustion engine know-how and data from static measurements.

7.2 Engine sources

For the engine model to be useful it has to accurately perform as a real engine. Some aspects of the engine can be modeled using known relationships. But things like efficiency and emissions has to come from a real engine.

Data for the SI engine comes from in house measurements in a SAAB 2.3 liter car engine. The engine used was the SAAB 9000 series, model year 1994.

The CI engine data is based on a typical European diesel engine with a displaced volume of 2.5 liter.

Throughout the project it has been a continuous struggle to get hold of data on which to base the models. This has been true for many aspects the project. Getting hold of realistic data for everything from battery to combustion engine performance and emissions is a real challenge.

The conclusion is that in order to obtain data, it is best to produce them

oneself.

7.3 Future work

The main shortage of the SI-engine model is the lack of a three way catalyst model. There has been a few attempts at making these kind of catalyst models. They have failed in one way or the other. The most common reason has been numerical difficulties which cause too long calculation times. So, an effort in making a reliable and fast catalyst model is very welcomed.

To try and fit the model to other makes of engines. The design of the model presented in this work will make it rather easy to adapt it to other engines and engine characteristics.

8

Bibliography

- [1] Lars-Ola Olsson. *Optimering av Körstrategi för SAAB 2.3l motor i SL:s Multiflexbuss*. ISSN 0282-1990.
- [2] Morten Hemmingsson. *A Powerflow Control Strategy to Minimize Energy Losses in Hybrid Electric Vehicles* ISBN 91-88934-11-X
- [3] Christian Andersson. *Observations on Electric Hybrid Bus Design*. ISBN 91-88934-18-7.
- [4] Reinmann R., Saitzkoff, A., Lassesson, B. and Strandh, P. *Fuel and Additive Influence on the Ion Current* SAE Transactions, Journal of Fuels and Lubricants, vol. 107, SAE Technical Paper 980161, 1998.
- [5] Bo Hjertstrand. *Konvertering av hybridbussar i Stockholm till etanoldrift* ISBN 91-89511-09-3.
- [6] Bengt Jacobsson. *Modular simulation tool for vehicle propulsion concerning energy consumption and Emissions*. PFF 8531-94-8701.
- [7] Rolf Egnell. *Otto Engine simulation in Dymola*. ISSN-0282-1990 ISBN-LUTMDN-TMVK-3184-SE.
- [8] M Thomas and M Ross. *Development of Second-by-Second Fuel Use and Emissions Models Based on an 1990s Composite Car*. SAE 971010.
- [9] Martin Müller, Elbert Hendricks and Spencer C. Sorenson. *Mean Value Modelling of Turbocharged Spark Ignition Engines*. SAE 980784.
- [10] Rolf Egnell. *α - 03 Simulinkmodell av en turboladdad ottomotor*. ISBN 0282-1990.
- [11] Göran Almkvist. *Transient Air to Fuel Ratio response in a Fuel Injected S.I. Engine*. ISBN 91-7197-097-5.

- [12] I. Arsie, C. Pianese and G. Rizzo. *Identification of manifold two-phase fuel flow model in a spark ignition engine with kalman filter and least square methods*. Proc. of the 7th IEEE Mediterranean Conference on "Control and Automation", Haifa, Israel, June 28-30, 1999, pp. 184-199.
- [13] John B. Heywood. *Internal Combustion Engine Fundamentals*. ISBN 0-07-100499-8.
- [14] Alaküla Mats, Andersson Christian, Egnell Rolf, Simonsson Bengt, Strandh Petter. *Transient Emissions Sampling (TES)* ISBN 91-89511-26-3.
- [15] Pierburg manual. *Pierburg systems manual*. AMA 2000.

A

Dictionary

In this thesis there are a few words that might need some further explanation.

Quasi stationary	When a model doesn't have an internal state.
Stoichiometric	When λ and ϕ equals one (1).
Adiabatic	occurring without heat transfer to the surroundings.
SI	Spark ignition.
CI	Compression Ignition.
HCCI	Homogeneous Charge Compression Ignition.
SAE	Society of Automotive Engineers.
IEEE	Institute of Electrical and Electronics Engineers.
CAD	Crank Angle Degree.
EI	Emission Index.
SCR	Selective Catalytic Reduction.
SNCR	Selective Non Catalytic Reduction.
MEP	Mean Effective Pressure.
BMEP	Brake Mean Effective Pressure.
IMEP	Indicated Mean Effective Pressure.

B

A small Simulink tutorial

The engines that have been presented in this thesis have all been implemented in Matlab/Simulink. Matlab is a script based language with matrix based numerics. It has the ability to solve matrix based linear equations. It has some very powerful graphical and visual features, which make programming faster than when using conventional codes. It is an extensively used *Language of Technical Computing*.

Simulink is a simulation program designed to handle continuous and discrete -time systems. It has a graphical interface where models are built up using blocks and wires. Simulink has its heritage from the analogy machine¹ that were used in earlier days. One problem with these early machines was that they could not handle algebraic loops This is still the case with Simulink. For example, an algebraic loop is created when the results of two operations are connected on the output side.

B.1 How it all comes together

A model is built up by picking up the desired icons with the drag-drop methodology, and then all is connected together with wires.

In Simulink source signals are found under the *Source* menu, source signals can come from internal sources like signal generators with arbitrary curve shapes. It is also possible to load external sources like for example files with drive cycles, or sampled data.

The output signal can be put in a scope for visual inspection as well as saved to a file or fed to a DAC². The output signal blocks are found in the

¹The analogy machine is a device where one can solve a problem with electrical circuits

²Digital to Analog Converter

menu called *Sinks*.

B.2 A small example - the low pass filter

Implementing a low pass filter is the first example. The low pass filter is described as Equation B.1.

$$Out = \frac{d}{dt} \frac{In - Out}{\tau} \quad (B.1)$$

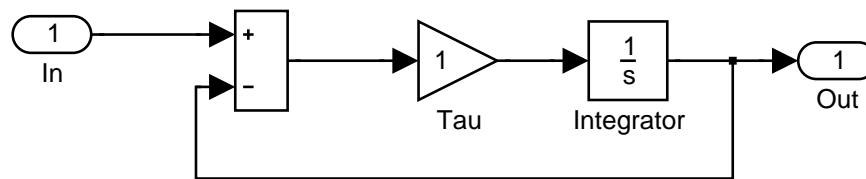


Figure B.1 Simulink example.

Figure B.1 shows the implementation of Equation B.1. Going from left to right, the following list describes the what function of the different icons have:

1. This is where the input signal comes The signal source can be from anywhere. It can be from an other part of Simulink or from an outside source like a sampled signal.
2. The next block is simple math.
3. The triangle is a gain block which multiplies the signal with a constant value. This is where the time constant τ is set.
4. The integrator, one of the most important blocks in Simulink.
5. Signal output.

B.3 A simple naturally aspirated SI engine

The next example is a small model of what could be called an air engine. It is basically a Simulink implementation of a throttle as described in section 5.1, and the mass balance around the inlet manifold, see section 4.1.

Figure B.2 shows the Simulink implementation of the air engine. It is a good point to try to have a clean and pedagogical layout of the model. The boxes labeled Throttle and Manifold are both sub models. This is Simulink code that has been encapsulated. This improves the layout and readability of the model. It has the added benefit of having boxes with the same interface.

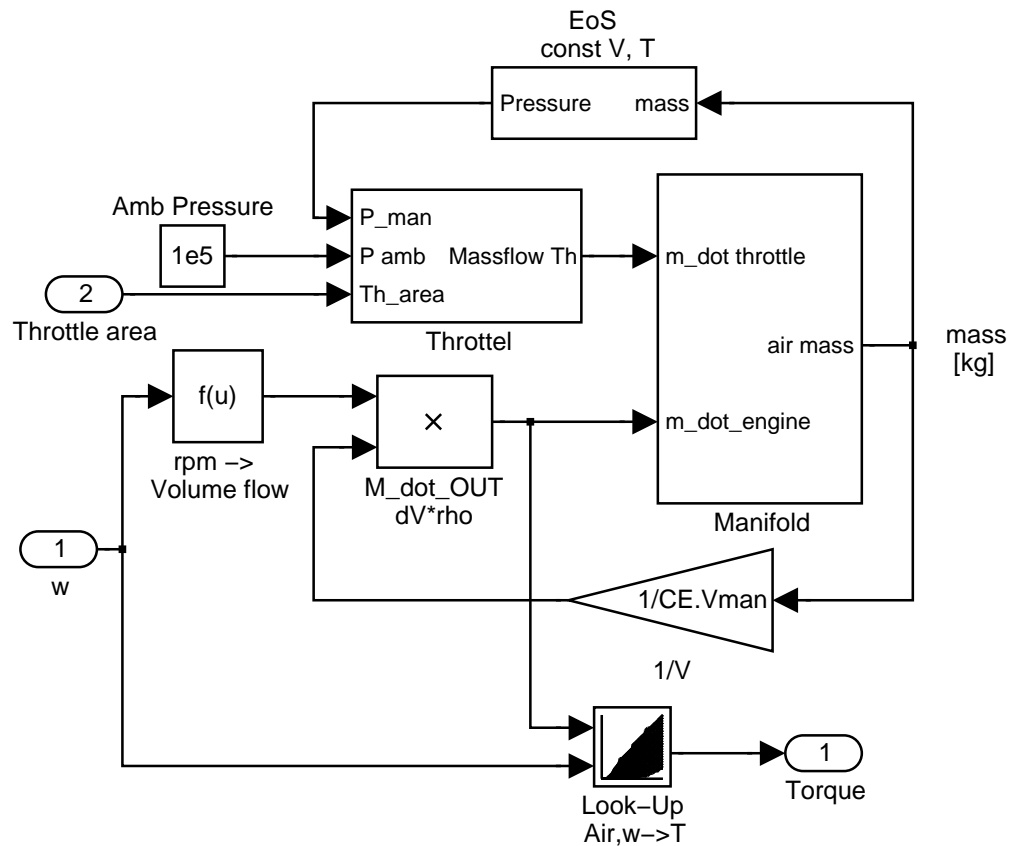


Figure B.2 A simple SI-engine model.

C

Simulink graphs

C.1 The CI engine

Figures C.1, C.2, C.3, C.4, C.5, C.6, C.7 show different parts of the Diesel engine model. They are the Simulink implementations of the equations given in Chapter 4.

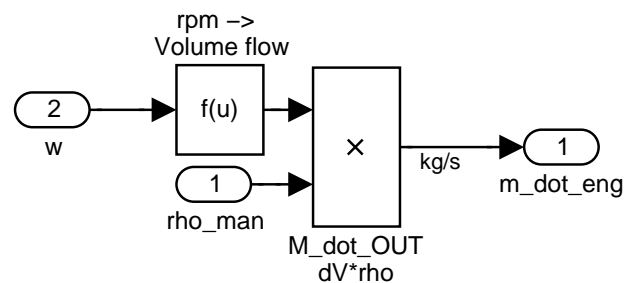


Figure C.1 Determine the mass flow into the engine body.

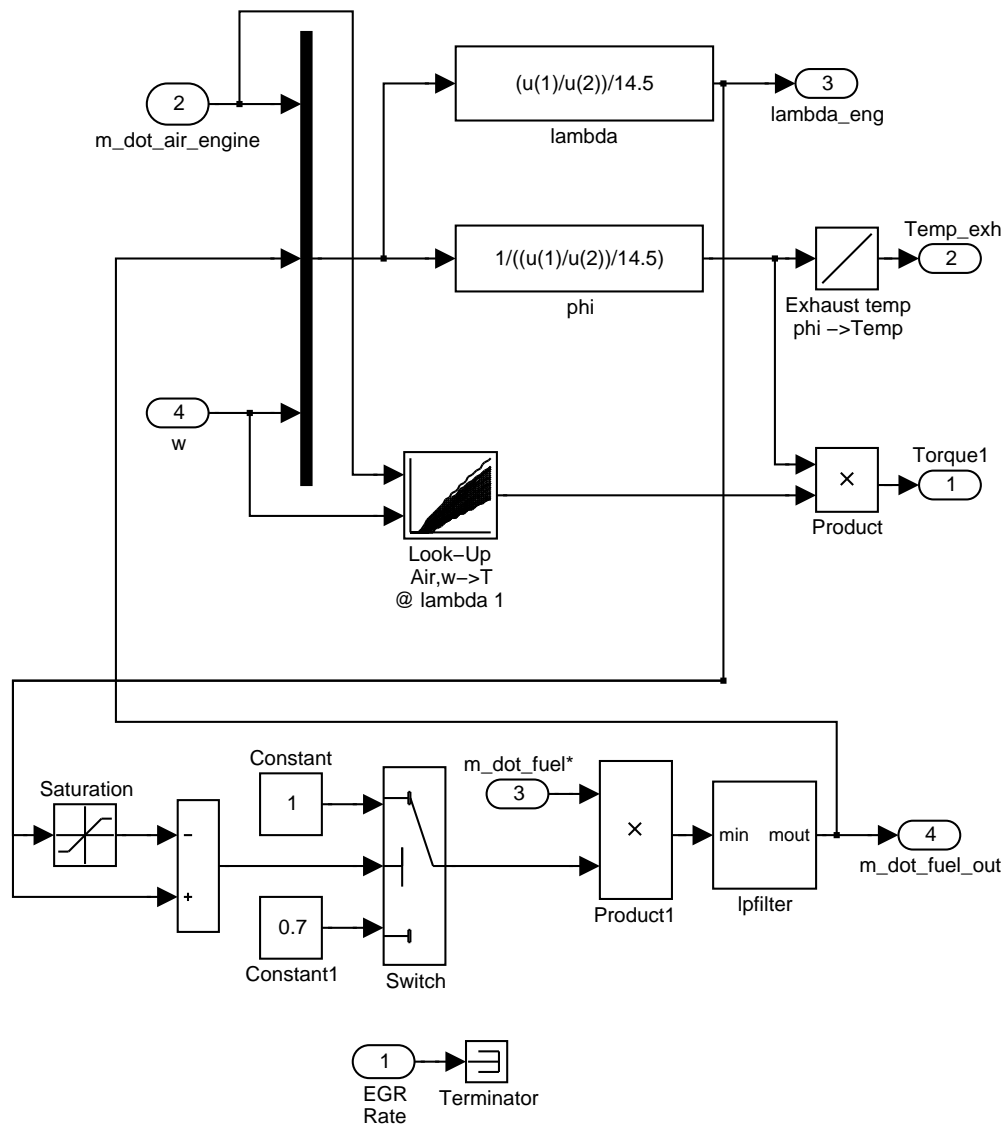


Figure C.2 Inside the engine combustion module.

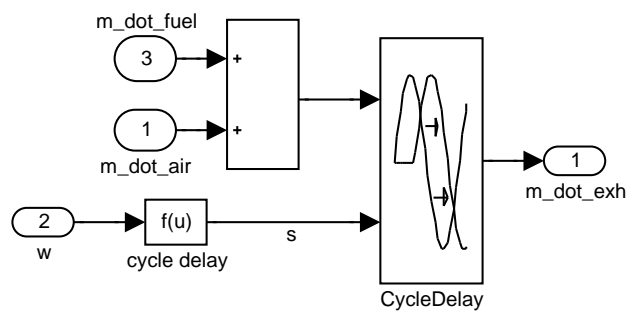


Figure C.3 The cycle delay, inside the engine body.

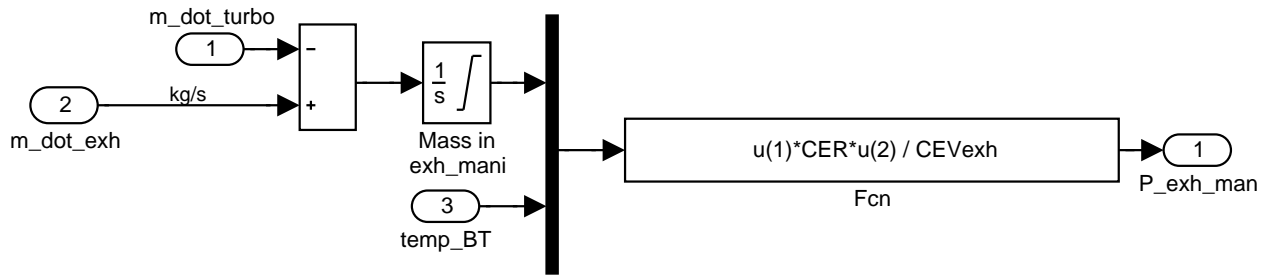


Figure C.4 The exhaust manifold.

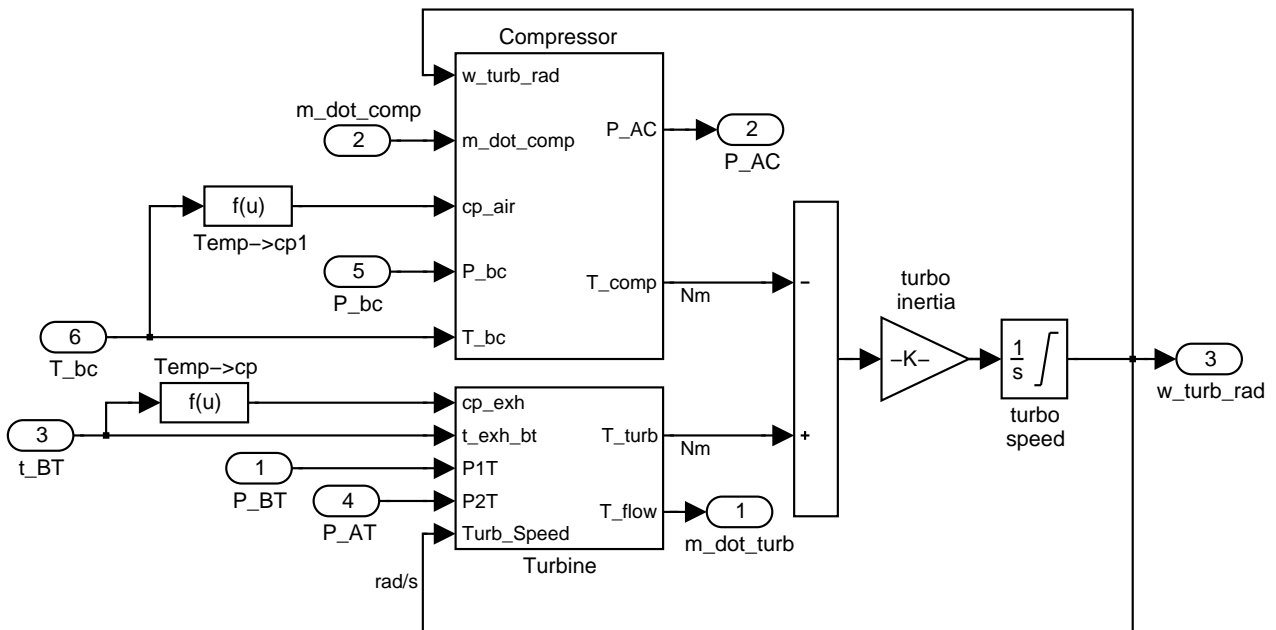


Figure C.5 The turbocharger.

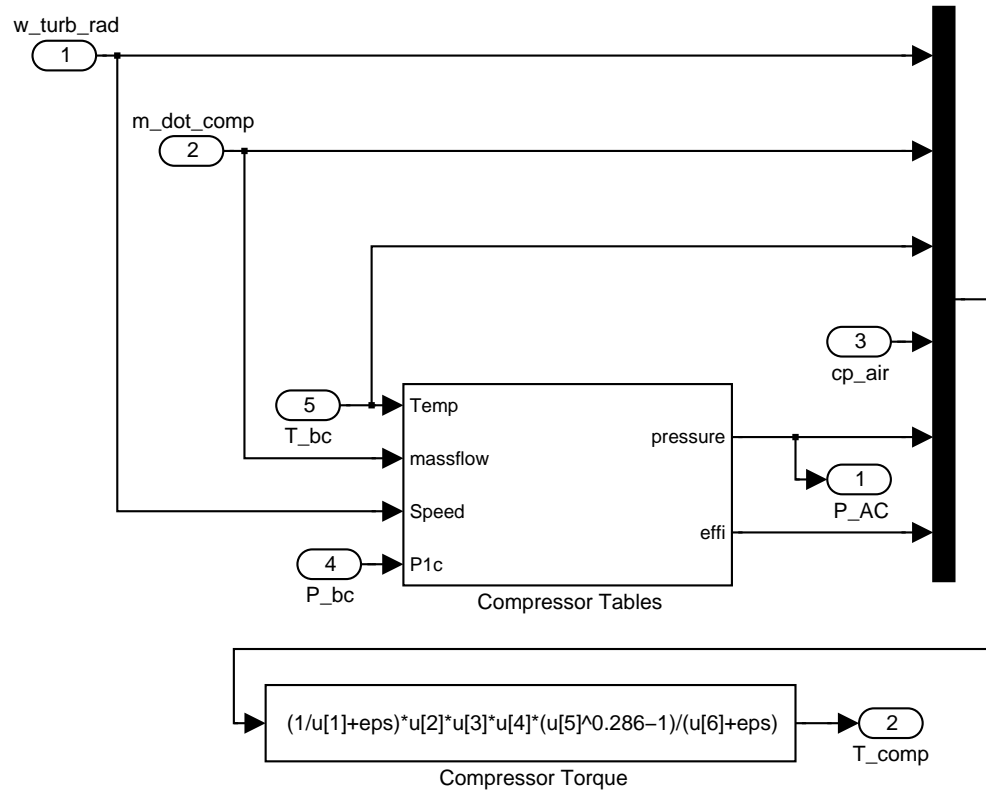


Figure C.6 The compressor.

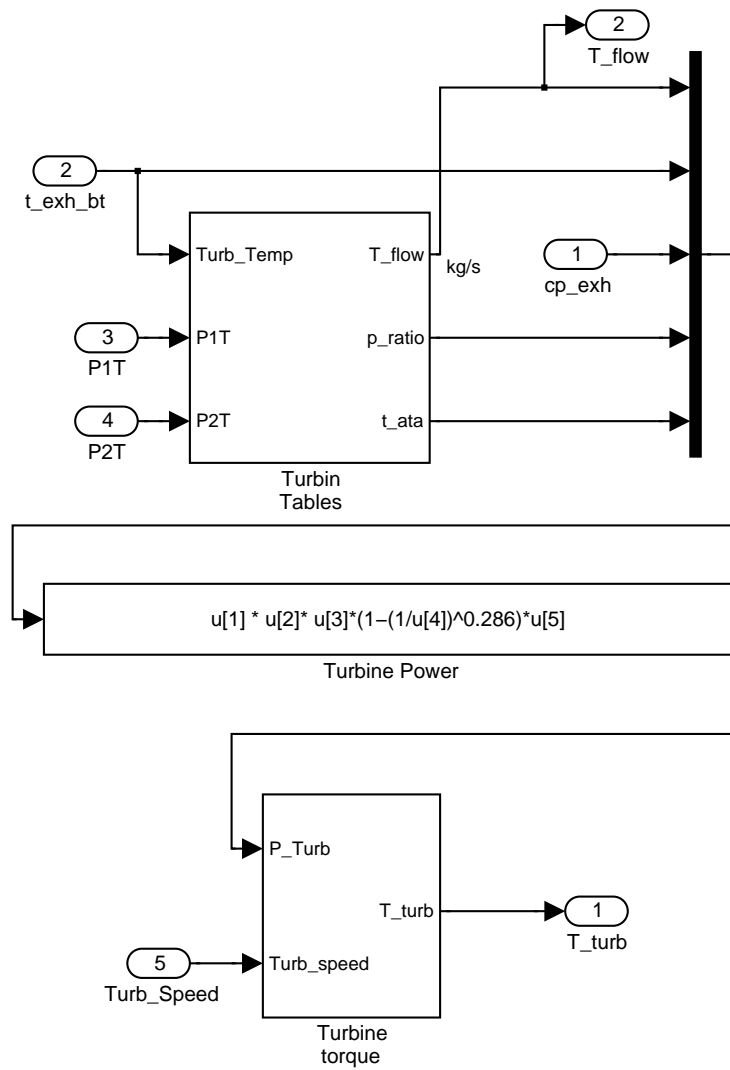


Figure C.7 The turbine.

C.2 The SI engine

Figures C.8 ,C.9 ,C.10 ,C.11 ,C.12 ,C.13 ,C.14 ,C.15 and C.16 are figures from the combustion engine model.

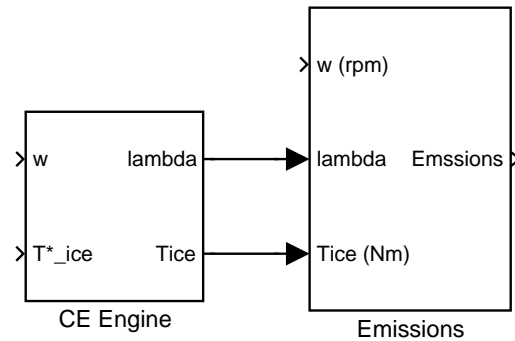


Figure C.8 The SI engine at the uppermost level.

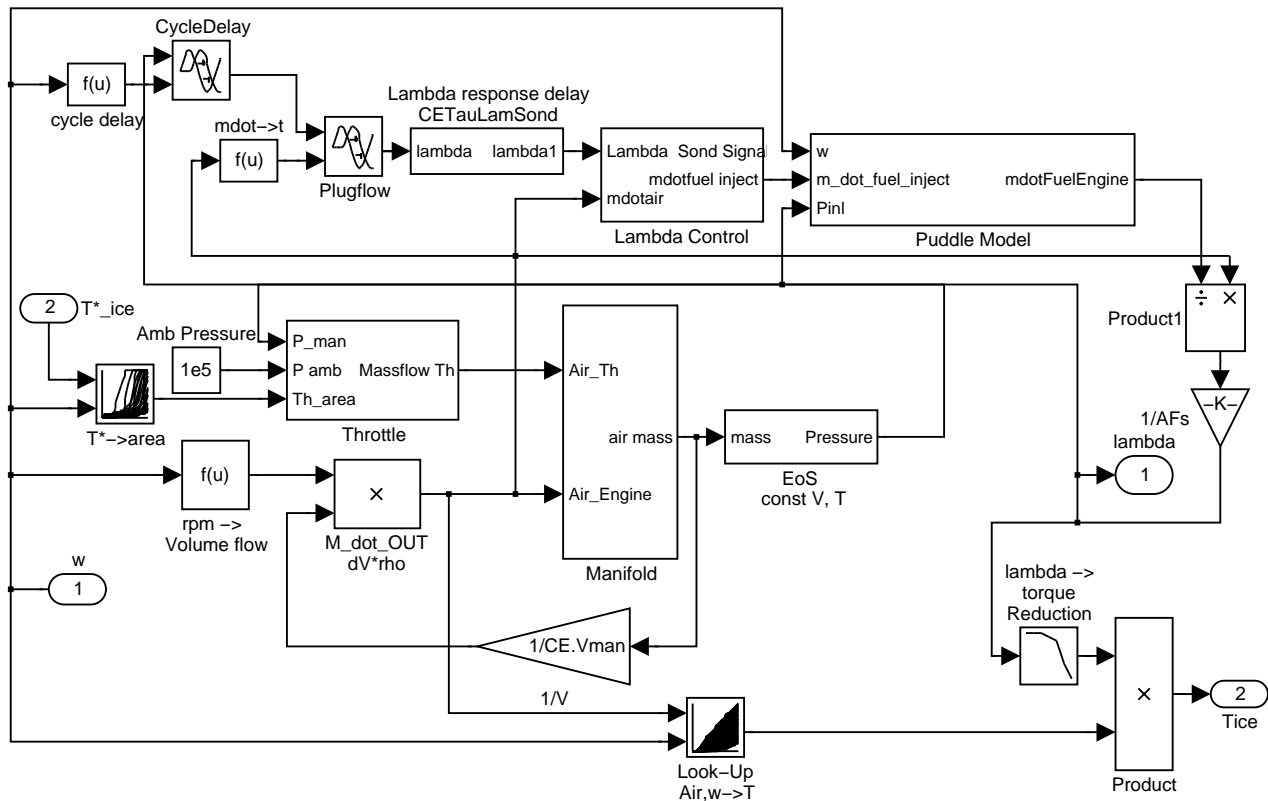
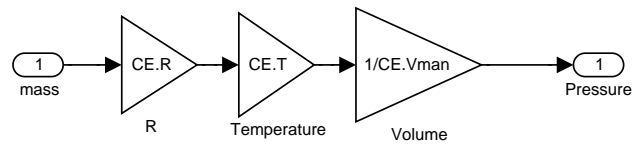


Figure C.9 Inside the combustion engine box.



Allmäna gaslagen == Equation of State

Figure C.10 Calculating the pressure in the inlet manifold.

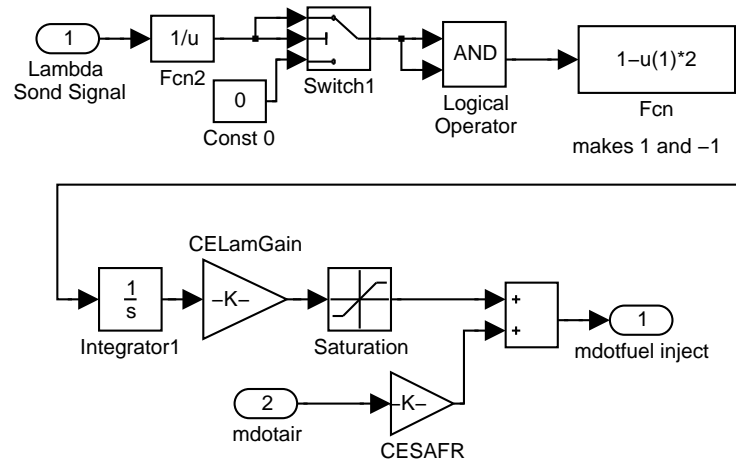


Figure C.11 λ -control algorithm.

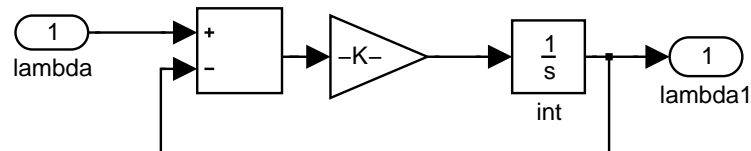


Figure C.12 Low pass filter for the λ -sensor.

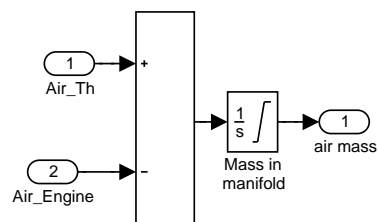


Figure C.13 The inlet manifold.

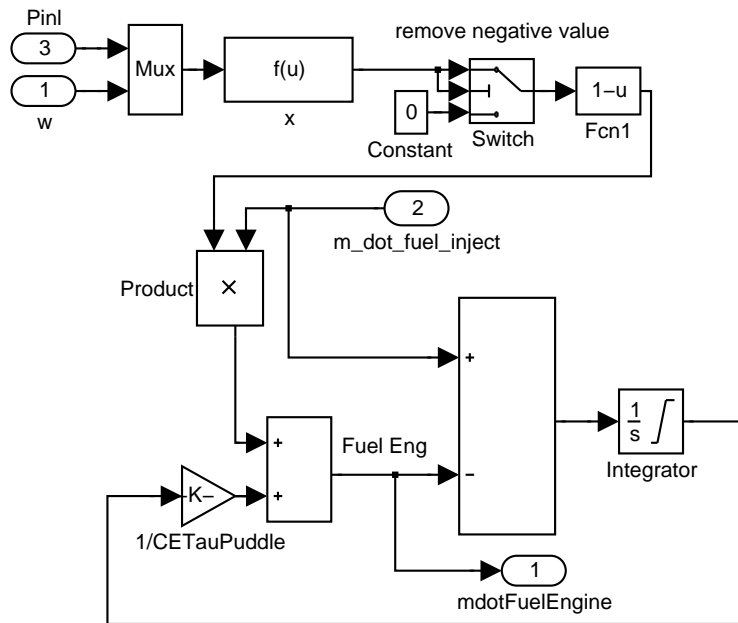


Figure C.14 The puddle model.

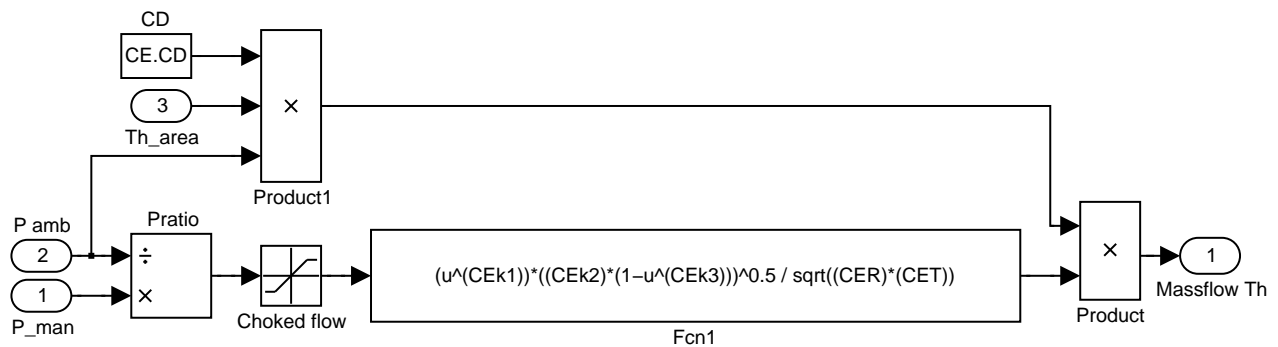


Figure C.15 The throttle.

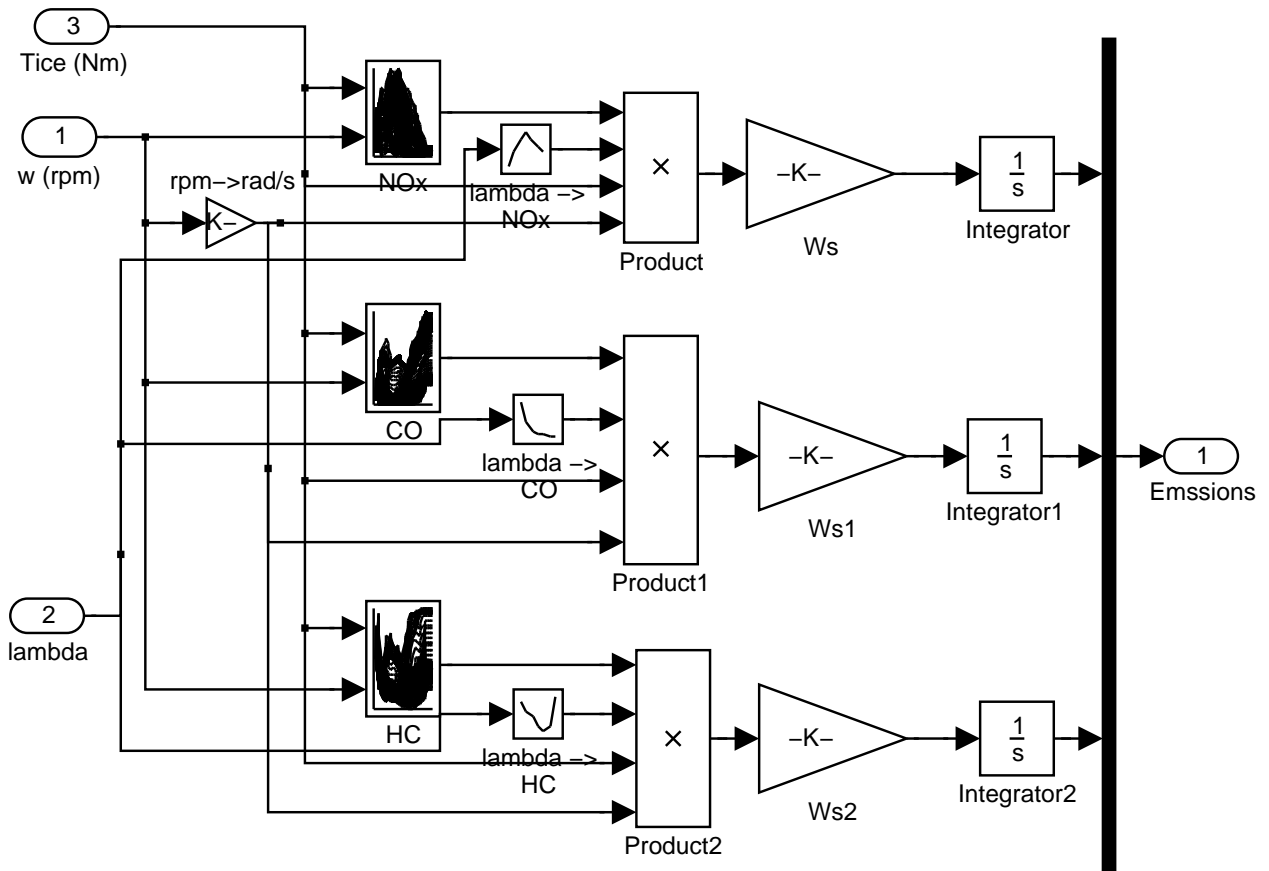


Figure C.16 Engine emission look-up and calculation.

D

Discussion about the thesis

This last appendix is written to address the questions that my opponent asked during the public defense of this licentiate thesis.

There are some points that have been corrected in the text itself. Below follows the questions of the opponent, followed by my answers.

- Question: What validates the use of the emptying and filling model in this simulation development?

Answer: In order to have access to fast simulation, there is a trade off between speed and precision.

- Question: What do you mean by regenerative braking causing an efficiency gain of 30%.

A: The answer is that by using regenerative braking, energy can be fed back into the battery. Assume that 50% of the brake energy is recovered. This will cause an increased mileage of approximately 30%.

- Q: What do you mean by stating that the inlet manifold has a time constant of 0.1 seconds?

A: If a test is being performed where the inlet pressure is changed from idle to full load, the time to fill and to empty is about 0.1 seconds. Hence I conclude that the inlet manifold has a time constant of about 0.1 second.

- Q: In section 5.1, is this a part of the engine manifold or just the control volume?

A: The throttle is an area restriction to determine the volume flow and its role is to determine the mass flow of air that is let into the inlet manifold.

- Q: How do you deal with *discharge coefficient* C_D between all the valves and channels?
A: The C_D for the throttle is given. For other flow restrictions the C_D -value is implicitly given, by comparing with measured static maps. However, no attempt is made to correct the C_D under transient conditions.
- Q: What about tuning effects in the inlet and exhaust manifolds?
A: In the model pipe tuning is included during static conditions, but not during transient conditions.
- Q: How can you claim that your model can predict transient behavior when you use static tables? How can you produce emission levels when these are also taken from static tables?
A: When it comes to the torque formation, this table is insensitive to transient flows, as long as the λ -value is within limits. The way that the table has been developed means that tuning effects in the manifold that occurs during stationary operation is taken into account. However, transient tuning effects are not taken into consideration and if they are big the model will not be correct.
Emissions are corrected against λ . So assuming that all cylinders run equal, the model should predict this correctly. But it is not a perfect simulation, but should be enough to be a good indicator.
- Q: Which role does the throttle have in the model?
A: The throttle is only based on Bernoulli equations and deals only with flow restriction to the inlet manifold.

E

Modeling SI Engines for Hybrid Vehicles

Modeling SI-engines for Hybrid Vehicles, written by myself and Rolf Egnell.
SAE 2001-01-0575.

Modeling SI-engines for Hybrid Vehicles

Petter Strandh, Rolf Egnell
Lund Institute of Technology, Sweden

Copyright © 2001 Society of Automotive Engineers, Inc.

ABSTRACT

One of the most attractive features of hybrid vehicles powered by SI-engines with three way catalysts is the potential of reaching extremely low emissions. In conventional drive trains, limitations in the air/fuel control result in lambda excursions during transients. These deviations from the ideal lambda result in increased emissions.

In a hybrid vehicle, rapid load and speed changes of the SI-engine could be limited to an acceptable level as the battery acts as a power buffer. However, the efficiency of charging and discharging the battery is rather low, which means that excessive power buffering will increase the fuel consumption of the vehicle. Thus it is of great importance to know what degree of speed and load changes the air/fuel control system could cope with without an increase in emissions.

Most SI-engine models for hybrid vehicles are quasi stationary, which means that data achieved at stationary load conditions are assumed to be representative for transient operation as well. In this paper a concept is presented in which stationary engine data is used, but corrected for the effects of lambda excursions.

In the present paper the model is described in depth and some calculated experiments are presented. It is found that load changes in the range of 20% to 90% at frequencies higher than 0.5 Hz will result in lambda excursions that probably will result in unacceptable emissions.

INTRODUCTION

Vehicles with drive lines including both IC engines, electrical motors and batteries, i.e. electric hybrid vehicles, are receiving more and more attention today. Toyota and

Honda have recently marketed passenger cars with this kind of system. The advantages of electric hybrid systems are low fuel consumption and emissions. In order to realize this potential, it is mandatory to optimize the electrical drive train to the characteristics of the SI engine. Due to the pumping losses, the efficiency of a gasoline engine is poor at low loads. Thus low loads must be avoided when using this type of engine in a hybrid system.

The TWC emission control is based on the principle of keeping the air/fuel ratio to the engine very close to the stoichiometric ratio, i.e. $\lambda = 1$. At a very narrow interval around $\lambda = 1$, the catalyst is capable of simultaneous conversion of CO, HC and NOx to harmless products. At very rapid changes of the flow through the engine, limitations in fuel flow control cause deviations from the ideal lambda window, and the catalyst will not be able to convert all harmful emissions. Although the catalyst, due to its storage capacity, is able to handle some deviations, spikes of high emissions will occur at too violent transients. Hence, when designing a low emission electric hybrid vehicle it is necessary to know the border frequency of load and speed changes below which the cleaning effect of the TWC system is intact.

In an electrical hybrid vehicle, the IC engine's load changes can be kept low and slow, thanks to the energy storage in the battery. However, energy transmission through the battery has low efficiency and thus increases the vehicle's fuel consumption. Obviously there exists an optimum rate of speed and load changes where the best compromise between low emissions and fuel economy can be found. The work presented in this paper concerns a model where the lambda variation due to transients can be studied. The SI engine modeling presented in this paper is part of a much larger generic hybrid modeling program. The objective of this program is to analyze various combinations of combustion engines, includ-

ing systems for exhaust cleaning, electrical energy converters and storages. Three types of hybrid systems will be studied. They are:

- Series hybrids
- Parallel hybrids
- Power split hybridises

Most models used to describe SI-engines in hybrid systems are based on data from stationary mapping of engines. Map-based models are accurate only if the load and speed transients are slow. In order to investigate the limits of the air fuel control at rapid changes, the model must respond to the dynamics during transients. In the present work, stationary engine maps based on speed and torque are transformed to maps based on speed and airflow, i.e. a certain measured torque corresponds to a certain measured airflow at a given speed.

In the model, the engine body is considered as an air pump and the flow capacity depends on the engine speed and the density in the inlet manifold. The density in turn depends on the throttle area and volume flow through the engine. The filling and emptying approach is applied to the inlet manifold. The calculated air mass flow is used to determine the fuel flow necessary to reach the desired lambda. Due to the effects of the location of the air mass measurement, wall wetting, delays caused by the residence time in engine and the exhaust manifold and the response time of the lambda sensor, the actual lambda differs from the ideal. The measured stationary data on torque and emissions at a given speed and air flow are corrected for the actual lambda value.

THE THEORY

The specific SI engine that is subjected to modeling is mapped during stationary conditions. This mapping gives the information of stationary torque, airflow, fuel flow and emissions. Based on this data, new maps are created where the stationary engine properties are given versus speed and airflow.

The simulation model is built up of the following three major parts:

- The air model
- The fuel flow model
- The fuel control model (λ -control)

THE AIR MODEL The air flow is used in the first stage of the model. This part consists of the engine body, the inlet manifold and the throttle.

The engine body In this model the *engine body* is regarded as a displacement pump with volume flow as function of engine speed, Equation 1. The mass flow of air entering the cylinder is determined by the density (ρ) in the inlet manifold, Equation 2.

$$\dot{V} = \frac{V_{engine} * \omega}{4\pi} \quad (1)$$

$$\dot{m}_{engine} = \rho * \dot{V}(\omega) \quad (2)$$

Where:

V_{engine}	$[m^3]$	engine displacement
ω	$[rad/s]$	engine speed
\dot{V}	$[m^3/s]$	volume flow through the engine
ρ	$[kg/m^3]$	density
\dot{m}_{engine}	$[kg/s]$	mass flow through the engine

The inlet manifold While the air is drawn into the engine, Equation 2, a balance is formed by the air going into the engine and the air going into the manifold from the throttle, Equation 3. This couples the airflow through the throttle to the pressure in the manifold. The density in the manifold determines how much air is drawn into the engine.

$$\dot{m}_{manifold} = \dot{m}_{throttle} - \dot{m}_{engine} \quad (3)$$

The equation of state gives both Equation 4 and 5.

$$\rho = \frac{m_{inlet\ manifold}}{V_{manifold}} \quad (4)$$

$$P_{manifold} = \frac{m_{inlet\ manifold} R T}{V_{manifold}} \quad (5)$$

Where:

$\dot{m}_{manifold}$	$[kg/s]$	mass of air in the manifold
$\dot{m}_{throttle}$	$[kg/s]$	air to the manifold
\dot{m}_{engine}	$[kg/s]$	air to the engine
$m_{inlet\ manifold}$	$[kg]$	mass of air in manifold
$V_{manifold}$	$[m^3]$	volume in manifold
ρ	$[kg/m^3]$	density
$P_{manifold}$	$[Pa]$	pressure in manifold
R	$[kJ/(kg * K)]$	gas constant
T	$[K]$	temperature

The throttle To control the amount of air that is going into the engine, there is a throttle in front of the inlet manifold. The throttle equation is identical to the equation that describes the compressible mass flow through an area, Equation 8. It becomes a part of the inlet manifold system as the P_{inlet} is a part of the equation. In the throttle, the inlet area is controlled by rotating a plate inside a tube just prior to the manifold.

When calculating the mass flow through the throttle it is essential to calculate the pressure ratio across the area. The flow dimensioning pressure ratio is given by the κ of the fluid. With the ideal gas law the critical pressure ratio is given by Equation 6.

$$\frac{P_m}{P_a} = \left(\frac{2}{\kappa + 1}\right)^{\kappa/(\kappa-1)} \quad (6)$$

The κ value of air is 1.4 and this yields to a critical pressure ratio of 0.5283. If the pressure ratio is critical, Equation 7 is used, otherwise Equation 8 is used.

$$\dot{m}_{th} = \frac{C_D A_{th} P_a}{\sqrt{RT}} \kappa^{1/2} \left(\frac{2}{\kappa + 1}\right)^{\kappa+1/2(\kappa-1)} \quad (7)$$

$$\dot{m}_{th} = C_D A_{th} \frac{P_a}{\sqrt{RT}} \frac{P_m}{P_a}^{\frac{1}{\kappa}} \sqrt{\frac{2\kappa}{\kappa-1} \left[1 - \left(\frac{P_m}{P_a}\right)^{\frac{\kappa-1}{\kappa}}\right]} \quad (8)$$

Where:

C_D	[-]	discharge coefficient
κ	[-]	ratio of specific heats
R	[kJ/(kg * K)]	gas constant
T	[K]	temperature
A_{th}	[m ²]	throttle area
P_a	[Pa]	ambient pressure
P_m	[Pa]	manifold pressure

Torque from airflow The input stationary measured data is transformed to speed and air flow based tables. A torque table is illustrated in Figure 1. In the model the torque is determined by looking up the output value in the table for the speed and air flow in question. See Equation 9.

$$T_{air\ flow} = f(\dot{m}_{in}, \omega) \quad (9)$$

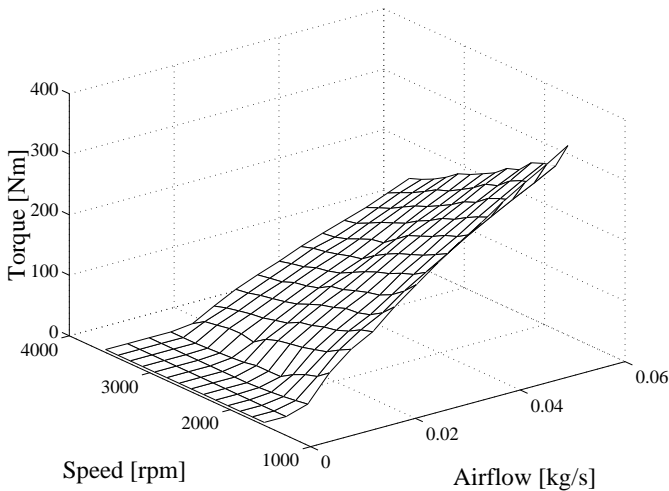


Figure 1: The Airmap

The air flow based tables include stationary effects of tuning. This effect appears as increased volumetric efficiency. It is assumed that this efficiency remains during transients. The tuning effects at transient load changes are not known.

As can be noted in Figure 1, the torque is very high at low engine speeds. The engine will never achieve this

high torque, since it is limited by the amount of air that can be drawn into the engine. At low engine speeds the airflow through the engine is low. In reality there is a limitation of the pressure in the manifold that cannot be higher than the ambient pressure. The torque could, however, be increased if the engine was supercharged.

The torque shown in Figure 1 is based on measured data from the engine running at $\lambda = 1$. Since this is not always the case, especially not during transients, the torque has to be corrected for the actual λ value, Equation 10. An example of such correction is shown in Figure 2.

$$T_{actual} = f(T_{air\ flow}, \lambda_{actual}) \quad (10)$$

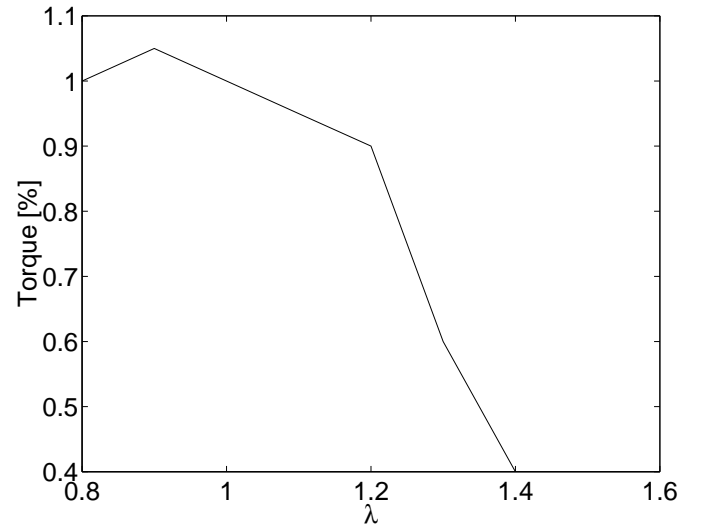


Figure 2: Torque reduction versus λ

THE FUEL SUPPLY MODEL The momentary air flow at different points is calculated with the air model, Figure 6. Air flow information could be picked by a sensor prior to the throttle or it can be calculated from the pressure and temperature in the manifold. In the latter case the volumetric efficiency must be known.

The air flow at the chosen point is used to calculate the momentary fuel supply while assuming stoichiometric air fuel ratio. In a port injected SI engine the fuel spray from the injectors is directed towards the inlet valves.

In the ideal case the fuel goes from the injector directly into the cylinder. However, part of the fuel that is injected into the port will stick to the walls. This is known as *wall wetting*. It is caused by fuel droplets sticking to the walls during the fuel injection. It can also come from back flow, this takes place during the later part of the intake stroke and during the valve overlap period.

The model used to describe the wall wetting originates from the PhD thesis, reference [1]. In this thesis, wall wetting effects are thoroughly investigated. Equation 11

describes how the fuel into the cylinder is a function of injected fuel, inlet manifold pressure and engine speed.

$$\dot{m}_{fuel\ engine} = f(\dot{m}_{fuel\ injected}, \omega, \dot{m}_{air}, P_{inlet}) + \frac{\dot{m}_{film}}{\tau_{puddle}} \quad (11)$$

Equation 12 shows the mass balance of fuel in the inlet manifold.

$$\dot{m}_{film} = \dot{m}_{fuel\ injected} - \dot{m}_{fuel\ engine} \quad (12)$$

Where:

T_{actual}	[Nm]	engine torque
$T_{air\ flow}$	[Nm]	engine torque at $\lambda = 1$
$\dot{m}_{fuel\ engine}$	[kg/s]	fuel entering the engine
$\dot{m}_{fuel\ injected}$	[kg/s]	fuel injected
\dot{m}_{air}	[kg/s]	air going into the engine
P_{inlet}	[Pa]	manifold pressure
\dot{m}_{film}	[kg]	total amount of fuel film
τ_{puddle}	[s]	fuel time constant
\dot{m}_{film}	[kg/s]	fuel film change rate

FUEL FLOW CONTROL The principles and functions of the computer-controlled fuel systems in vehicles are complex, and their details are classified as TOP SECRET of the manufacturers. The controller used in this work is very simple, and is based on measuring the airflow that is coming into the cylinder or by simulating a mass air flow meter prior to the throttle.

There are several ways of measuring the air that is about to enter the cylinders. Usually some kind of mass air flow meter is used. An alternative approach is to use the calculated value based on the density in the inlet manifold (ρ), engine speed (ω) together with a table containing volumetric efficiency. This method is usually referred to as speed density.

The present model receives its air flow information either from a simulated signal that comes from the throttle module, or from the inlet port using the speed density method.

To determine the amount of fuel to be injected, information regarding the airflow and, if it is a closed loop system, the measured lambda value is required. In Equation 13 the f is the closed loop function described below.

In Equation 14 the λ_{meas} is a function of the time delay for the engine cycle t_{engine} , the time delay from the plug flow in the exhaust manifold $t_{exhaust}$ and finally from the characteristic of the λ sensor τ_{sensor} .

$$\dot{m}_{fuel\ inj} = \dot{m}_{air} AFs + f(\lambda_{meas}) \quad (13)$$

$$\lambda_{meas} = f(\lambda_{real}, t_{engine}, t_{exhaust}, \tau_{sensor}) \quad (14)$$

Where:

$\dot{m}_{fuel\ inj}$	[kg/s]	fuel to be injected
\dot{m}_{air}	[kg/s]	air going into the engine
AFs	[-]	stoichiometric air fuel ratio
λ_{real}	[-]	real air fuel ratio in the engine
λ_{meas}	[-]	measured air fuel ratio
t_{engine}	[s]	time delay through the engine
$t_{exhaust}$	[s]	time delay through the manifold
τ_{sensor}	[s]	time constant of the λ -sensor

The closed loop λ control In Equation 13, the term $f(\lambda_{meas})$ is the closed loop control of λ . It determines whether the λ_{meas} value is above or below 1. If the λ value is too low it will ramp down the fuel flow until the value changes, and visa versa. There is also a limitation of the signal amplitude to prevent it from going too far. See the pseudo code below for the general idea:

```

if lambda_meas > 1 then
    lambda_control = lambda_control - 0.1
else
    lambda_control = lambda_control + 0.1
end
fuel = airflow * AFs + lambda_control;

```

IMPLEMENTATION OF λ TIME DELAYS

Engine delays The time delay in the engine (t_{engine}) is simply a function of engine speed (ω). This is the time duration that the air/fuel mixture resides inside the engine. Typically, the time of one engine cycle, two revolutions is shown in, Equation 15.

$$t_{engine} = \frac{60\pi}{\omega} \quad (15)$$

Exhaust manifold delays The time delay in the exhaust manifold is a bit more complicated. In the present model the flow in the exhaust manifold is regarded as a plug flow. This means that there is a transport time delay for the exhaust gases to reach the lambda sensor. In a plug flow there is no mixing along the fluid flow direction. This is shown below.

$$V_{plug\ flow} = \int_{t-d(t)}^t q(s) ds \quad (16)$$

The plug flow waiting time is solved using a variable time delay function, where the λ value is stored in a memory for the time dictated by the time it would take for the gas to go from the exhaust port to the λ sensor. Equation 17 describes this.

$$t_{plug\ flow} = \frac{V\rho}{\dot{m}_{engine}} \quad (17)$$

λ -sensor delays This was implemented as if the λ sensor was a low pass filter, Equation 18

$$\lambda_{meas} = \frac{d}{dt} \frac{\lambda_{calc} - \lambda_{meas}}{\tau} \quad (18)$$

Where:

$\dot{m}_{fuel\ inj}$	[kg/s]	fuel to be injected
\dot{m}_{air}	[kg/s]	air going into the engine
AFs	[-]	stoichiometric air fuel ratio
λ_{meas}	[-]	measured air fuel ratio
$\lambda_{control}$	[-]	lambda intergrator
λ_{calc}	[-]	theoretical value from the model
$air\ flow$	[kg/s]	measured airflow
$fuel$	[kg/s]	fuel to injected
τ	[s]	λ sensor time constant
V	[m ³]	volume in exhaust manifold
ρ	[kg/m ³]	density of the exhaust gasses

The λ sensor senses whether the λ value is above or below 1. Therefore the amplitude of the value is of no interest. λ sensors in ICE are usually binary, and can only indicate the presence or lack of oxygen. I.e, tell if there is oxygen in the exhaust gases or not.

EMISSIONS The emission data for the model are measured steady state at $\lambda = 1$. Speed and air flow tables are designed for emissions in the same way, as described for the torque above. Due to the transients, the actual λ value deviates from its mean value of 1. Then input emissions must be compensated for this.

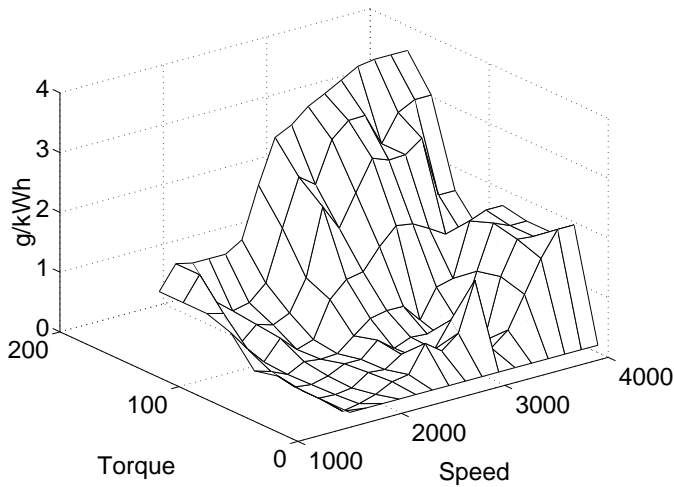


Figure 3: Specific CO Emissions

Figures 3, 4 and 5 come from measurements done at the department.

The factors that influence the regulated emissions as function of λ are well known. The actual emission value is adjusted with regard to the actual λ value. These relations are well known and can be observed in [3].

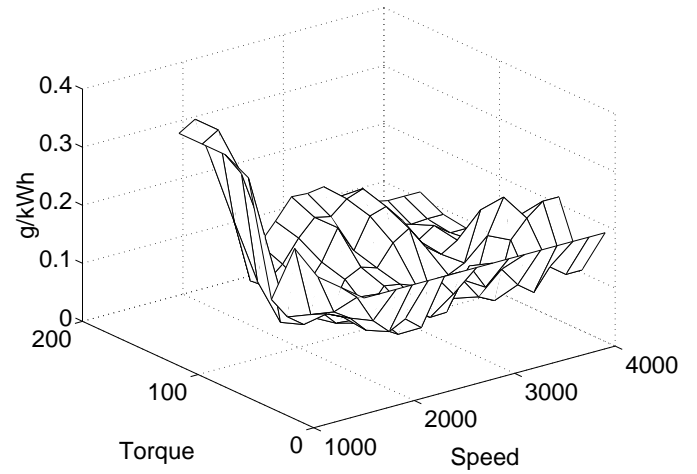


Figure 4: Specific HC Emissions

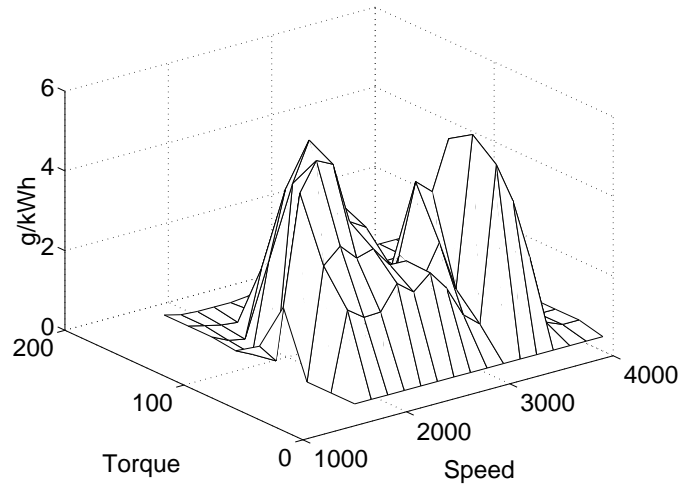


Figure 5: Specific NOx Emissions

SOFTWARE

The chosen programming language for this task was SIMULINK®. This language has a graphical interface that makes it possible in a highly visual environment to, build up the equations that describe the model. The model is built by using standard blocks connected by information carrying lines. This makes it fairly easy to change and develop the model.

IMPLEMENTING THE AIR PART OF THE MODEL

In Figure 6, the SIMULINK® program of the air engine part can be seen.

THE THROTTLE The box named *Throttle* contains Equation 8. It is controlled by the inlet area, the ambient pressure and the pressure in the manifold. The result is mass flow of air into the manifold.

THE MANIFOLD The box named *Manifold* contains Equation 3. Where the difference of the two air flows are integrated to yield the mass of air in the manifold.

By using Equation 5, the pressure in the manifold is calculated and passed to the throttle.

ENGINE BODY The volume flow that the engine is controlled by the engine speed and the engine displacement as in Equation 1. Next, the mass flow is calculated through Equation 2. The density in the manifold is given by Equation 4.

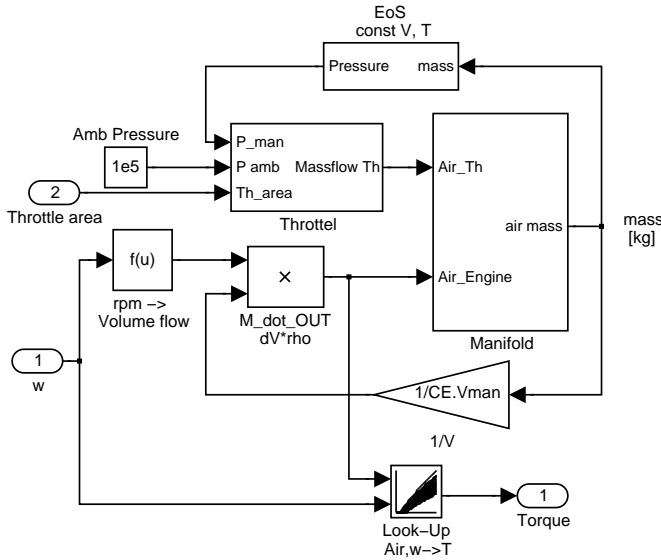


Figure 6: SIMULINK® program of the air model

FORMING TORQUE In this model torque is formed by combining engine speed and airflow through the engine. To do this conversion the airmap that is discussed earlier is used. It is used in the form of Equation 9 and can be seen in Figure 1.

IMPLEMENTING THE FUEL PART OF THE MODEL

Figure 7 shows the complete fuel model including fuel control, closed loop λ -control and the exhaust gas delays.

The air flow information is measured at the inlet port and sent to the lambda control box. Here the amount of fuel that is to be delivered is determined. The lambda algorithm and wall wetting equation make up the resulting amount of fuel that is to enter the engine body. From this the *real* lambda is calculated. This λ is delayed before it is fed into the lambda algorithm.

TIME SCALE

The time step in the model has to be chosen so that the fastest events could be captured at high enough resolution. The time scale of the changes of state in the mani-

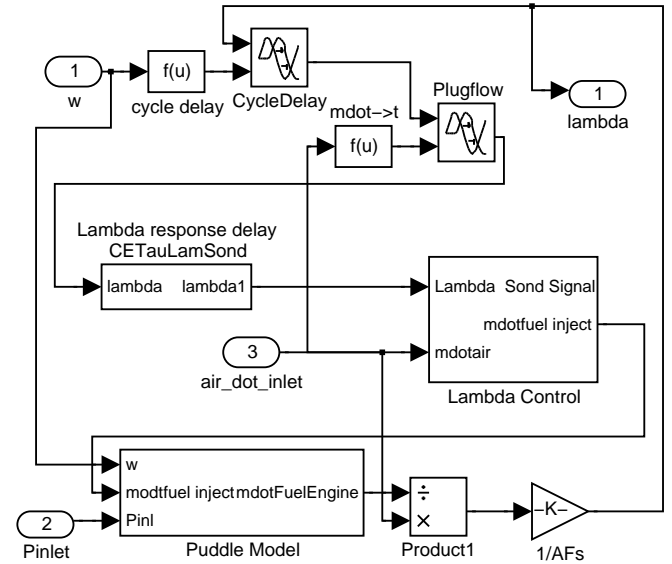


Figure 7: SIMULINK® program of the fuel model

fold is about 0.1 s. The corresponding time scales of the other components in the system are longer. Thus, the time scale of the manifold is dimensioning for the whole model. In order to get high enough resolution, a time step of 0.01s was used. If the sample time is higher than 0.1 the lambda closed loop control stops functioning. Using smaller step size did not affect the solution.

THE MODEL INPUT

The model is based on measured data from a SAAB 2.3l naturally aspirated engine. It is a 16 valve 4 cylinder engine, rated at 110kW at 5500rpm and 212Nm at 3800rpm. The data used for this model have been produced and measured at the department. Hence, the data regarding efficiency and emissions were readily available.

WALL WETTING DATA At the moment no measured data regarding the wall wetting are available. Thus, the parameters used to describe wall wetting, see Equation 11, are used as input. In the "Model Testing" section below the influence of these parameters on lambda excursion are demonstrated.

MODEL TESTING

As was mentioned above, the application for which the model was developed is a hybrid vehicle model. In this overarching model the input to the SI-engine is the engine speed. The demand on the SI-engine is defined as torque. The product of speed and torque is the power supplied to the hybrid system.

CONSTANT SPEED, VARIED TORQUE

Step down Figure 8 shows a test where the demanded torque is suddenly changed to a lower setting. The rich spike is due to of the wall wetting fuel that is drawn into the engine.

The torque begins at a value of 180Nm and ends at 20Nm. Engine speed is held constant at 2000rpm.

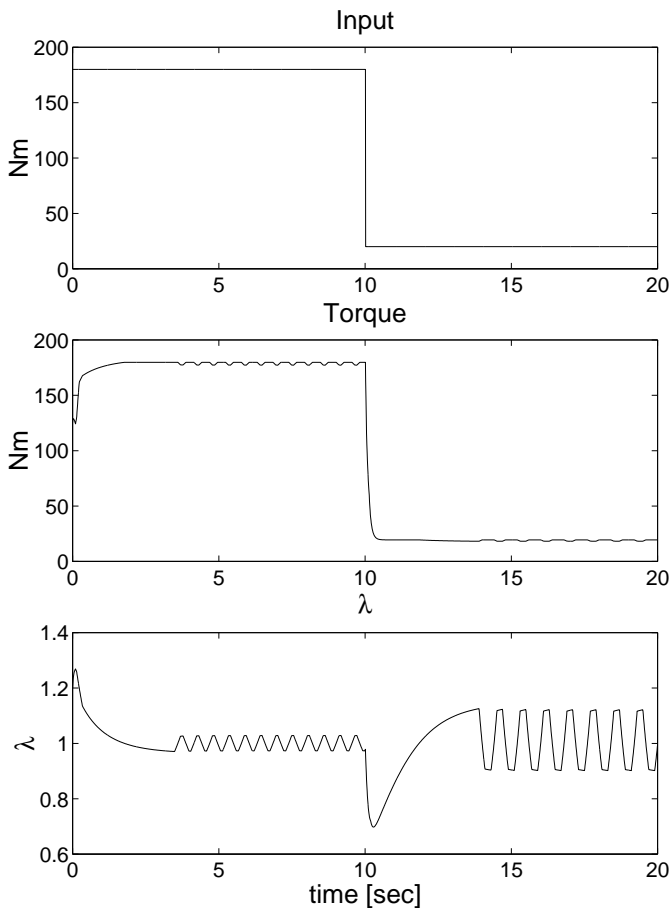


Figure 8: Step down test

Step up The experiment in Figure 9 is a test with an instantaneous positive step change.

The engine was run at a constant engine speed. The throttle is suddenly changed to a new value. The model is not equipped with transient compensation control. This means that the engine will be slow to recover from the stepped load change. Usually in production engines, fuel is added in an open loop fashion which means that shortly after the lean peak (seen in the Figure) a rich peak will follow, induced by the engine control unit (ECU).

The upper curve shows the input torque. It changes momentarily from 20 to 180Nm. The middle curve shows the step response of the engine. The response is governed by a time constant coming from the air flow and from the fuel flow. The lower curve shows the λ value. It rises because of the increased wall wetting. This is due to higher fuel flow and to higher inlet pressure that cause the fuel mass in the inlet to increase.

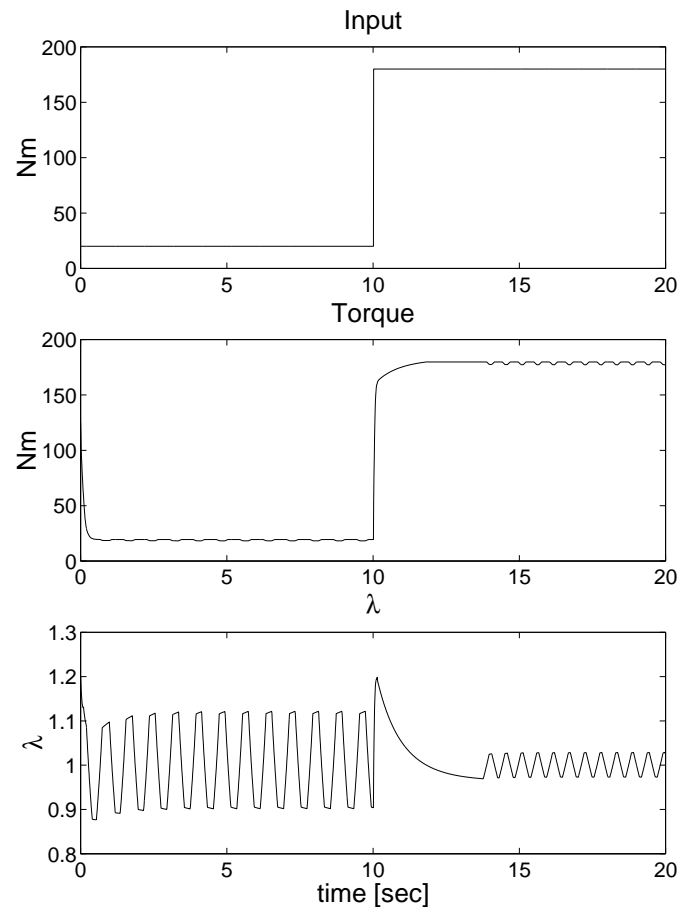


Figure 9: Step up test

SLOW RAMP TEST Ramping the torque with constant speed. In this experiment the torque was changed from 20 to 180Nm. But here it was slowly ramped, with a ramp time of 2 seconds. See Figure10.

The torque set signal is shown first, second the resulting torque from the engine and third the resulting λ -value. When the load change takes place the lambda signal becomes asymmetric, which would indicate that there is a shift in λ , that can result in an increased amount of engine exhaust emissions.

FAST RAMP TEST Ramping the torque with constant speed. In this experiment the torque was changed from 20 to 180Nm. But here it was ramped faster, with a ramp time of 0.5 seconds, as in Figure 11. In this test it took more time for the λ -value to settle.

In the Figure the input signal is first, resulting torque is in the middle and last the λ -value. Here the lambda ripple ceases for 1 second during the load change. It is lean before returning to a λ ripple.

FINDING THE BORDER FREQUENCY WHEN VARYING THE TORQUE In this trial the engine was set to run at an engine rpm of 2000, and then the torque demand was

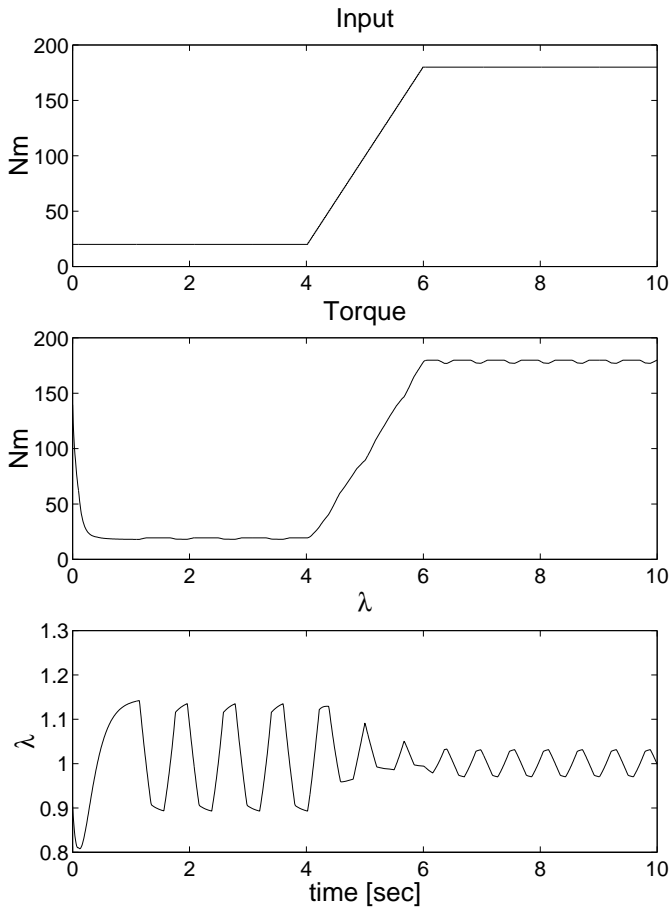


Figure 10: Slow ramped torque change

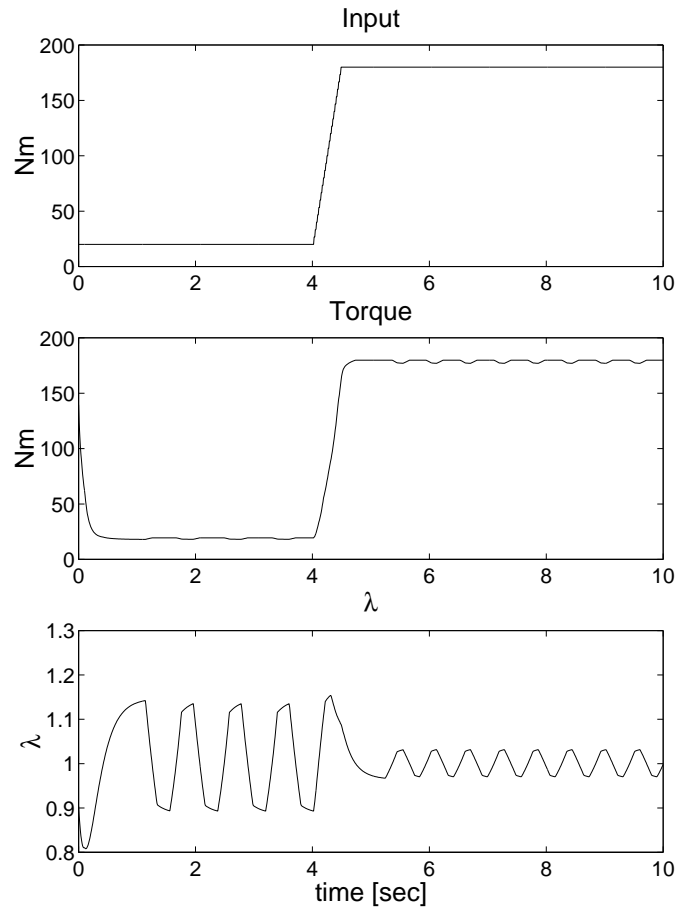


Figure 11: Fast ramped torque change

varied in a sinusoidal fashion. And it was varied from a mean value of 75Nm plus/minus 50Nm. At these large torque fluctuations the lambda control functioned properly if the frequency was below 0.5 [rad/s] or 0.08 [Hz]. If it is above this value the control no longer has any effect on the lambda value, which is now controlled by the load change.

The conclusion would be that wall wetting has a great effect on the amount of fuel that is about to enter the engine. If the wall wetting is smaller, the border frequency increases.

With a puddle time constant of 1 second the border frequency is about 0.5 (or 0.08 [Hz]); if the puddle constant is changed to 0.5 the frequency rises to 2 (or 0.31 [Hz]).

In Figure 12, the dark and light sectors show when the mixture is fuel lean or rich. At a low frequency it is possible to see a constant pattern of these shifts. But as the frequency increases towards 1 [rad/s] this pattern changes and the frequency is much lower. Here lambda control no longer has any effect, as the load changes are too rapid.

The conclusion from Figure 12 is that there is an upper limit to the load change frequency. This kind of load cycle is not really achieved under real conditions. But as in a hybrid vehicle it is possible to affect the way the en-

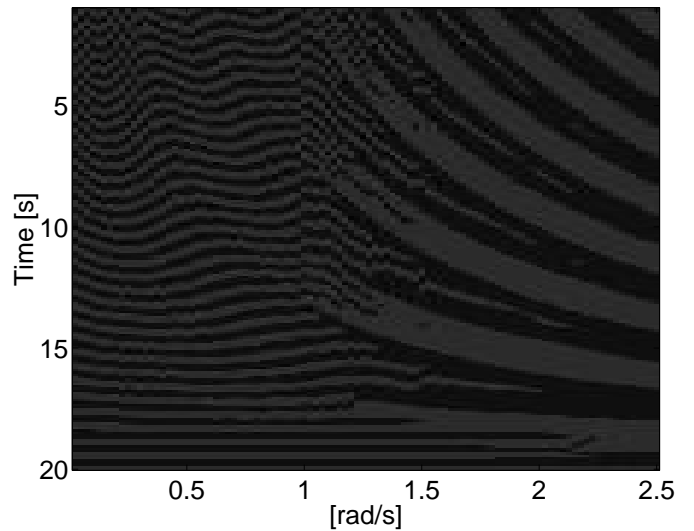


Figure 12: Lambda shifts

gine is loaded, this might be a way to determine maximum frequency of load change.

SHORTAGES OF THE MODEL

The model does not take into account residual gas or tuning effects during transients in the exhaust and inlet

manifold. The zero dimensional model has trouble solving problems of tuning. The absence of a commercial engine management model is a problem, as it largely affects the fuel management.

One severe drawback of the model is the absence of fuel transient control. On the other hand, if the model is correctly tuned. It would be possible to design a feed forward loop that takes wall wetting into consideration.

MODEL VERIFICATION

The model has not yet been verified with hard data. However, the model worked as expected. There are fine tunings to be made to fit the engine to every particular engine that is to be simulated. Since the core of the model is based on physical facts, it should be easy to adjust it to other makes of engines.

RESULTS

When the presented model is subjected to load changes a λ deviation can be detected. This λ deviation depends on the time delay of the close coupled signal and the wall wetting of fuel in the inlet manifold.

When the fuel evaporation from the puddle was increased, the border frequency increased. Decreasing the time constant (wall wetting) of the fuel in the inlet manifold made the frequency four times higher. So this is an important factor to consider when designing SI-engines.

CONCLUSION

A model describing the SI-engine has been developed. Its general characteristics are that of a typical engine. It shows the phenomena to be studied, but in order to compare this model to a real engine, it requires tuning and verification.

The model shows that there are shifts in the λ value at load changes. The faster and larger the load change the larger the deviation of λ .

One aim in this task was to find the border frequency. This means that over a certain load change frequency the λ value becomes irregular. This yields the assumption that the exhaust gas treatment works less efficiently. Evidence that the λ control works differently at different load frequencies can be seen in Figure 12.

REFERENCES

- [1] Göran Almkvist. *Transient Air to Fuel Ratio response in a Fuel Injected S.I. Engine*. ISBN 91-7197-097-5.
- [2] Rolf Egnell. *α - 03 Simulinkmodell av en turboladdad ottomotor*. ISBN 0282-1990.

[3] John B. Heywood. *Internal Combustion Engine Fundamentals*. ISBN 0-07-100499-8.

[4] Jim S. Cowart and Wai K. Cheng. *Trottle Movement Rate Effects on Transient Fuel Compensation in a Port-Fuel-Injected SI Engine*. SAE 2000-01-1937.

CONTACT

Petter Strandh
E-mail: petter.strandh@vok.lth.se

Rolf Egnell
E-mail: rolf.egnell@vok.lth.se

Dept Heat & Power Engineering
Div. Combustion Engines
Lund Institute of Technology
S-221 00 LUND
SWEDEN

F

Comparative Study of Generic Hybrid Topologies

This paper was presented in Berlin at the Electric Vehicle Symposium no.18 (EVS 18).

Comparative Study of Generic Hybrid Topologies

Karin Jonasson, Petter Strandh, Mats Alaküla

Abstract

This paper presents a detailed comparison of the performance, efficiency and emissions of four different hybrid topologies. The comparison is made by simulation with all motor models, battery models, control laws etc as similar as possible between the hybrid types. The simulation model uses an ICE model where efficiency and emissions are dynamically accounted for. The impact of transient operation of the ICE in the different hybrids is thus evaluated in as fair a comparison between different topologies as possible. All modelled hybrids are equipped with ICE and electrical machines with rated power and other properties as like a Toyota Prius as possible. The comparison is made when running a US06 driving cycle.

Keywords: HEV (hybrid electric vehicle), simulation, hybrid strategy, emissions, planetary gear.

1 Introduction

Hybrid electric vehicles are motivated by reduced fuel consumption and emissions due to a smoother use of the ICE being the prime energy converter. Several topologies can be put together that enables such smoothened operation of the ICE, like the series hybrid, the parallel hybrid and combinations of these like the strigear hybrid that uses a clutch to reconfigure between series and parallel configuration and the power split hybrid, that uses a planetary gear box that allows some of the energy to flow the “parallel way” to the wheels and some the “series way”.

The various vehicles that are commercially available, using any of the mentioned topologies, do not allow a direct comparison of performance since to many parameters are different, like vehicle weight, ICE size and type, control method, fuel etc. The work presented in this paper is made to make an as fair as possible comparison of different topologies. For this purpose, comprehensive simulation models are built, that include all major energy converters, all relevant limitations due to speed and torque etc. An ICE model is included that does not only model the behavior in stationary operation, but also in transient operation. This means that the consequences of different control laws are accounted for in the fuel consumption and emissions even in transient operation.

The result will stress the effects of the different topologies and form a foundation for choice of hybrid topology.

1.1 Main results

The most important result is that for a demanding driving cycle, like the US06, a parallel hybrid is the one that gives the lowest fuel consumption, closely followed by the strigear and power split hybrids while the series hybrid having the highest consumption. The simplicity with a pure parallel hybrid, having only one electrical machine with one power electronic converter makes it a strong alternative compared to the strigear and power split hybrids.

1.2 Outline

This paper will start with clarifying the hybrid vehicle concept and describe four possible topologies in som more detail. This will be followed by a description of the models components and the power distribution control used in the simulation models. There after, the simulated test vehicles are presented and their real counterpart. Then are the comparisons presented, followed by the simulation results. The paper ends with the conclusions.

2 Hybrid Vehicles

Hybrid vehicles in this paper, combine a combustion engine with at least one electric machine in the traction system. By combining the ICE and the electric machines in different ways, various topologies are obtained. By adding more motors and gears the numbers of possible topologies will increase rapidly. Below follows a description of the hybrid vehicles examined in this comparison. [1]

2.1 Parallel hybrid

The parallel hybrid vehicle (see figure 1) has a combination of drive systems where each driving shaft is connected to an energy source. There is a direct mechanical connection between the ICE and the wheels. This reduces the amount of power conversions from the prime energy source, which increase the efficiency of the vehicle.

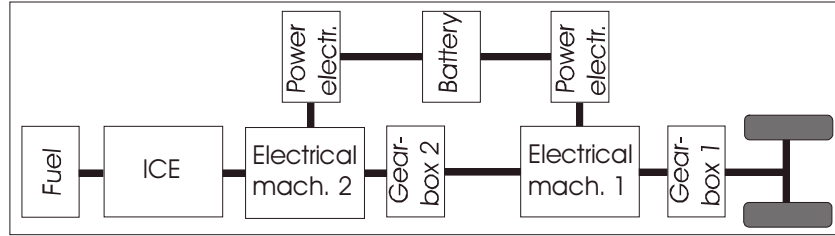


Figure 1: Parallel hybrid structure

2.2 Series hybrid

Series hybrid vehicles have a combination of energy sources (see figure 2). There is no mechanical connection between the ICE and the wheels. All energy from the prime energy source is converted to electric energy as an intermediate form before it can reach the wheels. This facilitates the ICE to be switched off in zero emission zones. The working point of the ICE can, owing to this, be chosen freely. The drawback is the amount of transformations the energy has to perform from the ICE to the wheels.

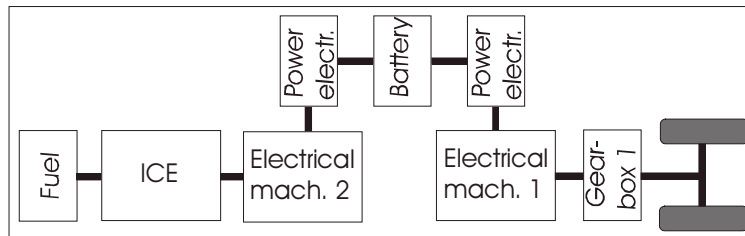


Figure 2: Series hybrid structure

2.3 Strigear hybrid

The Strigear hybrid is actually a combination of a parallel and a series hybrid vehicle (see figure 3) [2]. By replacing the single electrical machine in a parallel hybrid with two, with a clutch in between them, it is possible to switch between the two modes. The onboard computers are given the task to compare the predicted over all losses from the two hybrid concepts. The best solution is chosen, i.e. the clutch is engaged or disengaged. The name strigear is a short form of “sequentially run, triple gearbox connected engine/motor hybrid” [3].

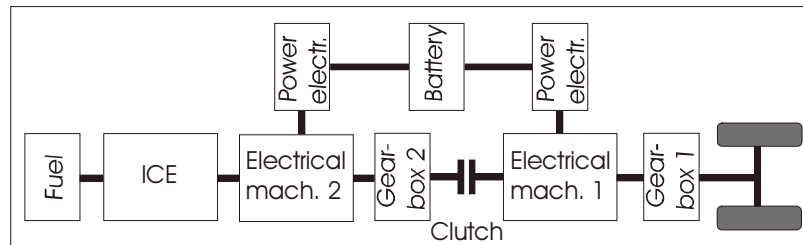


Figure 3: Strigear hybrid structure

This demands two electric machines, one extra clutch and computer capacity to handle the momentary loss comparison that is made. The benefit is to be able to choose the best configuration at any time.

2.4 Power split hybrid

The Power Split Hybrid (PSH), even called complex, combined or dual hybrid vehicle, has a blurred transformation between the series and parallel hybrid state (see figure 4). A planetary gearbox is used with two electrical machines (one on the ring wheel, one on the solar wheel and the ICE connected to the carrier). At most operating points some of the prime energy flows from the ICE directly to the wheels as in a parallel hybrid, and some flows via the electrical machines as in a series hybrid. The proportion between these two energy flows is speed dependent and at a certain speed it works as a pure parallel hybrid. In most other operating points it's partially a series hybrid, which means several conversions of the energy that flows the "series" way from the prime energy source to the wheels.

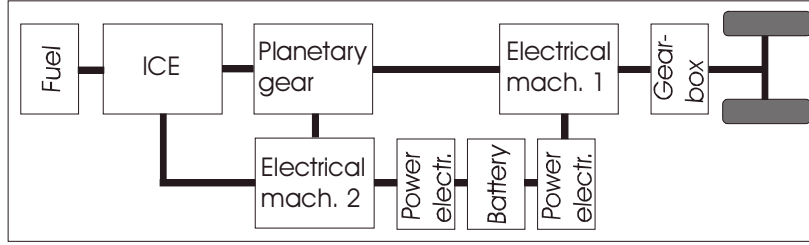


Figure 4: PSH structure

There are many possible combinations of a PSH. While using reduction gears, CVT, advanced planetary gear, clutches and different numbers of motors the possible number of combinations grows rapidly. The system can cause a power vicious circle that cost unnecessary high transmission losses.

2.4.1 Planetary gear

The planetary gear (see figure 5) has three shafts, which are connected to the sun-, carrier- and the ring wheel. They are connected to the electrical machine 2, the ICE and the electrical machine 1 respectively. The size and number of the wheels, number of pinions, number of planets, wheel inertia, rotational friction etc influences the behavior of the gear.

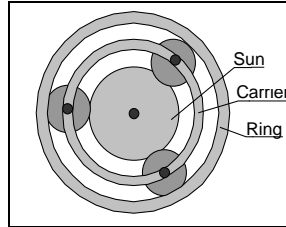


Figure 5: Planetary gear

In the simulation model the fundamental dynamic equations for the planetary gear have been used. By forming a matrix and replacing the expressions formed by invariables (moment of inertia, numbers of teeth, number of planet-wheels and mass of the planet wheel) with k_{11} , k_{12} and k_{13} etc, the equations are given the following structure where T_{frict} is the load on the ring wheel due to road and rolling friction on the car. [4]

$$\frac{d}{dt} \begin{bmatrix} \omega_r \\ \omega_c \\ \omega_s \end{bmatrix} = \begin{bmatrix} k_{11} & k_{12} & k_{13} \\ k_{21} & k_{22} & k_{23} \\ k_{31} & k_{32} & k_{33} \end{bmatrix} \cdot \begin{bmatrix} T_r \\ T_c \\ T_s \end{bmatrix} + \begin{bmatrix} k_{11} \\ k_{21} \\ k_{31} \end{bmatrix} \cdot T_{frict} \quad (1)$$

In the strigear hybrid there is also an instantaneous comparison of the estimated total losses in the series and the parallel hybrid mode. Based on this estimate, the most suitable configuration (series or

parallel) is selected and the clutch is operated accordingly. The selection signal is low pass filtered and is given a suitable hysteresis so the system won't get too spasmodic.

Electric machine 1 and 2. In these models the electrical machines and corresponding power electronics are represented together as a look up table of efficiency depending on speed (~ voltage) and torque (~current). In addition the maximum torque is limited taking field weakening operation into account. Transient torque boost is not represented.

ICE. This sub model contains a quasi-stationary model with transient behaviour. This means that it is built up basically by using tables, but also has dynamic equations for describing the inlet manifold states, the fuel delivery and wall wetting as well as closed loop control of the air/fuel ratio. This makes it behave like a naturally aspirated gasoline engine, with a three-way catalyst. However, the catalyst as such is not modelled in the present version of the sub model.

Transmission. The model includes the basic equations for the gearboxes, including a fixed efficiency (99%) of each gear step. In the parallel hybrid a 5 speed automatically shifted “manual” gear box is used. In the planetary gear the ICE is connected to the carrier, the electrical machine 2 to the sun wheel and finally the electrical machine 1 and the wheels of the vehicle are connected to the ring wheel.

Friction forces. The air and rolling resistance are calculated as a function of the speed and vehicle size, and fed back to the transmission expressed as a torque input to the gearbox.

Battery. The battery model represents the battery losses with a fixed charge/discharge efficiency of 95%. A thermal model is included with one thermal node inside the battery pack for a rough estimate of the battery temperature with the various topologies and control methods. One of the output level shows the state of charge (SOC), which has a reference value of 70 % to avoid an over charge.

3.4 Power distribution - details of the control of energy flows

In the power distribution block, the references for the required torque from each of the main energy converters are calculated. These torques are calculated as a function of the instantaneous tractive power demand, the auxiliary power demand, the deviation of SOC in the battery and finally the actual speed and the speed reference of the vehicle and the different machines.

A fundamental consideration within this block is that the dynamic operation of the ICE must be limited. It can be argued that an ICE consumes unproportional amounts of fuel and generates unproportional amounts of emissions when making changes of operating point with a certain rate, compared to the fuel consumption and emissions in stationary operation [5]. The simplest way to limit the dynamic operation of an ICE is to low pass filter the power requirement on the ICE. The filter time constant must thus be selected to ensure quasi-static operation of the ICE. The ICE power requirement is thus given by equation 2.

$$\frac{dP_{ice}}{dt} = \frac{P_{tractive} + P_{aux} + k(SOC^* - SOC) - P_{ice}}{\tau_{ice}} \quad (2)$$

The stationary efficiency or emissions of an ICE can be expressed in a map as a function of speed and torque. This disregards temperature dependence, ageing dependence etc. From this map the best operating point for any power level within the ICE's operating range can be selected. Figure 7a) shows the efficiency map and the optimum torque and efficiency as a function of the requested power derived from the efficiency map.

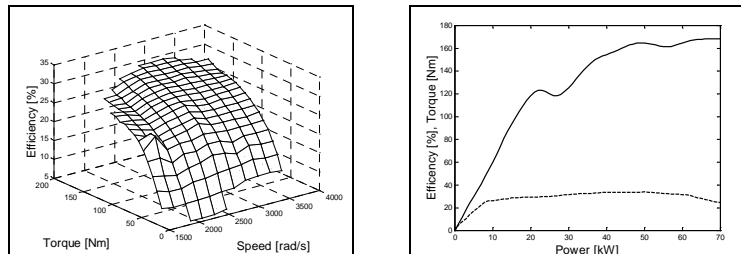


Figure 7: a) Efficiency map for ICE. b) The optimal working point for the ICE.

In all hybrid models used in this paper, the torque and speed references for the ICE is calculated from P_{ice}^* via a look up table like the one in figure 7 b), the references being denoted T_{ice}^* and ω_{ice}^* . The ways to realize these references are slightly different in the different hybrids according to the following sections.

3.4.1 Series hybrid strategy

The tractive torque is entirely supplied by electrical machine 1 (EM1) in figure 2, and its reference can be calculated directly from the wheel torque reference given by the driver according to equation 3 where gr_1 is the gear ratio in the final gear of the drive train.

$$T_{em1}^* = \frac{T_{wheel}^*}{gr_1} \quad (3)$$

The torque reference for the second electrical machine (EM2) is calculated to obtain the desired speed of the ICE, according to equation 4 where K_s is the proportionality gain of the EM2 and the ICE speed controller.

$$T_{em2}^* = K_s \cdot (\omega_{ice}^* - \omega_{ice}) - T_{ice}^* \quad (4)$$

3.4.2 Parallel hybrid strategy

Since the ICE in the parallel hybrid is mechanically connected to the wheels, the speed reference for the ICE can only be reached if the gearbox is able to set up as suitable gear ratio (gr_2) given the instantaneous combination of vehicle speed and ICE speed reference. The most suitable gear ratio is selected and a set of new references for the ICE torque and speed are calculated by equations 5 and 6.

$$gr_{2,min} < gr_2 = \frac{v_{vehicle}}{r_{wheel} \cdot \omega_{ice}^*} \text{ "in 5 fixed steps"} < gr_{2,max} \quad (5)$$

$$\omega_{ice}^* = \frac{v_{vehicle}}{r_{wheel}} \cdot gr_2 \quad \& \quad T_{ice}^* = \frac{T_{ice}^* \cdot \omega_{ice}^*}{\omega_{ice}^*} \quad (6)$$

Given the new set of ICE torque and speed references, the torque references for the electrical machine(s) are calculated according to equation 7 and 8. Since the simulation model contains two electric machines, the torque demand is distributed proportional to the best of their ability given the operating conditions. Consideration is taking to the two gearboxes, which are included in the model. This is made in equation 7 and 8.

$$T_{em1}^* = \frac{T_{wheel}^* - (T_{ice}^* \cdot gr_1 \cdot gr_2)}{gr_1} \cdot \frac{T_{em1,max} \cdot gr_1}{T_{em1,max} \cdot gr_1 + T_{em2,max} \cdot gr_1 \cdot gr_2} \quad (7)$$

$$T_{em2}^* = \frac{T_{wheel}^* - (T_{ice}^* \cdot gr_1 \cdot gr_2)}{gr_1 \cdot gr_2} \cdot \frac{T_{em2,max} \cdot gr_1 \cdot gr_2}{T_{em1,max} \cdot gr_1 + T_{em2,max} \cdot gr_1 \cdot gr_2} \quad (8)$$

If only one machine is used, the specification for the other of the two in the model is set to zero maximum torque in equation 7 and 8. The maximum torque values, used in equations 7 and 8, are momentary values taking field weakening into account, and do thus vary with speed.

3.4.3 Strigear hybrid strategy

The strigear hybrid is able to run as a series or a parallel hybrid depending on the position of the clutch. The selection of the clutch position is based upon a comparison of two loss estimates, one for each topology. The loss estimates are calculated from equation 9 and 10.

$$\begin{aligned} \hat{P}_{loss,serie} = & \hat{P}_{loss,em1} + \hat{P}_{loss,em2} + \hat{P}_{loss,ice} + P_{em1} \cdot (1 - \eta_{gr_1}) + \\ & + (P_{em1} + P_{em2}) \cdot (1 - \eta_{batt}) \end{aligned} \quad (9)$$

$$\begin{aligned}\hat{P}_{loss, parallel} = & \hat{P}_{loss, em1} + \hat{P}_{loss, em2} + \hat{P}_{loss, ice} + (P_{em1} + P_{em2}) \cdot (1 - \eta_{batt}) \\ & + P_{em1} \cdot (1 - \eta_{gr1}) + (P_{ice} + P_{em2}) \cdot (1 - \eta_{gr1}) \cdot (1 - \eta_{gr2})\end{aligned}\quad (10)$$

η_{gr1} and η_{gr2} are the efficiencies of the gear boxes 1 and 2 respectively. The selection rule is simple; the configuration with the lowest estimated losses is used. The comparison of the two loss estimates is low pass filtered and a small hysteresis is used to limit the number of clutch position changes.

3.4.4 Power split strategy

In this case the ring motor (EM1) is used to produce the instantaneous torque for traction. The combination of the ICE and the solar motor (EM2) are used to supply the low pass filtered power by using EM2 to speed control the ICE.

Since the torque demand for the ICE is known, equation 11 can be used to calculate the additional torque references, see also equation 12 - 14.

$$\begin{bmatrix} T_{em1}^* \\ T_{em2}^* \end{bmatrix} = \begin{bmatrix} k_{11} & k_{13} \\ k_{31} & k_{33} \end{bmatrix}^{-1} \cdot \begin{bmatrix} \frac{(\omega_{em1}^* - \omega_{em1})}{\tau_x} \\ \frac{(\omega_{em2}^* - \omega_{em2})}{\tau_z} \end{bmatrix} - \begin{bmatrix} k_{12} \\ k_{32} \end{bmatrix} \cdot T_{ice}^* + \begin{bmatrix} 1 \\ 0 \end{bmatrix} \cdot \frac{T_{wheel}^*}{gr_1} \quad (11)$$

where

$$\omega_{em1}^* = \frac{gr_1}{r_{wheel}} \cdot v^* \quad (12)$$

$$\omega_{em2}^* = R_{planet} \cdot \omega_{em1}^* + (1 - R_{planet}) \cdot \omega_{ice}^* \quad (13)$$

$$R_{planet} = \frac{\omega_{solar} - \omega_{carrier}}{\omega_{ring} - \omega_{carrier}} \quad (14)$$

4 The particular case simulated

4.1 Reference vehicle

In this comparison a vehicle is chosen which is as alike the Toyota Prius, available in the European market, as possible. Table 1 shows the most important data of the Prius [6]:

Table 1: Data for Toyota Prius, used as input in the simulation models.

Property	Value
Vehicle mass (total) [kg]	1645
Front area [m ²]	2.52
Max power EM1 [kW]	33
Max torque EM1 [Nm]	304
Max speed EM1 [rad/s]	585
Max power EM2 [kW]	33
Max torque EM2 [Nm]	68
Max speed EM2 [rad/s]	471
Max power ICE [kW]	53
Max torque ICE [Nm]	140
Gear ratio ring wheel/wheel axis	3.5
Battery type	NiMH
Maximum charge [kWh]	1.7

4.1.1 Machine sizes

The machine sizes are selected to correspond to the Prius data, known by the authors, as good as possible. Table 2 shows the selected data used in the simulations. Note that the pure series hybrid has a smaller ICE and a larger EM1, with preserved total installed power

Table 2: Data for the electrical machines in the simulation models.

Property	Series	Parallel	Stigear	PowerSplit
Max power EM1 [kW]	43	33	33	33
Max torque EM1 [Nm]	514	394	789	304
Max speed EM1 [rad/s]	167	167	167	585
Max power EM2 [kW]	33	33	33	33
Max torque EM2 [Nm]	70	140	140	140
Max speed EM2 [rad/s]	471	471	471	471
Max power ICE [kW]	43	53	53	53
Max torque ICE [Nm]	91	112	112	112

The electrical machines are modelled as a look up table with efficiency, where also the power electronic losses are included. This is motivated by the fact that speed and voltage are almost proportional in stationary operation and that current and torque are almost proportional in stationary operation. Each electrical machine is given the efficiency characteristic shown in figure 8, but the speed and torque axes that are scaled according to the specifications in table 2.

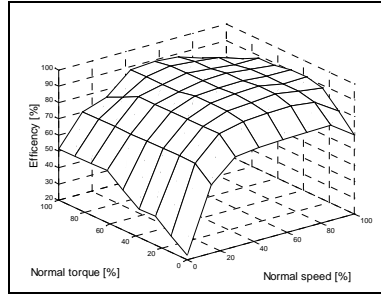


Figure 8: The normalized value for efficiency, used in the electric machines.

4.1.2 ICE

The ICE model describes a naturally aspirated gasoline engine. Input data are the engine speed and the torque demand. Outputs are the actual torque, the fuel consumption and the emissions. During simulation, the engine model tries to deliver the demanded torque as accurately as possible, taking into consideration the different dynamic phenomena in the inlet manifold and in fuel flow characteristics. In short the inlet manifold can be regarded as a low pass filter with a time constant of about 0.1s. The model also contains a fuel model, which includes equations that describes how much of the injected fuel that instantaneously enters the engine and how much is stuck to the walls of the inlet port. This is called the wall-wetting model. There is also a closed loop model for adjusting the fuel injection to achieve the desired stoichiometric air/fuel mixture. If the delivered fuel does not exactly match the air in the engine, the operation of the three-way catalyst is jeopardized with the consequence of an increase in vehicle exhaust emissions.

The interesting part of the engine model is the formation of torque. The airflow is derived from the manifold and throttle sub model. The engine speed is known. By using these two variables as input to a look up table, the torque at stoichiometric conditions is derived. This torque is then corrected to achieve the torque at the actual air/fuel ratio. A graphical representation of such a look up table, also called air map, is shown in figure 9. Air maps can be derived from efficiency maps or fuel consumption maps.

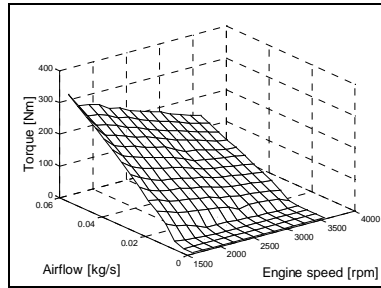


Figure 9: Shows the airmap that is the core of the ICE model.

One of the most interesting variables in a study like this is the size of the ICE. The maximum efficiency for a naturally aspirated SI engine can be found at full torque and around the middle of the engines operating speed range. So in order to minimize the fuel consumption, the engine size should be chosen so that the dominating load points of the application, in this case the hybrid vehicle, are found within this region.

The scaling of the ICE has been achieved by changing the number of cylinders. By this procedure it is reasonable to assume that the engine maintains its main characteristics, apart from the torque. By decreasing the number of cylinders the friction losses in the engine should be higher and, hence, decreasing the efficiency somewhat. This has, however, not been taken into consideration in the present model.

Figure 10 shows how calculated engine data compares to measured data. A real engine has been run in transient operation and logged. Afterwards the model engine has been run according to the same cycle. In the figure the upper curve shows how the air fuel ratio differs between the real engine and the simulated engine. The lower curve is the torque change. Conclusions from the graph is that the wall-wetting model, to some extent describes the wall wetting that occurs in the real engine.

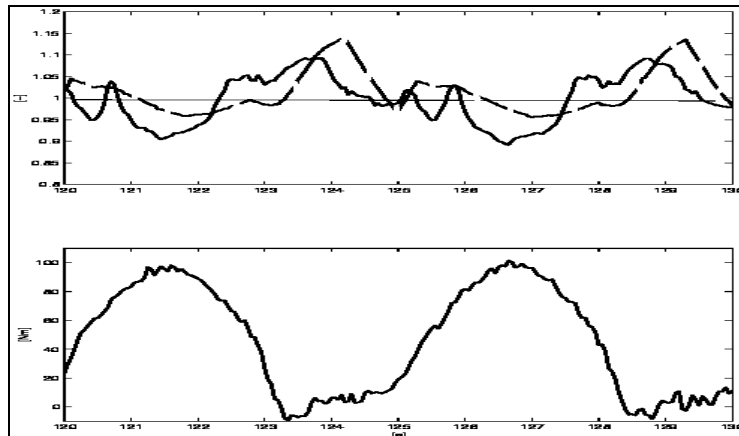


Figure 10: Upper graph: Dashed line is the simulated air fuel ratio and the solid line is taken from real engine tests. Lower graph: Torque change.

The way that the model has been built makes it possible to simulate other makes and sizes of engines, as long as they are naturally aspirated. This is accomplished by modifying the air map, the inlet manifold size and the exhaust manifold size combined with control parameters from the engine control unit.

In the present model, emissions are calculated using values that have been measured after the catalyst. The emissions data comes from in house measurements performed on a SAAB 2.3l naturally aspirated engine. When the engine operates in a transient mode, during a fast load change and when the fuel air ratio is deviated from the stoichimetric, the emissions are assumed to increase by the same percentage as the emissions increase before the catalyst. Thus, it is assumed that the conversion efficiency of the catalyst is maintained outside the “lambda” window. This could be the case for fast and not so far lambda excursions, due to the storage capability of the catalyst.

4.1.3 Battery

The battery model is based on the assumption of a constant efficiency (η_{batt}) when changing the SOC. The total electric power handled by the battery is the sum of the power to the two electrical machines and the auxiliary power. The sum is called P_{batt} . The losses in the battery are thus calculated according to equation 15.

$$P_{loss,batt} = (1 - \eta_{batt}) \cdot P_{batt} \quad (15)$$

The state of charge (SOC) of the battery is calculated as an integral of the battery power reduced by the losses according to equation 16.

$$SOC = \begin{cases} \frac{\int (P_{batt} - P_{loss,batt})}{W_{batt,max}} = \frac{\int \eta_{batt} \cdot P_{batt}}{W_{batt,max}} & \text{when charging} \\ \frac{\int (P_{batt} + P_{loss,batt})}{W_{batt,max}} = \frac{\int P_{batt}}{W_{batt,max} \eta_{batt}} & \text{when discharging} \end{cases} \quad (16)$$

A thermal model is also included according to equation 17.

$$\frac{dt_{batt}}{dt} = \frac{P_{loss,batt}}{C_{batt_thermal}} - \frac{t_{batt} - t_{outer}}{C_{batt_thermal} \cdot R_{batt_thermal}} \quad (17)$$

where t_{batt} and t_{outer} is the temperature inside and outside the battery. C_{batt} and R_{batt} are the thermal capacitance and thermal resistance respectively. The battery data used in the simulations are given in table 3.

Table 3: Battery data used in the simulations

Property	Value
Maximum energy [kWh]	1.7
Charging efficiency [%]	95

4.1 Drive cycle

The simulations in this paper have been made with the US06 cycle, which is a driving cycle that describes highway driving. It contains examples of aggressive accelerations and high speed driving. It is 12.8 km long and has a mean velocity of 78 km/h and with a maximum speed of 130 km/h. See figure 11a) and b).

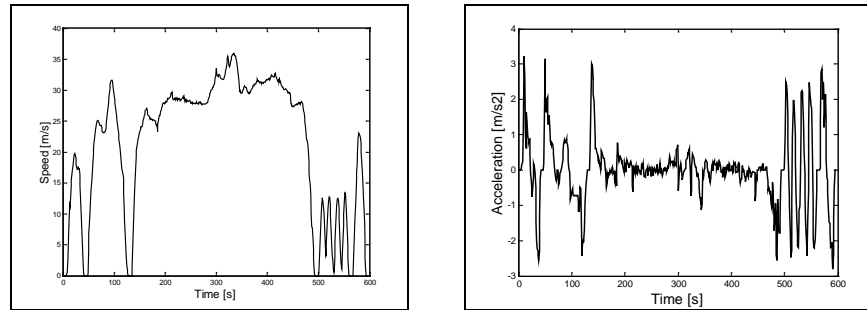


Figure 11: Drive cycle US06: a) Velocity b): Acceleration

The US06 Supplemental Federal Test Procedure (SFTP) is developed to address the shortcomings with the FTP-75 test cycle in the representation of aggressive, high speed and/or high acceleration driving behavior, rapid speed fluctuations and driving behavior following startup. [8]

5 Results

The different topologies are simulated with two different time constants, in the determination of the ICE power reference, see equation 2. The time constants are chosen to 10 seconds and 2 seconds. The

longer time constant guarantees quasi steady state operation of the ICE, with retained emission-control. The shorter time constant is on the verge of transient operation of the ICE. Table 4 shows the total fuel consumption and the emissions.

Table 4: Emissions and fuel consumption for the hybrids.

Hybrid	τ_{ice} [s]	Fuel [l/100 km]	NO _x [g]	CO [g]	HC [g]
Series	2	9.0	2.8	9.2	0.42
Parallel	2	6.0	2.5	4.9	0.32
Strigear	2	6.3	2.4	5.3	0.35
Power split	2	6.8	2.8	4.2	0.34
Serie	10	9.0	3.1	8.6	0.43
Parallel	10	6.3	2.6	4.9	0.34
Strigear	10	6.5	2.4	5.7	0.40
Power split	10	7.1	2.8	3.2	0.41

The vehicles are able to follow the drive cycle. Figure 12 a) shows one section from one of the simulations with the parallel hybrid. The charge controller is able to retain the SOC, which cycle is shown in figure 12 b) and c) shows the total tractive power and the ICE power. The ICE power is the low pass filtered traction demand.

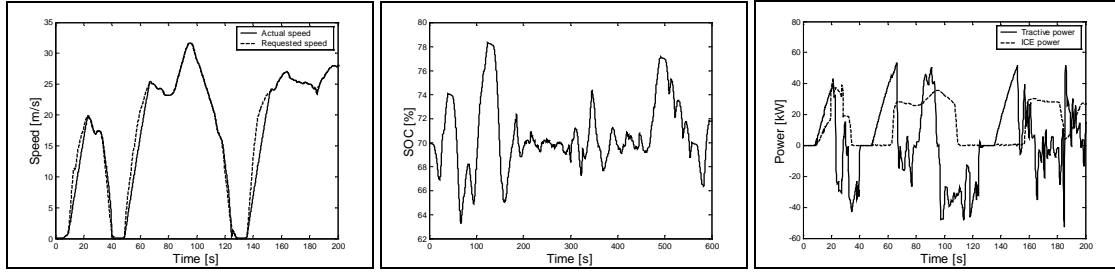


Figure 12: The parallel hybrid vehicle simulated with $\tau_{ice} = 10$ s. The figure shows the first 200 seconds. a) The actual speed (solid) and the requested speed (dashed). b) SOC c) Tractive power (solid) and ICE power (dashed).

The hybrid's machines perform within their speed and torque limitations, which is shown in figure 13.

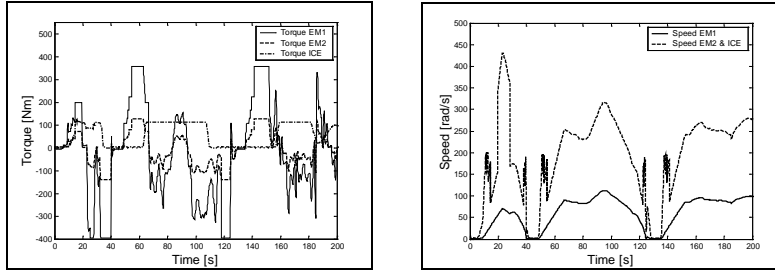


Figure 13: Same simulation as above. a) Torques from EM1 (solid), EM2 (dashed) and ICE (dash-dotted). b) Engine speed for EM1 (solid), EM2 and ICE (dashed, the two last machines have the same value).

6 Conclusions

From the simulations it can be concluded that the highest efficiency, as expected, is reached with topologies allowing a direct path from the ICE to the wheels with a minimum of energy conversions. The pure parallel hybrid is the best, but the difference to the strigear and power split hybrids is small. The series hybrid comes out last, and is not suitable for the high power applications like a Prius size vehicle running the US06 drive cycle. It can thus be argued that the pure parallel hybrid, equipped only with one electrical machine is the best solution due to the low complexity in combination with high performance.

7 References

- [1] J. van Mierlo, G. Maggetto, *Comparison of power algorithms in hybrid vehicles*, EVS 15, 30th September to 3rd October 1998, Brussels, Belgium.
- [2] L. Stridsberg, *Dual Electric Motor Hybrid Powertrain*, EVS 15, 30th September to 3rd October 1998, Brussels, Belgium.
- [3] www.powertrain.se, 2001-07-11
- [4] L. Vedmar, *Transmissioner*, Maskinelement, Lunds tekniska högskola, 1998, Lund, Sweden.
- [5] C. Andersson, *Observations on electric hybrid bus design*, Licentiate thesis, Department of Industrial Electrical Engineering and Automation, Lund University 2001.
- [6] *PRIUS, New Car Features, May 2000*, Toyota Motor Company, 2000, Japan.
- [7] P. Strandh, *Modeling SI-engines for hybrid vehicles*, SAE 2001-01-0575.
- [8] www.dieselnet.com/standards/cycles/ftp_us06.html, 2001-07-10.

8 Authors

Karin Jonasson, BSc (Conservation), BSc (Civil Engineering).

University of Lund, Dept. of Industrial Electrical Engineering and Automation, Box 118, 221 00 Lund, Sweden;
Phone: +46-46-222 74 99, Fax: +46-46-14 21 14, E-mail: karin.jonasson@iea.lth.se

K. Jonasson got the BSc (Conservation) degree at Gothenburg University and the BSc (Civil Engineering) degree at Lund University.

From 1995 to 1996 she was at Göteborg Energi AB, from 1996-1997 at Melcom Elektronik and from 1997 to 1998 at Jonasson Agency Consulting. Since 1998 she is a PhD student at Lund University, Department of Electrical Engineering and Automation.

Petter Strandh, BSc (Mechanical).

University of Lund, Dept Heat and Power Engineering, Div Combustion Engines, Box 118, 221 00 Lund, Sweden; Phone: +46 46 222 41 39, Fax: +46 46 222 47 17, E-mail: petter.strandh@vok.lth.se.

P Strandh got his BSc degree in 1997 at Lund University.

Since 1997 he is a PhD student at Lund University, Dept Heat and Power Engineering, Div Combustion Engines.

Mats Alaküla,

University of Lund, Dept. of Industrial Electrical Engineering and Automation, Box 118, 221 00 Lund, Sweden;
Phone: +46-46-222 92 84, Fax: +46-46-14 21 14, E-mail: mats.alakula@iea.lth.se

M. Alaküla got his engineering education at Chalmers University of Technology, Göteborg, where he graduated in Electrical Engineering in 1986. From 1986 to 1989 he was a Ph.D student at the Department of Electrical Machines and Power Electronics and received his Licentiate degree at the same Department in 1989. From 1989 on he has been working in the field of electrical drives at the Department of Industrial Electrical Engineering and Automation (IEA) at the Lund Institute of Technology. In 1993 he received his Ph.D. degree and he is since April 1994 appointed as full professor in Industrial Electrical Engineering at IEA. His main field of interest is various aspects of electrical drives and applications with combustion engines.

G

Norpie - paper

Simulation and verification of a hybrid bus, was written by Christian Andersson, Karin Jonasson, myself and Mats Alaküla.

Simulation and verification of a hybrid bus

Christian Andersson

University of Lund
Department of Industrial
Electrical Engineering and
Automation
Box 118
S-221 00 Lund
Sweden
Phone +46 46 222 74 99
Fax +46 46 14 21 14
Email:
Christian.Andersson@iea.lth.se

Karin Jonasson

University of Lund
Department of Industrial
Electrical Engineering and
Automation
Box 118
S-221 00 Lund
Sweden
Phone +46 46 222 74 99
Fax +46 46 14 21 14
Email:
Karin.Jonasson@iea.lth.se

Petter Strandh

University of Lund
Department of Heat and Power
Engineering
Divisions of Combustions
Engines
Box 118
S-221 00 Lund
Sweden
Phone +46 46 222 41 39
Fax +46 46 222 47 17
Email:
Petter.Strandh@iea.lth.se

Mats Alakula

University of Lund
Department of Industrial
Electrical Engineering and
Automation
Box 118
S-221 00 Lund
Sweden
Phone +46 46 222 92 84
Fax +46 46 14 21 14
Email: Mats.Alakula@iea.lth.se

ABSTRACT

A simulation model of a Hybrid Electric Bus (HEB) is presented in this paper. The model is verified through an existing HEB equipped with a measurement system. Finally some alternatives charging strategies and their consequences for the real HEB are presented.

Keywords: HEB (hybrid electric bus), charging strategies, simulation, emissions, gas motor, drive cycle.

1 INTRODUCTION

As a further step in the attempt to make the public transports in Malmö, Sweden, more environment adapted, HEB has been introduced in the ordinary bus fleet. The measurements that have been undertaken in this paper are made upon one of these HEB. This bus normally operates the distance Malmö city – the Copenhagen bridge, a distance of 20 km back and forth. The bus is a natural gas-electric hybrid bus. For further detail see table 1. Finally some alternative charging strategies for the bus are developed and their consequences are shown.

2 DRIVING CYCLES

A driving cycle consists of a predetermined speed and time vector. The vehicle is supposed to follow the vector as accurate as possible. The survey in this paper uses two driving cycles. It is the well-known Braunschweig cycle and a recorded driving cycle from a city bus in Malmö.

The Braunschweig City Driving Cycle was developed at the Technical University of Braunschweig. It was developed to simulate and test an urban bus driving cycle. When a vehicle is tested it is run on a chassis dynamometer. The cycle is frequently used in research with comparing simulation models. This cycle is quite demanding and has quick accelerations and retardations. The maximum speed is 58.2 km/h and the average speed is 22.4 km/h. Maximum acceleration is 2.14 m/s².

The Malmö cycle is a randomly selected recording of the bus velocity going from the town center to an exhibition site at the outskirts of Malmö. It is not as demanding as the Braunschweig cycle. The maximum speed is 49.7 km/h and the average speed is 20.9 km/h. Maximum acceleration is 1.36 m/s².

Another interesting point regarding this cycle is the duration and frequency of the bus stops. The stops gives the hybrid system time to recharge and the ICE usually has to be run with lowered power to reduce noise at the bus stop.

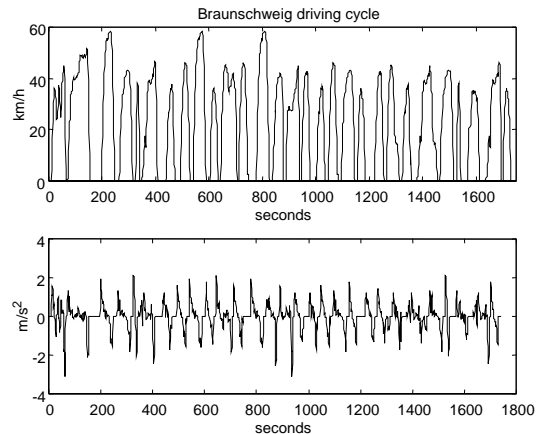


Fig. 1: Braunschweig driving cycle, speed and acceleration.

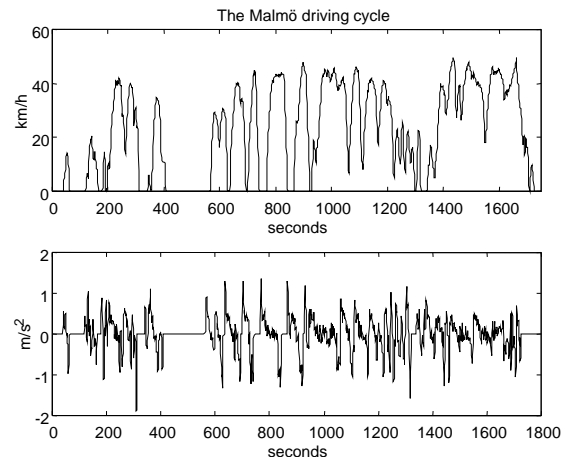


Fig. 2: The Malmö bus route, speed and acceleration.

3 EMISSIONS

At certain conditions ideal combustion can occur. This means that all hydrocarbons (HC) will be transformed into only carbon dioxide and water. This is called stoichiometry and is known as $\lambda=1$.

3.1 Regulated emissions

The most serious drawbacks with the combustion engines are their emissions. All fuel can never be transformed into only carbon dioxide and water, there will always be some residual products. When studying emissions, HC, carbon monoxide (CO) and nitrogen oxides (NO_x) are usually the ones in focus, since those are governed by legislative restrictions. But the exhaust gases also include other poisonous substances, such as formaldehyde and poly aromatic hydrocarbons.

The NO_x causes acid rain, which destroys the forests, and is poisonous. The carbon monoxide is a poisonous gas, which causes choking, and the hydrocarbons can cause cancer.

CO is formed during combustion with lack of oxygen. It is also formed due to an uneven fuel mixture. HC is formed by a surplus or a deficit of oxygen. NO_x is formed at high temperatures (>1800 K) when oxygen and nitrogen in the air react.

3.2 Emissions in the simulation model

The emissions maps used in the simulation model, have been formed and scaled to fit the size of the motor in the actual hybrid bus. As base for the scaled maps the emissions from a Scania DS 11-motor (biogas) have been used, which is similar to the one in the bus. The emission tables that are used in the model do not consider the use of an oxidizing catalyst.

The most interesting emission due to its impact on the environment is NO_x, which is not affected by the catalyst. A survey is undertaken in Finland of the involved bus's emissions. All regulated emissions, particles and other unregulated emissions will be measured. The results of this survey are predicted to the summer 2000.

3.3 Transient emissions

When running the engine through fast transients it's possible that the emissions from the engine will increase, due to a shift in the air fuel ratio. When the ratio is fuel rich, large amounts of NO_x are formed, but when the ratio is excessively lean the engine can misfire, resulting in large amounts of unburned HC. It's important not to make too fast load variation to avoid increased exhaust emissions.

4 DESCRIPTION OF THE VEHICLE

The bus that is used for verifying the simulation program is an electric series hybrid bus. The bus is constructed to take total of 57 passengers, 32 seated. It is a low floor city bus, 10 meters long. The chassis is built of composite and carbon fibre. This makes the bus very light. The construction is also environmental friendly because it is built of 100 % recyclable materials.

4.1 Engine

The Internal Combustion Engine (ICE) is a 6-cylinder turbo charged lean burn natural gas engine of 145 kW, equipped with a catalyst converter. The engine comes from Cummins.

4.2 Generator and driving motor

The generator and the two driving motors are of the same size and of the same construction. The generator is very compact and delivers maximum 125 kW and the driving motors deliver 55 kW each. They are permanent magnet machines from MagnetMotor. In this way the generator can supply the wheel-motors with enough energy, so the energy doesn't have to come from the battery to supply the driving-motors when peak power is needed.

4.3 Battery

The bus has a NiMH battery from Varta, which consists of 280 cells. The battery weighs approximately 500 kg. The battery is used as a power source when the bus is in emission free operation with the ICE turned off. The bus can run 20 km in battery mode.

4.4 Break chopper

When the battery reaches a certain state of charge they cannot receive more regenerated power from the driving motors. The power will then go to the break chopper, which will heat the cooling water for the engine.

4.5 Auxiliary system

The compressor and the pump are coupled mechanically to the engine. When the battery drives the bus and the engine is off, there is a special electrical motor for this application.

There is also a 24 V system in the bus and a separate generator to be used when the engine is on and a special DC/DC converter to be used when the engine is off.

4.6 Measuring system

A laptop containing LabView®, has been located onboard the bus and has continuously stored the measured data. The base in the measuring system constitutes is SCXI, a data acquisition system from National Instruments.

The onboard system has approximately 30 separate channels, which is sampled by 16 bits resolution. The onboard measuring system is collecting data from 25 sensors. All signals in the system are sampled with 5 Hz, hereby the transient behavior can be recorded also.

4.7 Sensors

All sensors used for the measuring are mounted after the bus was built. The reasons why the new sensors were mounted instead of using the sensors and measuring system installed by the bus-manufacturer, where that the already installed system did not have enough sampling speed and the accuracy of the sensors was not guaranteed by the bus-manufacturer.

aerodynamics and rolling resistance components. All the components have been chosen to imitate the real bus and its conditions as much as possible.

The simulated vehicle includes the possibilities to measure the emissions HC, CO and NO_x during the simulation. The levels of exhaust gases is presented instantaneously in graphs and also stored in a vector. Even the fuel consumption is measured and is present, since its level depends on different strategies. No transient behaviours are measured in the model.

The simulated driving cycles use velocity as a function of time. Besides that the model can also use velocity as a function of distance in its simulations. Using velocity as a function of time can give the result that if the speed differs from the supposed one, the bus stop will occur on the wrong place. If velocity is used as a function of distance there might be a problem with the pause time at the bus stop. To make it possible for the passengers of the simulated vehicle to get on and off the bus at the bus stop, a delay of 20 seconds is added at all bus stops.

6.3 Verification

Fuel consumption, speed and power flow are measured on the bus, see Fig. 4. The measured signals are only showed during 200 seconds of the Malmö cycle. This is made for clarity. The fuel consumption of the 10,4 km long bus route is 2,39 kg with the 6-cylinder Cummins engine.

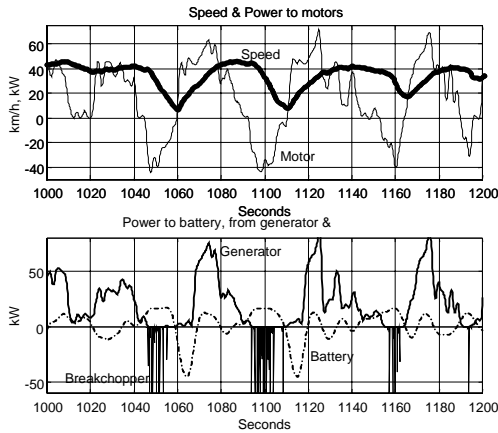


Fig. 4: Data measured from the hybrid bus in city traffic.

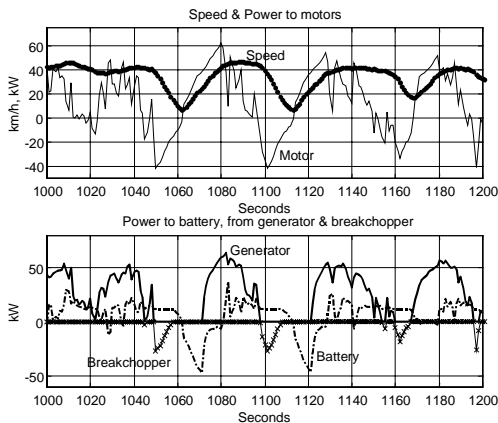


Fig. 5: Data from the simulated bus.

Fig. 5 shows the simulated bus with the same charging strategy as the real bus but with the Scania engine. On the Scania engine emissions and efficiency tests have been undertaken. The engine is actually too big (8-cylinder) so it has been scaled down (the number of cylinders have been reduced) to suit this application. For the simulation the motor has been reduced to the half size. The engine is hereby a 4-cylinder with peak power of 100 kW. The fuel consumption of the 10,4 km bus route then becomes 2,58 kg with the 4-cylinder Scania engine, see table 2.

6.4 Charging strategies

The SOC always ends at the same level as it started at, in this case 90 %. This makes the different cycles comparable and therefore a peak appears at the ICE at the end of each driving cycle. The charge power is depending on the wheel power and the state of charge reference minus actual. This gives the required charge power.

$$\frac{dP_{ice}}{dt} = \frac{P_{drive} + k(soc^* - soc) - P_{ice}}{\tau_{ice}} \quad (1)$$

T_{ice} (1) is the low pass filter time constant for the ICE. The emissions are strongly depending of the selection of T_{ice} . A small T_{ice} entail a quick change of the ICE's operation point and vice versa. The simulations have been made with T_{ice} equal 1, 10 and 100. With a choice of a small T_{ice} the model will not take consideration to any transient behaviour.

Since the battery size influences the bus's behaviour it is of deceive importance. The present battery will do about 20 km. Smaller battery capacity will of course be less heavy, but the ability to run in an emission free zone will also be reduced. It should be observed that the SOC vary only very little during the driving cycle, no matter which cycle that's been chosen.

6.4.1 Sensitivity analysis

By optimising the charging strategies in the bus a smoother power flow is achieved. The battery and the ICE might also be able to reduce and thereby will the weight of the bus decrease. This makes the bus cheaper to obtain and also to run, since the fuel consumption will decrease. See table 2. The possible weight loss is nevertheless of little importance compared to the vehicle's total weight.

	No. of cyl.	Battery size[%]	Fuel [kg]	Batt loss [kWh]	NO _x [g]	
Real	-	100	2.39	-	-	M
Sim	4	100	2.58	0.340	14.7	M
Sim	4	100	2.97	0.493	17.8	B

Table 2: The real bus and the simulated configuration (M=Malmö cycle, B=Braunschweig cycle).

With the aim to achieve an optimised strategy the ICE power is low pass filtered, see (1). T_{ice} is varied in the simulations between 1, 10 and 100 seconds. Owing to this there is a possibility to avoid the transient behaviour of the ICE. A smoother power flow leads to less emissions, which is of high priority. A short T_{ice} makes it possible to reduce the size of the battery, see table 3.

τ_{ice} [s]	No. of cyl.	Battery size[%]	Fuel [kg]	Batt loss [kWh]	NO _x [g]	
1	3	100	2.39	0.284	14.1	M
10	3	100	2.57	0.601	14.0	M
100	3	100	2.83	0.752	13.6	M
10	3	100	2.85	0.861	16.9	B

Table 3: The bus with variation in τ_{ice} (M=Malmö cycle, B=Braunschweig cycle).

The size of the ICE is also used as a variable parameter according to the charging strategy. Cutting down the number of cylinders reduces the size. When the motor size is to low, the efficiency becomes high to the price of strongly increasing emissions (NO_x), see table 4.

τ_{ice} [s]	No. of cyl.	Battery size[%]	Fuel [kg]	Batt loss [kWh]	NO _x [g]	
10	3	100	2.57	0.601	14.0	M
10	2	100	2.35	0.625	18.1	M
10	4	100	2.73	0.592	13.9	M
10	2	100	2.61	0.885	21.5	B
10	3	100	2.85	0.861	16.9	B

Table 4: The bus with variation in engine size (M=Malmö cycle, B=Braunschweig cycle).

The battery size can also be used as a variable parameter. In the simulations the size was varied from 50 % to 150 %. Smaller battery is cheaper and lighter, but the battery losses increased. Larger battery gave the opposite result. See table 5.

τ_{ice} [s]	No. of cyl.	Battery size[%]	Fuel [kg]	Batt loss [kWh]	NO _x [g]	
10	3	100	2.57	0.601	14.0	M
10	3	50	2.67	0.903	14.8	M
1	4	50	2.61	0.385	13.4	M
100	2	150	2.60	0.622	13.5	M
100	2	150	3.01	0.905	14.2	B

Table 5: The bus with variation of battery size and engine (M=Malmö cycle, B=Braunschweig cycle).

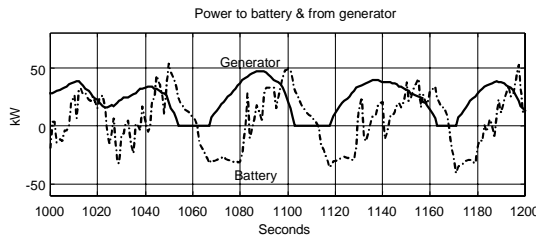


Fig. 6: An optimized simulated vehicle with $T_{ice}=10$, 3 cylinders and 100 % battery capacity.

To solve the problem with over charged batteries one solution could be to only allow the battery to be charged by generator to

SOC 70 or 75 %. When the bus is breaking the battery can take care of all the power that the drive motors generate. In this manner the heat losses due to overcharging will be reduced.

7 CONCLUSIONS

To choose driving cycles for a simulation model one has to assume that the performance demands of the vehicle is known. For instance the used Braunschweig cycle is very demanding compared with the Malmö cycle. It might not be necessary to construct a HEB to be able to drive a very tough cycle when it is only going to be used in city traffic. No one buys a Formula 1 car for transport his or her groceries. It doesn't fit that purpose.

One of the goals with this study is to get a vehicle with an ICE that is as small as possible and that can work smoothly and with lower emissions. This is due to a small ICE is lighter and cheaper.

Using different charging strategies has of course great impact on the vehicle's performance. An increasing T_{ice} gives a lower efficiency since the requested power decreases from the ICE. If the size of the ICE is decreased, the efficiency will increase to the price of increasing NO_x.

With increasing size of the battery their losses will decrease but the costs and weight will increase. If the main aim is to be able to drive in battery mode for long distances it is of great interests that the bus has a large energy storage possibility. If that is not the case a power storage is wanted.

REFERENCES

- [1] Braunschweig city driving cycle, 2000-04-27, www.dieselnet.com/standards/cycles/braunschweig.html.
- [2] R. EGNELL, *Motorer för gasbussar LITA- och STAB-projekten*, Vitskövle 1993.
- [3] J. B. HEYWOOD, *Internal Combustion Engine Fundamentals* 2nd edition Singapore 1988.
- [4] A. MALMQUIST, L. ROSENDAHL, N. BERG, O. ALÈN, *Second generation gas turbine driven hybrid city bus*, proceedings of Electric Vehicle Symposium 15, Brussels, Belgium, 1998.
- [5] J. VAN MIERLO, *Simulation of a complex parallel-series hybrid drive train*, Electric Vehicle Symposium 16, Beijing, China, 1999.
- [6] D. SUTANTO, H. L. CHAN and C.C. FOK, *Battery, Model for Use in Electric Vehicles and Battery Storage System*, 8th European Conference on Power Electronics and Applications, Lausanne, Switzerland 1999.